

ANALYSIS OF XYLOGLUCAN ENDOTRANSGLYCOSYLASE/HYDROLASES  
ENZYMES TO SEEK THEIR EVOLUTIONARY ORIGINS



by

Tuğçe Bayrakdar Turgut

Submitted to Graduate School of Natural and Applied Sciences  
in Partial Fulfillment of the Requirements  
for the Degree of Master of Science in  
Biotechnology

Yeditepe University

2017

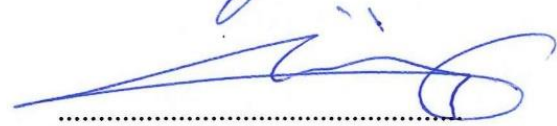
ANALYSIS OF XYLOGLUCAN ENDOTRANSGLYCOSYLASE/HYDROLASES  
ENZYMES TO SEEK THEIR EVOLUTIONARY ORIGINS

APPROVED BY:

Assist. Prof. Dr. Andrew John Harvey  
(Thesis Supervisor)

  
.....

Assoc. Prof. Dr. Gizem Dinler Doğanay

  
.....

Assist. Prof. Dr. Bahar Soğurmaz Özdemir

  
.....

DATE OF APPROVAL: .... / .... / 2017

## ACKNOWLEDGEMENTS

I wish to express my sincere gratitude to my advisor Assis. Prof. Dr. Andrew John Harvey for his support of my study, for giving me guidance and helping me with great patience.

I would like to thank Research Assistant Merve Seven who gave support of this project and valuable advices were appreciated. I would also want to thank my precious laboratory members of Plant Biotechnology Group; Dilara Tüzün, Ezgi Türksever and Burcu Gür for making the working environment fun, helping me during the laboratory and sharing this challenging journey with me.

I greatly thank to the Scientific and Technological Research Council of Turkey (TUBITAK) for its generous financial support during MSc studies by supporting from the research project 114Z270 “Looking Backward to Move Forward: An Analysis of the Evolution of Xyloglucan-Active Enzymes”.

Finally, special thanks to my parents, my husband and numerous friends who encouraged, showed patience and never gave up on me along this process, always offering support and love.

## ABSTRACT

### ANALYSIS OF XYLOGLUCAN ENDOTRANSGLYCOSYLASE/HYDROLASES ENZYMES TO SEEK THEIR EVOLUTIONARY ORIGINS

Xyloglucan is an important polysaccharide and is involved in strengthening the cell wall in both monocot and eudicot species. The xyloglucan endotransglycosylase/hydrolase (XTH) enzymes can degrade or remodel xyloglucan within the cell walls. The characterization of the xyloglucan substrates have a great importance since their involvements in the process of cell wall components and properties of the cell wall. The part of the cell wall where XTH enzyme shows activity, protects the plants from the outer elements and interacts with the environment. To be able to manipulate cell wall properties in order to enhance the yield and protect the plant from outer stresses, it is important to understand the functions of the enzymes that are modifying the carbohydrate matrix. XTH is one of the members of glycoside hydrolases 16 (GH16) enzyme family and it cleaves and re-ligate or irreversibly hydrolyzes xyloglucan. The aim of this study is investigating ancestral and EG16 group XTH enzyme members including OsXTH30, OsEG16-31 (*Oryza sativa*), BdXTH2 (*Brachypodium distachyon*), and HvEG16-10 (*Hordeum vulgare*). Heterologous expression, production and purification of the enzymes was performed as well as characterizing the enzymes and analyzing their kinetic studies. OsEG16-31, and HvEG16-10 enzymes could not be heterologously expressed during the period of this study, but XTH activity levels were detected from OsXTH30 and BdXTH2. The characterization of BdXTH2 enzyme showed higher affinity for tamarind seed xyloglucan as a donor substrate. The characterization and enzymatic activities of ancestral forms of XTH gene products is aimed since these genes have a role in seed germination, stress tolerance, organogenesis, cell expansion, and fruit ripening.

## ÖZET

### KSİLOGLUKAN ENDOTRANSGLİKOZİLAZ/HİDROLAZ ENZİMLERİNİN EVİRİM ORJİNLERİNİ İNCELEMELİK İÇİN ANALİZİ

Xyloglucan önemli bir polisakkarittir ve aynı zamanda hem monokot hem de ödikot türünün hücre duvarı güçlendirilmesinde görev almaktadır. Ksiloglukan endotransglikozilaz/hidrolaz (XTH) enzimi, hücre duvarları içindeki ksiloglukanı parçalayabilir veya yeniden şekillendirebilir. Ksiloglukan substratlarının karakterizasyonu, hücre duvarı bileşenleri ve hücre duvarı özellikleri ile ilgili olduğundan büyük önem taşımaktadır. XTH enziminin aktivite gösterdiği hücre duvarı kısmı, bitkileri dış elementlerden korur ve çevre ile etkileşime girer. Verimi arttırmak ve bitkiyi dış streslerden korumak ve hücre duvar özelliklerini manipüle edebilmek için karbonhidrat matrisini modifiye eden enzimlerin işlevlerini anlamak önemlidir. XTH, glikozid hidrolazlar 16 (GH16) enzim ailesinin üyelerinden biridir ve ksiloglukanın parçalanmasını ve yeniden bağlanmasını veya geri dönüşümü olmadan hidrolize edilmesini sağlar. Bu çalışmanın amacı, OsXTH30, OsEG16-31 (*Oryza sativa*), BdXTH2 (*Brachypodium distachyon*) ve HvEG16-10 (*Hordeum vulgare*) dahil olmak üzere atalasal ve EG16 grubu XTH enzim üyelerini araştırmaktır. Enzimlerin karakterize edilmesi ve kinetik çalışmalarının analiz edilmesi için enzimlerin heterolog ifadeleri, üretimi ve saflaştırılması gerçekleştirilmiştir. OsEG16-31 ve HvEG16-10 enzimleri heterolog olarak eksprese edilememiştir. Ancak XHT aktivitesi, OsXTH30 ve BdXTH2 enzimlerinde tespit edilmiştir. BdXTH2 enziminin karakterizasyonunda hint hurması tohumu ksiloglukanına donör substratı olarak daha yüksek afinite gösterdiği görülmüştür. XTH genleri, tohum çimlenmesi, stres toleransı, organogenez, hücre genleşmesi ve meyve olgunlaşması gibi görevlerde rol aldığından dolayı, bu gen ürünlerinin atasal formlarının karakterizasyonu ve enzimatik faaliyetlerinin incelenmesi amaçlanmıştır.

## TABLE OF CONTENTS

ACKNOWLEDGEMENTS.....	iii
ABSTRACT.....	iv
ÖZET .....	v
LIST OF FIGURES .....	ix
LIST OF TABLES.....	xii
LIST OF SYMBOLS/ABBREVIATIONS.....	xiii
1. INTRODUCTION .....	1
1.2. PLANT CELL WALL .....	1
1.2. PLANT CELL WALL STRUCTURE.....	2
1.3. CELLULOSE.....	4
1.4. XYLOGLUCAN .....	8
1.5. MIXED-LINKED B-GLUCANS .....	12
1.6. XYLAN.....	13
1.7. MANNAN.....	14
1.8. PECTIN.....	15
1.9. XYLOGLUCAN ENDOTRANSGLYCOSYLASE/HYDROLASE (XTH) ENZYMES.....	16
1.10. POLYSACCHARIDES AND OLIGOSACCHARIDE SUBSTRATES.....	21
1.11 HETEROLOGOUS EXPRESSION AND THE <i>PICHA PASTORIS</i> SYSTEM ...	23
2. MATERIALS.....	25
2.1. EQUIPMENTS AND MATERIALS .....	25
2.2. CHEMICALS.....	26
3. METHODS .....	32
3.1. TARGET ENZYME SELECTION.....	32
3.2. PRODUCTION AND PURIFICATION OF OsXTH30, HvEG16 AND OsEG16-31 ENZYMES.....	32
3.2.1. Reproducing colonies and Preparation of Glycerol Stock .....	32
3.2.2. Plasmid Isolation.....	32
3.2.3. Preparation of <i>Pichia pastoris</i> Competent Cells.....	33

3.2.4. Plasmid Digestion .....	34
3.2.5. Phenol Extraction and Ethanol Precipitation of Plasmid DNA .....	34
3.2.6. <i>Pichia pastoris</i> Transformation .....	35
3.2.7. Selection of Colonies Which Producing the Target Enzyme.....	35
3.2.8. Enzyme Activity Assay.....	37
3.2.9. Large Scale Production and Protein Purification.....	37
3.2.10. Bradford Protein Assay.....	39
3.2.11. Western Blot, Silver Nitrate Staining and Dot Blot Analysis.....	39
3.2.12. pH Optimization and Activity Analysis.....	40
3.2.13. Enzyme Kinetic Analysis.....	40
3.3. ENZYME KINETIC ANALYSIS OF BDXTH2 .....	40
4. RESULTS .....	42
4.1. PRODUCTION AND PURIFICATION OF OsXTH30.....	42
4.1.1. Big Scale Production and Purification of OsXTH30 in 3 lt of BMMY Medium .....	42
4.1.1.1. Transformation into <i>Pichia pastoris</i> and positive colony selection of OsXTH30 .....	42
4.1.1.2. Expression of OsXTH30 in <i>Pichia pastoris</i> .....	44
4.1.1.3. Purification of OsXTH30 Enzyme with Chromatography.....	45
4.1.1.4. Detection of OsXTH30 Using SDS-PAGE, Western Blotting, Silver Nitrate Staining and Dot Blot Analysis.....	47
4.1.1.5. Bradford Assay and the Enzyme Activity Analysis .....	49
4.1.2. Big Scale Production and Purification of OsXTH30 in 1.7 lt of BMMY Medium .....	51
4.1.2.1. Expression of OsXTH30 in <i>Pichia pastoris</i> .....	51
4.1.2.2. Purification of OsXTH30 Enzyme with Chromatography .....	52
4.1.2.3. Detection of OsXTH30 Enzyme Using SDS-PAGE, Western Blotting, Silver Nitrate Staining.....	54

4.1.2.4. Bradford Assay and the Enzyme Activity Analysis .....	56
4.2. CHARACTERIZATION OF BDXTH2 .....	58
4.1.2. pH Optimization.....	58
4.2.2. Enzyme Activity Analysis .....	59
4.2.3. Kinetic Studies .....	61
4.3. PRODUCTION AND PURIFICATION OF OsEG16-31 AND HvEG16-10.....	63
4.3.1. Positive Colony Selection of OsEG16-31 and HvEG16-10 .....	63
5. DISCUSSION .....	65
6. CONCLUSION.....	68
REFERENCES .....	69



## LIST OF FIGURES

Figure 1.1. Structure of the primary cell wall.....	3
Figure 1.2. <i>Arabidopsis</i> leaf cell based plant cell wall structure. The cellulose amount is decreased compared to a living cell for better visibility.....	4
Figure 1.3. Representation of cellulose biosynthesis.....	5
Figure 1.4 Cellulose synthase complexes formed by CESA .....	6
Figure 1.5. Phylogenetic tree of cellulose synthase and cellulose synthase-like gene families in higher plants.....	7
Figure 1.6. Representation of <i>Arabidopsis</i> xyloglucan.....	8
Figure 1.7. Nomenclatures and chemical structures of Xyloglucan side chain compositions .....	9
Figure 1.8. Representation of the xyloglucan with different oligosaccharide units .....	10
Figure 1.9. Structures of the different XyG from different plant species .....	11
Figure 1.10. Structure of mixed linked (1;3,1;4)- $\beta$ -D-glucan.....	12
Figure 1.11. Representation of xyloglucan endotransglucosylase/hydrolase (XTH) activity .....	16
Figure 1.12 Chemical mechanism of the glycosyl transfer reaction by hydrolysis and transglycosylation .....	18

Figure 1.13 Structure of PttXET16A.....	19
Figure 1.14 Representation of xyloglucan endotransglucosylase activity.....	19
Figure 1.15 Phylogenetic tree of XTH enzymes according to their on amino acid sequences .....	21
Figure 1.17 Representation of some of the main polysaccharides that are used as donor...23	
Figure 1.15. Oligosaccharides that are used as acceptor substrates.....	24
Figure 4.1 YPDS agar with transformant and nontransformant <i>P. pastoris</i> colonies for colony selection of pPICZ $\alpha$ -C/OsXTH30 .....	45
Figure 4.2 Detection of OsXTH30 protein produced by heterologous expression of transformant <i>P. pastoris</i> colonies by using SDS-PAGE.....	46
Figure 4.3 Purification OsXTH30 protein by the affinity chromatography of using the GE Healthcare HisTrap FF column.....	48
Figure 4.4 The GE Healthcare Superdex 75 16/100 size exclusion column chromatogram of OsXTH30 enzyme .....	48
Figure 4.5. Analysis of the OsXTH30 protein fractions from 46 to 94 after purification with GE Healthcare Superdex 75 16/100 gel filtration column.....	50
Figure 4.6. Western blot analysis of the OsXTH30 protein of pool 1 (f46-57) and pool 2 (f58-70). Protein marker band sizes and fraction numbers are indicated on the image .....	51
Figure 4.7. Standard curve of Bradford assay using BSA measured at 595 nm.....	52

Figure 4.8. Chromatogram of heterologously expressed OsXTH30 enzyme using GE Healthcare HisTrap FF column.....	55
Figure 4.9. Chromatogram of heterologously expressed OsXTH30 enzyme using The GE Healthcare Superdex 75 16/100 size exclusion column .....	55
Figure 4.10. Analysis of the protein content of OsXTH30 protein in fractions resulting from GE Healthcare Superdex 75 16/100 gel filtration chromatography .....	57
Figure 4.11. Standard curve of Bradford assay using BSA measured at 595 nm.....	58
Figure 4.12. Enzyme activity results of the OsXTH30 enzyme after the GE Healthcare Superdex 75 16/100 gel filtration column. Enzyme reactions were set by using TXG-XGO donor-acceptor couples detected by the HPLC.....	59
Figure 4.13. The enzyme activity-time plot of different polysaccharide-oligosaccharide substrate pairs of OsXTH30 enzyme .....	60
Figure 4.14 pH optimization of the BdXTH2 by using the TXG-XGO couples that have different pH values prepared with McIlvaine buffers.....	61
Figure 4.15. Relative Specific enzyme activities of BdXTH2 according to the Table 4.6. TXG-XGO couple was used for comparison.....	63
Figure 4.16. Detection of the optimum TXG concentration using with 50µM of X7 for BdXTH2 activity.....	64
Figure 4.17. Detection of the optimum X7 concentration with %0.2 w:v of TXG for BdXTH2 activity .....	64
Figure 4.18 Lineweaver-Burke graph of BdXTH2 enzyme with 0.2% of TXG with various X7 concentration.....	65

Figure 4.19. Detection of heterologously expressed HvEG16 and OsEG1631 enzymes of selected colonies using polyacrylamide gel electrophoresis.....66



## LIST OF TABLES

Table 2.1. List of equipment, materials and company names.....	27
Table 2.2. List of chemicals and company names .....	29
Table 2.3 Polysaccharide donors listed with abbreviations and catalog numbers.....	32
Table 2.4. Oligosaccharide acceptors listed with abbreviations and catalog numbers.....	32
Table 4.1. The enzyme activities of undiluted OsXTH30 enzyme along the production and purification periods with TXG-XGO donor acceptor couple for 24 hours.....	47
Table 4.2. Protein fraction concentrations of purified pools belongs to the OsXTH30 enzyme .....	52
Table 4.3. The enzyme activities of purified pools belongs to the OsXTH30 enzyme .....	53
Table 4.4. The enzyme activities of undiluted OsXTH30 enzyme along the production and purification periods with TXG-XGO donor acceptor couple for 1 hour .....	54
Table 4.5. Protein concentrations of purified OsXTH30 enzyme pools.....	58
Table 4.6. Specific enzyme activity of BdXTH2 with different substrate couples .....	62

**LIST OF SYMBOLS/ABBREVIATIONS**

AOX1	Alcohol oxidase 1
BA	1,3:1,4- $\beta$ -glucotetraose A
BB	1,3:1,4- $\beta$ -glucotetraose B
BBG	Barley $\beta$ -glucan
BC	1,3:1,4- $\beta$ -glucotetraose C
BMGY	Buffered Glycerol Complex Medium
BMMY	Buffered Methanol Complex Medium
BSA	Bovine Serum Albumin
CAZy	Carbohydrate-Active enzymes
CESA	Cellulose synthase
Csl	Cellulose Synthase-Like
CT	1,4- $\beta$ -cellotetraose
ddH <sub>2</sub> O	Double Distilled Water
DGM	Di-galactosyl mannopentaose
DTT	Dithiothreitol
EDTA	Ethylenediaminetetraacetic acid
GAXs	Glucuronoarabinoxylans
GH	Glycoside hydrolases
GM	Galactosyl mannotriose
HEC	Hydoxyl-ethyl cellulose

HPLC	High Performance Liquid Chromatography
IPTG	Isopropyl- $\beta$ -D-thiogalactopyranosid
LB	Luria-Bertani
LT	Laminaritetraose
MLGs	Mixed linked $\beta$ -glucans
MXE	Xyloglucan endotransglucosylase
Ni-NTA	Nichel- Nitrilotriacetic Acid
PBS	Phosphate-buffered saline
PMSF	Phenylmethylsulfonyl Fluoride
SOC	Super Optimal Broth With Added Glucose
TAE	Tris-Acetate EDTA
TBS	Tris Buffered Saline
TBS- T	Tris Buffered Saline- Tween 20
TCA	Trichloroacetic acid

# **1. INTRODUCTION**

## **1.1. PLANT CELL WALL**

The cell wall consists of complex and diverse structures during cell division, growth and differentiation. The selectively permeable cell wall is responsible for cell-cell adhesion and for intercellular communication. There are about 40 different types of cells in a plant. Their diversity can be distinguished by the chemistry, size, format and components of the cell wall. The fact that even plants of the same species show cellular differentiation, arises from environmental conditions and developmental stages of the plants [1]. Components of the cell wall also depends on the growth phase and location in the cell wall beside the type of the cell [2].

Most cells use turgor pressure to resist positive pressure produced within the cell and this pressure help them to stand upright. Plant cell walls have also developed defense mechanisms to protect plants against invasive microorganisms and abiotic stresses. In general, plant cell walls can be grouped into two groups; primary walls and secondary walls. The primary cell wall is being formed during cell growth and secondary cell wall is stored in some cells after cell growth and after expansion stops. Although primary cell walls are rigid structures that are eliminated outside the plasma membrane and are malleable and flexible. They do not interfere with the expansion of the cells, and adapt to the physiological needs of the plant.

Plant cell wall structure is made of 80-90% carbohydrate, 10% glycosylated proteins, and lignin. Different kinds of polymers constitute the cell wall such as; cellulose, hemicellulose, pectin and structural proteins [3]. Polysaccharides represent an important and renewable source of carbon fixed by photosynthesis and the resulting biofuels are important as a biomass source for industry. Cell walls have been used as fuel for thousands of years, such as wood from dicotyledonous species, and peat supplied from Sphagnum moss are used as fuel sources [4]. It is being attempted to convert plant cell wall polysaccharides into renewable energy fuels and to use them to provide dietary benefits. Increasing plant performance requires a number of changes and modifications in the wall components. Success has been observed in non-cellulosic polysaccharides, but it has been understood in



research that it is not easy to make radical changes in the cellulosic process. However, the contribution of genetically modified and non-GM technologies to human health and biofuels by changing the cell wall structure is still under development [5].

The cell wall also prevents the cell from being attacked by pathogens. Extracellular components that act on cell wall elements in uninfected plants activate the defense mechanism of the cell. Activation of this mechanism also implies the presence of signal transduction chains that can be activated by glycans [6]. It has been suggested that during the degradation of the cell wall, complex molecules are released to activate the defense system [7]. Some other studies have showed that cell wall polysaccharide fragments and proteoglycans are involved in during development [8,9].

## **1.2. PLANT WALL STRUCTURE**

Cell walls generally consist of three parts, the middle lamella, the primary cell wall and the secondary cell wall. The middle lamella is the first layer formed during cytokinesis, which combines two cell walls during cell division. The primary cell wall is usually 0.1-10  $\mu\text{m}$  thick but it plays an important role in biomass accumulation, as it is continues to be formed during in cell growth and development [4]. The structure of the primary cell wall should be resistant to turgor pressure and build to be resistant during cell expansion. Primary cell wall components can be classified as polysaccharides, such as cellulose, hemicellulose, and pectin. Hemicelluloses and pxylogluectins are generally called matrix polysaccharides. Even though matrix polysaccharides are synthesized in the Golgi, cellulose is formed at the plasma membrane in the form of microfibrils [10].

When some cell types are subjected to stress due to a mechanical effect, they resort to cell wall synthesis once cell division is complete and the cell is fully grown [6]. The secondary cell wall, which is not found in all cell types, is formed after cell growth has ceased, and provide mechanical stability, strength and modularity to cells. The contents of secondary cell walls in some types of plant cells may have different functions, depending on the type of cell they are in. For instance, xylem cells containing lignin plays a role in strengthening and waterproofing the cell wall [4]. The researches concentrated on the primary cell wall, as the wall composition changes in the secondary cell wall compared to the cell type. Non-cellulosic polysaccharides and glycoproteins form the primary cell wall in a matrix

distributed among the cellulosic microfibrils in the matrix. For example, covalent linkage of xyloglucan, which is hemicellulose, is frequently observed with pectin in Angiosperms [11].

The complex structure of the growing cell wall consists of cellulose, and other polysaccharides that can be assembled into 2 groups; pectins and hemicelluloses and these complex polysaccharides called collectively called matrix polysaccharides. Cellulose microfibrillar crystals are inflexible fibers in layers that are embedded in these matrix polysaccharides. Pectins are complex polysaccharides that separate microfibrils from each other during cell growth and stabilize them when growth is over. Homogalacturonan, arabinans, rhamnogalacturonans I and II, galactans, and other polysaccharides are the main pectin domains. Hemicelluloses are polysaccharides that form a flexible and rigid structure that binds to celluloses. Xyloglucan and arabinoxylan can be mentioned as the main hemicelluloses, especially for dicots [12].

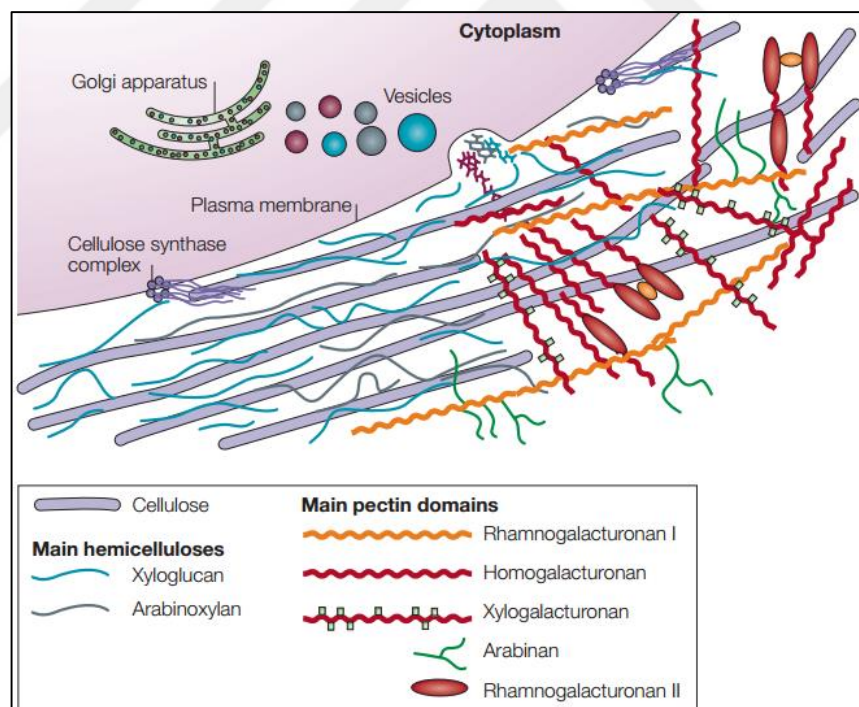


Figure 1.1. Structure of the primary cell wall [12].

The cell wall compositions of monocot and dicot plants differ from each other. The amount of cellulose in the monocot plants in the primary cell wall is around %20-30 whereas in dicot plants this amount is %15-30. Hemicelluloses in the primary cell wall have markedly

different percentages in monocot and dicot plants; xylan is %20-40 in monocots and %5 in dicots, xyloglucan is %1-5 in monocots and %20-25 in dicots. Monocot plants have %10-30 of mixed-linked glucans whereas there is none in dicots [13].

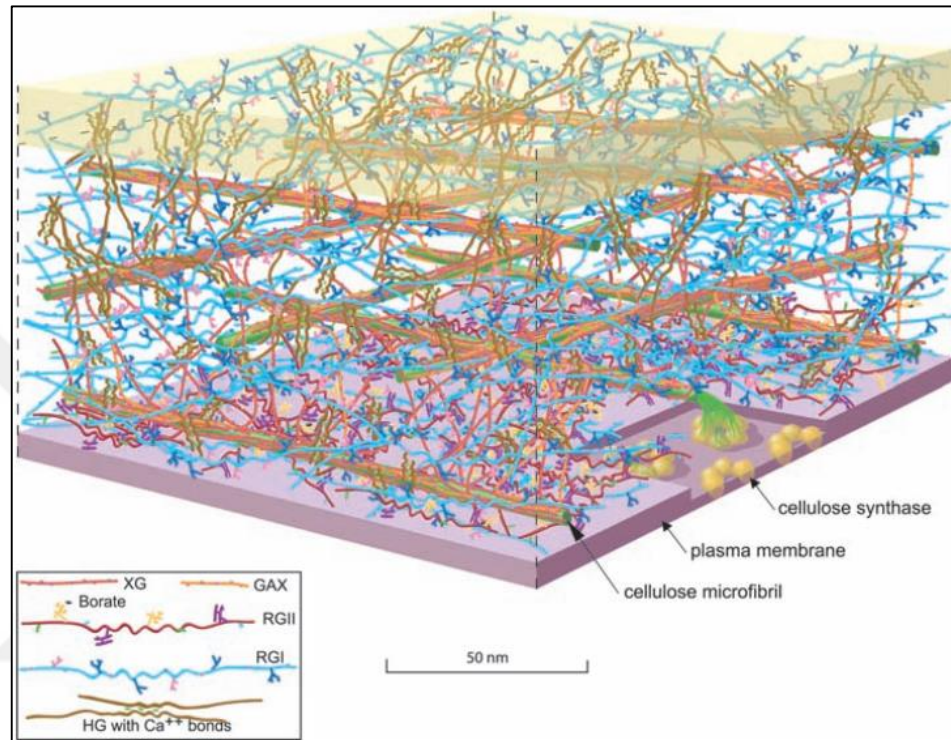


Figure 1.2 *Arabidopsis* leaf cell based plant cell wall structure. The cellulose amount is decreased compared to a living cell for better visibility [6].

### 1.3. CELLULOSE

Cellulose is the most abundant biopolymer found on Earth and has structural and functionally important tasks as it is found all over the plant cell wall [14]. Cellulose acts as a bridge to connect other plant cell wall elements. Cellulose is composed of (1,4)-linked  $\beta$ -D-glucans. The parallel structure of many glucans creates a chemically robust material that is resistant to attacks. Cellulose is formed from large membrane complex, which extracts microfibrils from the cell surface, which is called the cellulose synthase complex. This large multi-protein cellulose synthase complex synthesizes in the plasma membrane by combining 18-36 glucan chains at the same time on a single microfibril [3]. These elongated cellulose microfibrils are 3-5 nm wide and are aligned with each other. Cellulose synthase enzyme

complexes are in the form of hexameric rosettes and are in the approximate range of 25-30 nm [15].

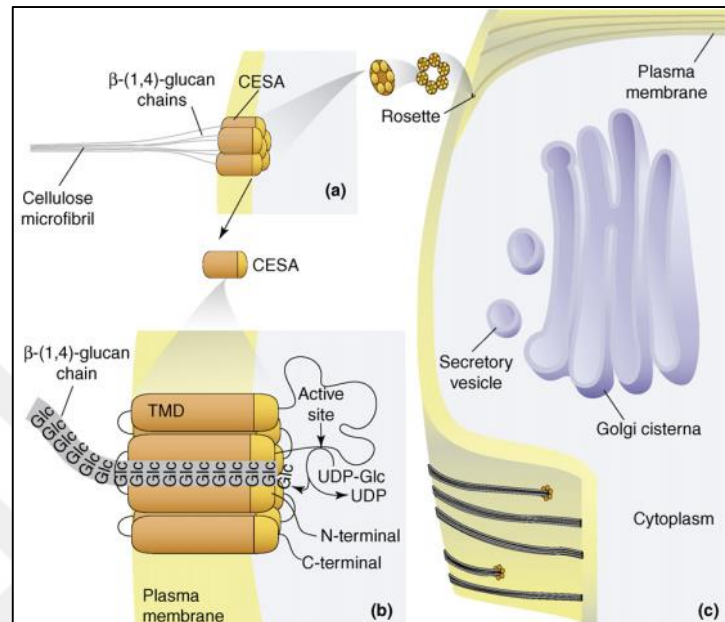


Figure 1.3. Representation of cellulose biosynthesis. (a) Rosettes producing cellulose microfibrils in the cell wall. (b) CESA proteins forms rosette subunits which forms hexameric rosette. (c) Matrix polysaccharides deposited to the outer cell with Golgi after they are synthesized [16].

It has been said that each hexameric rosette consists of six rosette subunits and these subunits contain six CESA proteins. Thus, it is assumed that there are 36 of CESA proteins in 1 rosette [16]. After CESA genes were identified for the plant cellulose synthesis and forming microfibrils, it has been found that CESA family contain 10 genes and each of the genes expressed in different cells and tissues [17]. For example, *Arabidopsis* has 10 CESA genes whereas there are at least 10 CESA genes in rice and the poplar has 18 of them [18,19]. When UDP-glucose (cytosolic uridine-diphosphoglucose) is used as substrate, it has been observed that each rosette subunit forms a  $\beta$ -1,4-glucan chain and joins it into microfibrils outside the plasma membrane [16].

It has been concluded that three different CESA genes must be present in order to obtain a functional cellulose synthesis complex [20,21]. Also, different groups of genes are required

for the formation of cellulose in the primary and secondary cell walls. For instance, *CESA1*, *CESA3* and *CESA6* are involved in building primary cell wall and *CESA4*, *CESA7* and *CESA8* genes are involved in building secondary cell wall for *Arabidopsis* [22].

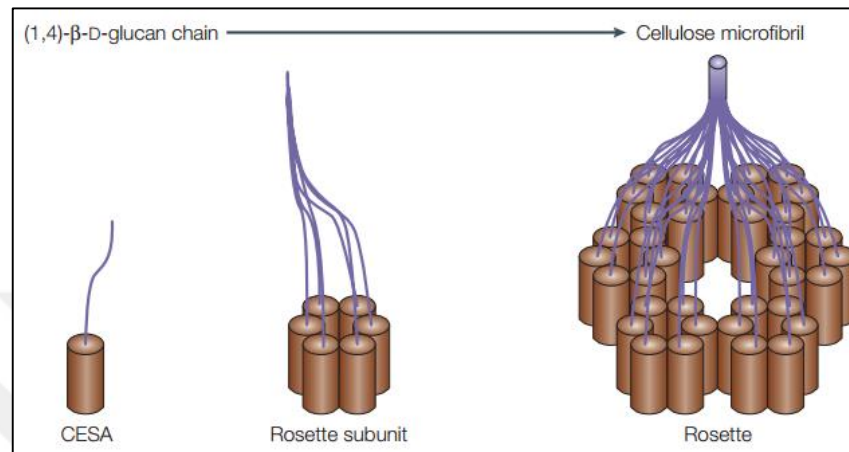


Figure 1.4. Cellulose synthase complexes formed by CESA. Rosette units are formed by 6 rosette subunit which is formed by 6 CESA proteins [23].

The matrix polysaccharides have a greater variety of glycosidic bonds and sugar groups than cellulose. Although glycosyltransferases related genes are difficult to identify, approximately 20 were characterized [24]. CESA proteins belong to the Cellulose Synthase-like (CSL) gene family, and in this superfamily there are other families named as CSLA, CLSB, CSLC, CSLD, CSLE, CSLF, CSLG, CSLH and CSLJ [25].

CSL proteins have sequence fragments that are characteristic of β-glycosyltransferases. However, in CSL proteins, there is no N-terminal region like CESA protein have with a zinc domains which causes protein dimerization. Because of these similarities, it is thought that CSL proteins are involved in the synthesis of hemicelluloses with β-D-glycan backbones such as xyloglucan, xylan, mannan and other hemicelluloses in the Golgi [23].

The synthesis of wall polysaccharides in grasses has been investigated by genomic studies and it has been understood that the CSLF and H families are involved in the synthesis of (1,3; 1,4)-β -D-glucan [26,27]. Also, studies showed that *CSLA* genes are involved in production of β-mannan synthase which is responsible for building the mannan backbone structure of some of the hemicelluloses. For instance, galactomannan containing guar gum

is used as food thickener and has  $\beta$ -mannan backbone. Galactomannan from the guar gum was observed to be synthesized by a *CSLA* gene [28].

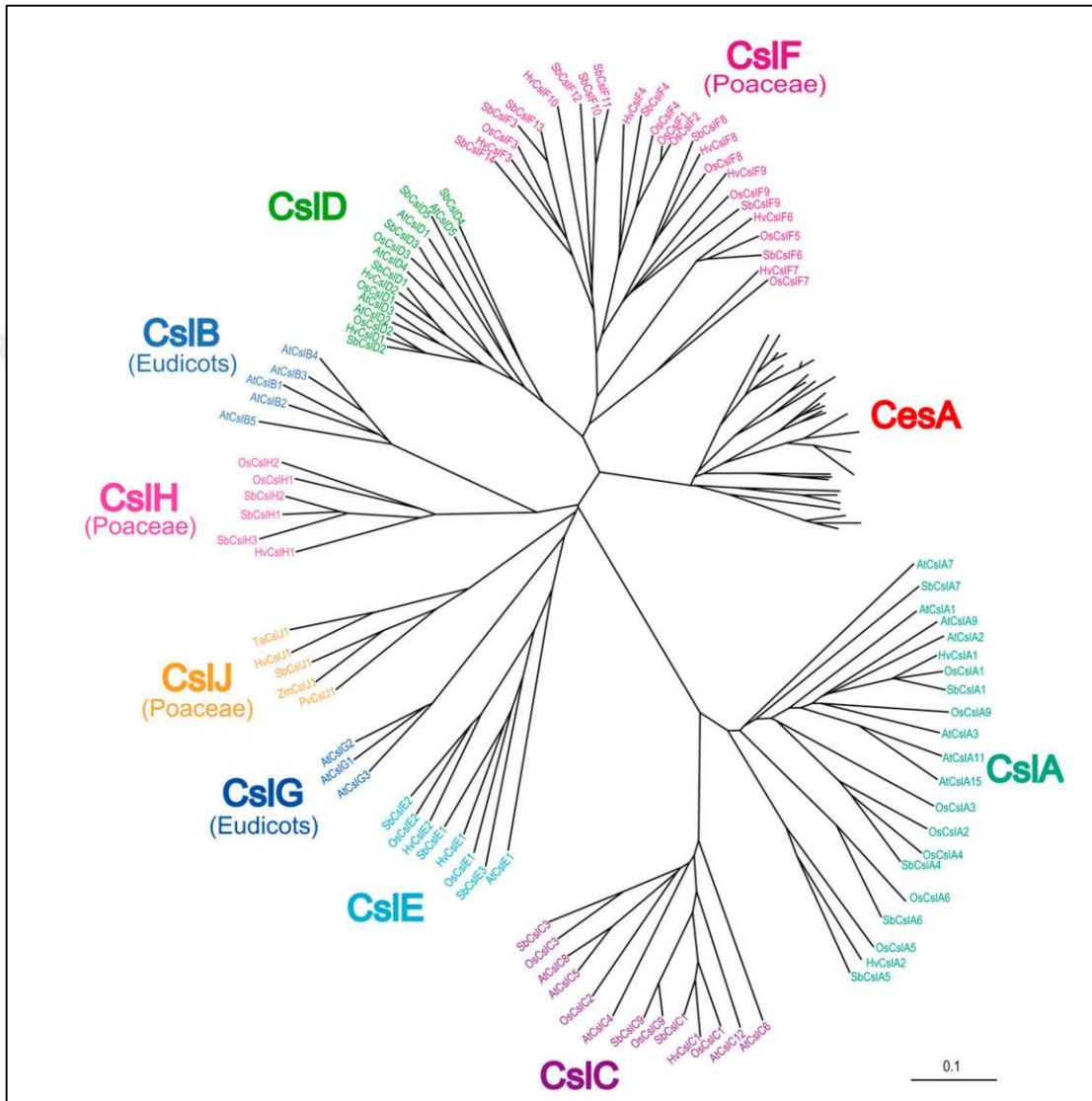


Figure 1.5. Phylogenetic tree of cellulose synthase and cellulose synthase-like gene families in higher plants [29].

In the phylogenetic tree (Figure 1.5) of the *CSL* genes, the *CSL* gene families have close to 50 groups, many of which are subgroups. When these groups are examined, it is observed that the *CSLF* and *CSLH* genes are only Poaceae specific and *CSLB* and *CSLG* groups can

be seen only in eudicots [30]. The *CSLJ* group is not found in rice and *Brachypodium* but is found in barley, wheat, sorghum and maize [29].

#### 1.4. XYLOGLUCAN

Once the polysaccharides of the matrix are secreted, they form a cell wall structure that is robust and expansible with newly synthesized cellulosic microfibrils and wall polymers that was already existing in the cell wall. Since the interactions between the polysaccharides are thought to be formed by enzymatic reactions and physico-chemical effects, the expansion of the cell wall has not been fully resolved [23].

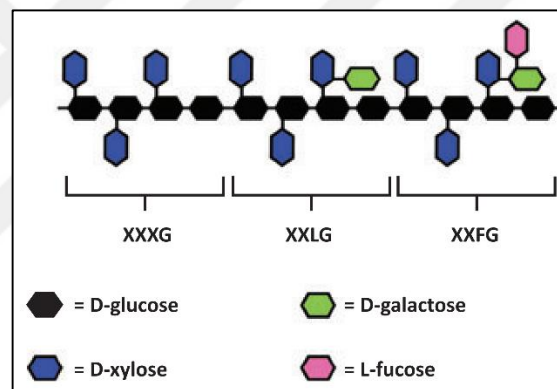


Figure 1.6. Representation of *Arabidopsis* xyloglucan [3].

Xyloglucan (XyG) is a hemicellulose that is very abundant in the primary cell wall and it has highly branched 1,4-β-linked glucan backbone with 1-6-α-xylosyl residues. The amount of the xyloglucan can vary between the species. Flowering plants have around 25% in primary cell wall whereas, grasses less than 2% [31]. It is known that XyGs are involved in the growth of cells because they link to cellulose via hydrogen bonds to microfibrils in the cell wall [32,33]. In addition to the primary cell wall, XyG is found in a form that is thick, non-lignified in the secondary cell wall of some species of the cotyledons or endosperms of seeds [31].

Galactosyl and fructosyl-galactosyl groups are added to some of the xylose in dicotyledons while monocotyledons have less xylosyl residues [34,35]. Moreover, the 1,4-β-glucan

backbone provides rigidity of the cell between microfibrils, xyloglucan also plays a role in both cell viability and cell degradation [36].

XyGs have  $\alpha$ -Xyl residues bound to glucose from O-6 side. The sidechains of XyG with xylosyl residues creates different structures and a diversity of nomenclature [37]. It was started to be described as a single letter nomenclature according to the sidechains of XyGs [38] (Figure 1.7).

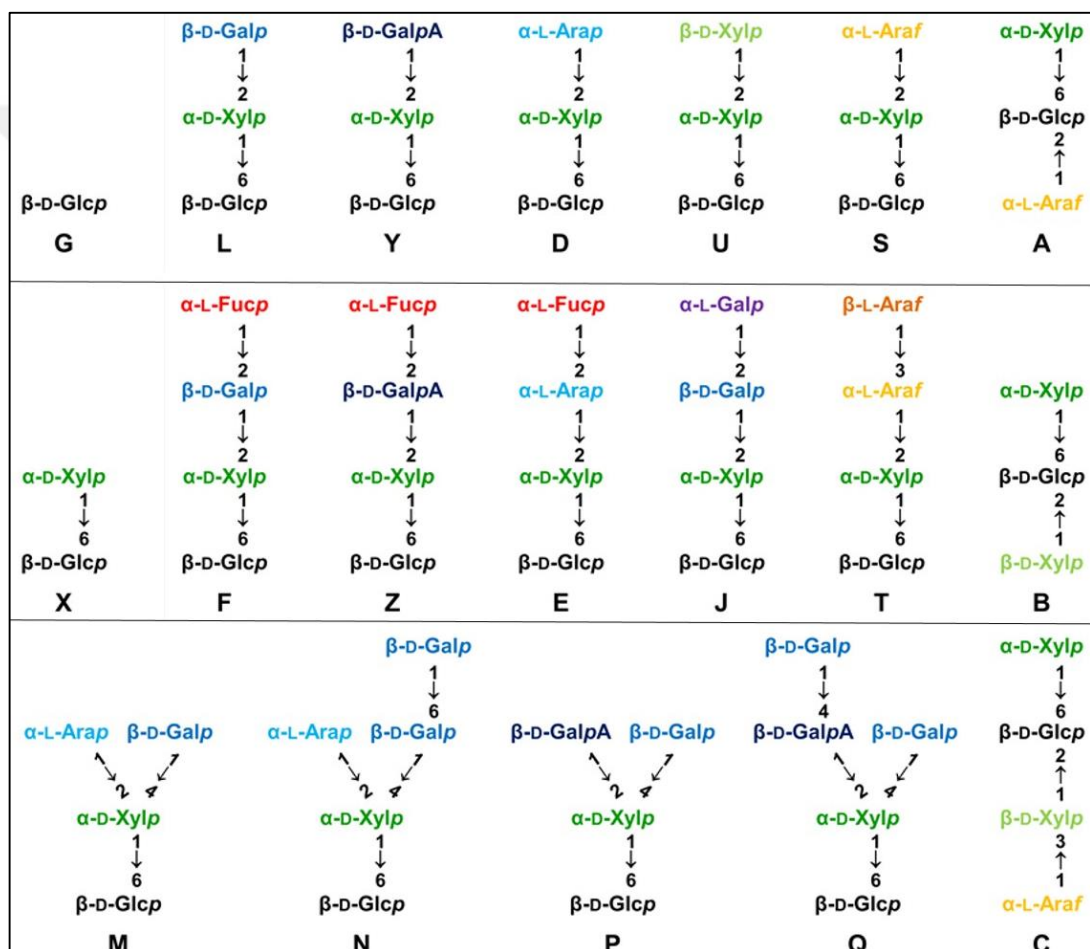


Figure 1.7. Nomenclatures and chemical structures of Xyloglucan side chain compositions.  $\beta$ -(1,4)-glucosyl backbones are represented as black, numbers are showing the hydroxyl group of the sugar that is bound to the carbon of the other sugar and arrows show the direction of the glycosidic bonds [39].



The xyloglucan sidechains are usually started with  $\alpha$ -D-Xylp residues, these residues have their own sidechains that can grow up to 4 glycosyl residues long. Up to now, 19 XyG sidechains have been identified (Figure 1.7). Only a small subset of these XyG sidechains is observed in any one species. XyG side chains are named with single letters, for example, the glucosyl backbone is named with the letter G if there is no substitution and if a xylosyl unit is added to the glucosyl backbone from O-6 than it named as X. When the xylosyl residue is further substituted such as in  $\beta$ -D-Galp-(1,2)- $\alpha$ -D-Xylp it is named as L, whereas  $\alpha$ -L-Fucp-(1,2)- $\beta$ -D-Galp-(1,2)- $\alpha$ -D-Xylp substitution will give the name F to the side chain [39].

D-galactose, D-xylose, D-galacturonic acid, L-arabinopyranose, L-fucose, L-arabinofuranose and L-galactose are also present as glycosyl units in the sidechains. Sidechains can be grouped according to their similarities. D, L, S, Y and U motifs can be grouped since they are similar except their type of glycosyl group that is linked to the xylosyl from O-2 position. Other group can be grouped together as F, E, J and Z motifs because of their  $\alpha$ -(1,2)-L-fucosyl residues. Generally eudicotyledons and gymnosperms have these 3 side chains with unbranched glycosyl backbone [40].

XyG subunits show differences both between species and their cell types. It can be observed that a lot of the vascular plants produce a repeat unit of XXXG in their XyG, while grasses synthesize XXGGG with lower amount of xylosyl attached to the glucan backbone [41,42]. Generally the XXXG kind of XyG contains XXXG, XXLG, XXFG and XLFG subunits based on the developmental stage and the plant types [43]. Equisetum and Selaginella type of plants have  $\alpha$ -l-Ara linked Fuc type of XyG from the O-2 [37]. It was observed that Gal residues of XyG from *Arabidopsis* and sycamore can have acetyl groups in XXLG, XXFG and XLFG [44].

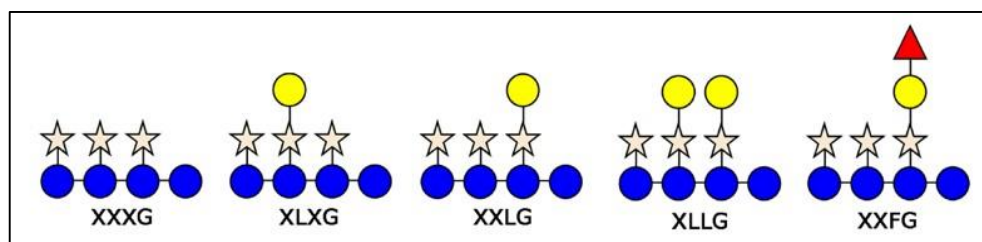


Figure 1.8. Representation of the xyloglucan with different oligosaccharide units; XXXG, XLXG, XXLG, XLLG and XXFG. (Glucosyl units are represented by blue circles, xylosyl

units are represented by orange stars, galactoses are represented by yellow circles, fucose is represented by red triangle [45].

XyG sidechains that are oriented to create different oligosaccharide motifs can be observed by digesting them by endoglucanases and cleaving the glucosyl units [46]. Cleaved oligosaccharides from XyG of *Arabidopsis* and other dicot species give the XXXG motif and this motif have xylosylated glucosyl and an unsubstituted glucosyl unit [43]. Plants in the Poaceae family such as rice (*Oryza sativa*) and barley (*Hordeum vulgare*) have the XXGG<sub>n</sub> motif with decreasing degree of xylosylated XyG backbone, which n is generally from 1 to 3 [42,47].

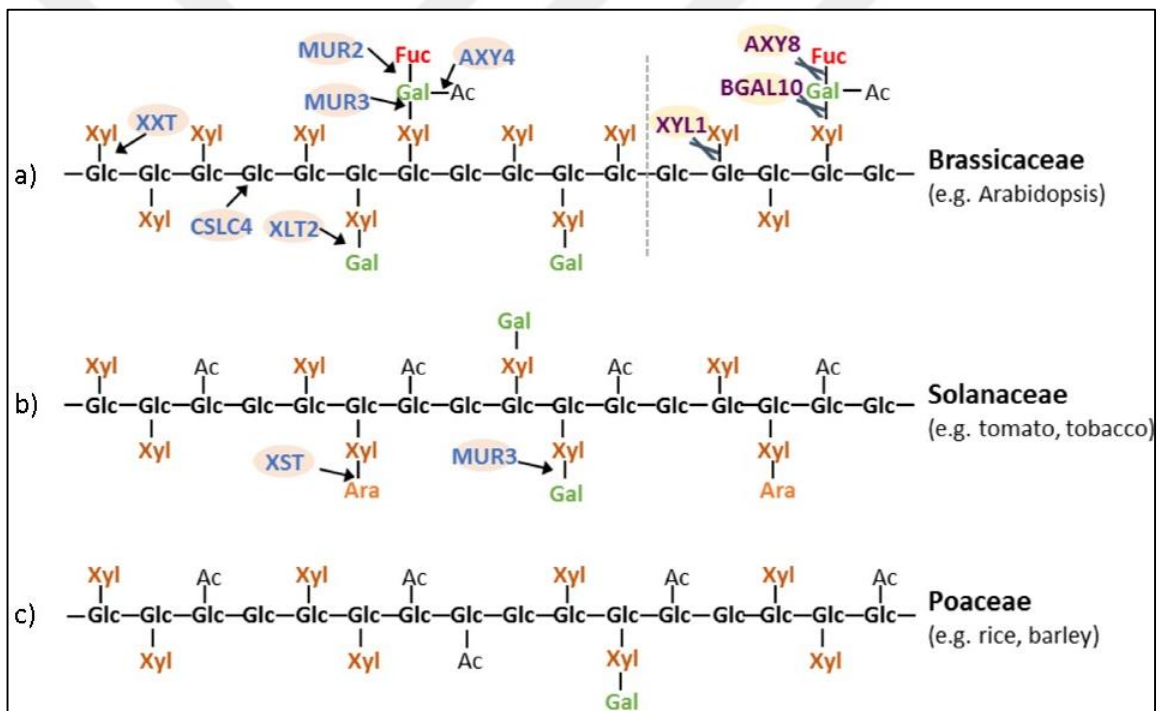


Figure 1.9. Structures of the different XyG from different plant species such as *Arabidopsis*, *Solanum lycopersicum* (tomato), *Nicotiana tabacum* (tobacco), *Oryza sativa* (rice), *Hordeum vulgare* (barley) [40].

The non-covalent links between the XyG and the cellulose microfibrils has been associated with the expansion and prevention of self-linkage of the microfibrils in the primary cell wall [48]. A glucan synthase is needed for XyG biosynthesis for the formation of the glucan backbone, and this is thought to be carried out by one or more members of the CslC synthase

clade [49]. In addition, glycosyl transferases are necessary in order to add other units to glucan chain to obtain different kinds of XyG side chains. Different and specific types of glycosyl transferases are required since each linkage thought to be made by an individual transferase. Thus, more than one transferase couples are needed to obtain subunits. For example in order to achieve XLFG subunit, three (1,6)- $\alpha$ -xylosyltransferases, two (1,2)- $\beta$ -galactosyltransferases, one (1,2)- $\alpha$ -fucosyltransferase and at least one (1,4)- $\beta$ -glucan synthase should be used [49].

### 1.5. MIXED-LINKED B-GLUCANS

The Poaceae family of the Poales, which contains the cereals and grasses, is a part of the commelinid monocots and this group of plants have (1;3,1;4)- $\beta$ -D-glucan, also known as mixed-linked glucan (MLG) in their cell wall [50]. A typical MLG form of a Poalean can be demonstrated like; “...G3G4G4G3G4G4G4G3G4G4G3G4G4G3G...” where  $\beta$ -D-glucopyranose abbreviated as “G”, (1 $\rightarrow$ 3) and (1 $\rightarrow$ 4) bonds are represented as “3” and “4”. Underlined parts of MLG shows the cello-oligosaccharide units [51].

MLG is a homopolysaccharide which is formed from linkages of (1,3) and (1,4) bonds to  $\beta$ -D-glucopyranose units [52]. MLG has an important role in the Poaceae in building the cell wall structure and cell wall growth, and is also involved in polysaccharide storage in the endosperm.

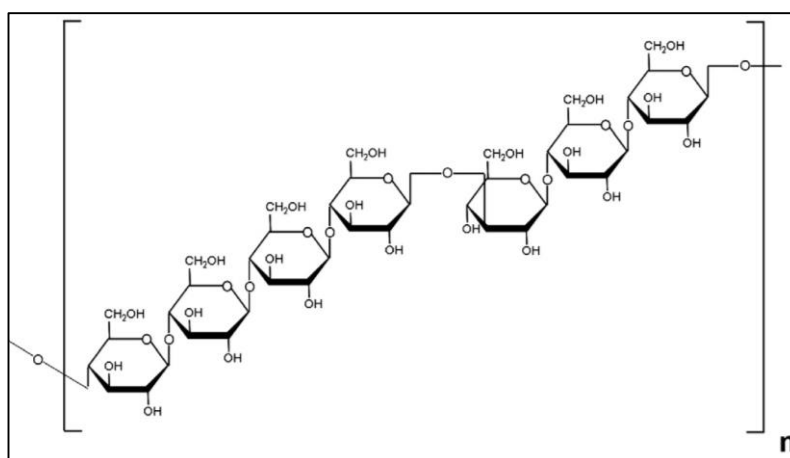


Figure 1.10. Structure of mixed linked (1;3,1;4)-  $\beta$ -D-glucan [53].

Research has been focused on MLG since it has health benefits considering the dietary fiber inside of MLG and economic value [54,55]. It was observed that MLG is not present in the meristematic cells of the Poaceae cell walls until the elongation starts. The MLG is started to be synthesized with the elongation and hydrolyzed with the decreased level of elongation of non-growing cells [41,56]. The presence of MLG on the cell wall of Poales is thought to be an important development in the variety of plants and in the evolution of plants [2,57,58]. Researchers are also interested in the possibility of the presence of MLG in other land plants and with an unexpected discovery that concluded that MLG is also present in the cell wall of *Equisetum arvense* (horse tail) [59].

There is an enzyme called lichenase which is an MLG-specific endoglucanase, and hydrolyses MLG from (1,3) and (1,4) bonds. As a result of this reaction oligosaccharides are released such as trisaccharides and tetrasaccharides. The flexibility and solubility of MLG comes from the (1;3) bonds whereas insolubility and rigidity arises from extended regions of (1;4) linkages [60,61].

## 1.6. XYLAN

Xylan is a polysaccharide that mainly consists of linear chains of  $\beta$ -1,4-linked xylosyl units and it is found in both primary and secondary cell walls, cross-linking hemicelluloses [62]. Xylan constitutes 20% of the primary cell wall [63]. In general, unlike xylan in dicots, xylan in grass plants can cross-link lignin with ferulic acid and substitute from O-2 in the side chains of arabinosyl units [63].

Some of the xylan synthase genes in grasses that have been found through studies belong to the Glycosyl Transferase Families; GT43, GT47 and GT61. Glycosyltransferases and acyl-CoA transferases with these genes are involved in the synthesis of xylan in grasses [65,66]. One of the genes that is a member of rice and wheat is a member of GT61 and is responsible from the addition of arabinosyl residues to the xylan backbone. The other genes that from rice group is found to substitute xylosyl to arabinosyl from O-2 side in xylan [67].

Xylan with an attached arabinose residue to its backbone is called arabinoxylans and glucuronoarabinoxylans (GAXs). Despite the fact that the cereal endosperm arabinoxylans

contain very little glucuronic acid, there is a tendency to have more glucuronic acid and 4-O-methyl glucuronosyl residues of the heteroxylans in the vegetative parts of the grass which make GAX a more suitable name although they are generally called arabinoxylans [63].

Xylan is a polymer that has begun to gain attention with the understanding that it is an important source for biofuel production. The investigation of cell wall biosynthesis is important for understanding and facilitating biofuel production. Xylan, the building material of the secondary cell wall, makes fermentation difficult because it is formed from pentose sugars, which require different enzymes and/or microorganisms to degrade them. Manipulating xylan biosynthesis may facilitate digestion of other cell wall polymers and understanding of cellulose-producing enzymes [68,69].

### 1.7. MANNAN

Mannan is another polysaccharide that is present in the hemicelluloses groups of the plant species [4]. Heteromannans are grouped as mannans, glucomannans, galactomannans and galactoglucomannans. Mannan and galactomannans have 1,4- $\beta$  linked mannose backbone while glucomannan and galactoglucomannan are 1,4- $\beta$  linked heteropolymers that contain mannosyl and glucosyl residues in their backbones. Galactomannan and galactoglucomannan may contain mannosyl residues that are linked with  $\alpha$ -1,6-linked galactosyl residues [63]. Also, the mannose backbone can be acetylated at their O-2 and O-3 sites [70]. When the substitution of the backbone of the mannan increases, the solubility of the polymer also increases [71,72].

Mannan polysaccharides are used in many plants and algae for structural and storage purposes especially in seeds [73,74]. Different tissues and cells of *Arabidopsis* contain mannan polysaccharides but still studies must be performed in order to understand its purpose in the cell wall [75,76]. Mannan can be found very commonly in land plants, also in mosses and lycophytes [77].

Despite the role in seed storage of galactomannan, the function of the mannans are not exactly known. The deletion of the synthase genes of glucomannan in *Arabidopsis* created a plant without any glucomannan in its cell walls, however there was no clear phenotype observed [78].

## 1.8. PECTIN

Pectins are complex heterogeneous polysaccharides that are in the cell walls. Dicot plants and non-graminaceous monocots have approximately 35% pectins in their primary cell walls. Grass plants consist of pectin between 2-10% in their primary cell walls and 5% in the woody tissues [79]. Pectin can also be dissolved in aqueous buffers, acidic or calcium chelators [12].

Pectic polysaccharides can be found in various places in plants, such as; dividing and growing cells, the soft parts of the plant cells and middle lamella. Pectin is also found in the secondary cell wall between xylem and woody fibers in the tissue. Pectin is present in cell walls of all higher plant and gymnosperms, pteridophytes, bryophytes and the Chara [80].

It has been suggested that the increase in RG-II pectin in vascular plants throughout evolution is related to an important role of pectin in primary and secondary cell wall structure and is related to the upright posture of the plant [81]. A thorough understanding of pectin structure and synthesis is essential for potentially modifying wall structure, and will be important to ensure the production of plants that can be fully decomposed from lignocellulosic biomass for biofuel production [82,83].

Some of the studies indicate that pectin has many roles in the cell wall such as growth, development, defense, structure, wall porosity, hydration of the seeds etc. [83]. It has also been used in industry as a stabilizing agent for food and cosmetics, also it has been used in pharmaceutical studies, used for lowering cholesterol, and even in reducing cancer [84].

## 1.9. XYLOGLUCAN ENDOTRANSGLYCOSYLASE/HYDROLASE (XTH) ENZYMES

Endotransglycosylases are enzymes that are involved in integrating newly released matrix polysaccharides into the cell wall, by cutting and re-linking glucans [85–87]. The xyloglucan endotransglucosylase (XET) from such enzymes cuts the xyloglucan backbone and re-links the free end of another cut xyloglucan with glycosidic bonds. Some of the XTH enzymes also have hydrolase activity and are called xyloglucan hydrolase (XEH) enzymes.

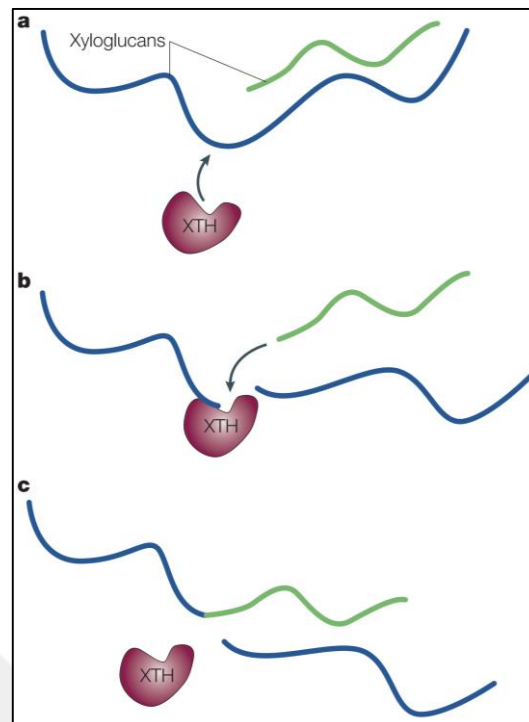


Figure 1. 11. Representation of xyloglucan endotransglucosylase/hydrolase (XTH) activity. a) XTH bind the one of the xyloglucan chain (blue). b) XTH cuts xyloglucan chain while still attached to catalytic side. Other xyloglucan chain (green) is ready to bind and perform of second reaction. c) Two of the xyloglucan molecules ligated and xyloglucan fragment is released [12].

According to molecular modeling studies of some of the XTH family members, it was assumed that they can also use hemicelluloses other than xyloglucan, such as arabinoxylan and (1,3;1,4)- $\beta$ -D-glucan. This hetero-transglycosylase ability has been demonstrated with a number of different XTH enzymes from both semi-purified, purified, and heterologously expressed enzymes [47,88,89]. XTH is involved in many tasks in the cell wall. It has been indicated that XTH acts in a wall adaptation of new xyloglucans, in the expansion of the cell wall strengthening and loosening, softening of fruits, detaching of xyloglucans from cellulose surface [33,90–94]. Studies have shown that there is an characterized endotransglycosylase enzyme that targets mannan, and it is also presumed there are other endotransglycosylases for xylan and other polysaccharides that have not been discovered [12].

XTHs cleave the xyloglucan backbone and use it as a substrate while attaching it from reducing end to another xyloglucan chain from the non-reducing end (Figure 1.11) [95].

XTH are proteins that have a highly conserved active site motif determined as DEIDFEFLG or DEIDIEFLG and their optimum pH is between 5 and 6 [33]. XETs have been classified in the Carbohydrate Active Enzymes (CAZymes) which links saccharides with glycosidic bonds and XTHs can be classified in the Glycosyl Hydrolase 16 (GH16) family of the CAZy group [96]. Glycosyltransferases, carbohydrate esterases polysaccharide, lyases and carbohydrate-binding modules are other groups that belong to the CAZy classification beside glycoside hydrolases (GH) [97,98].

GH16 family which is encoded by the XTH gene is the only family has shown the endolytic activity specific to xyloglucan in plants (Rose et al., 2002). As in other GH16 enzymes, genes in the XTH subfamily benefit from the mechanism of glycosyl transfer displacement and retention (Figure 1. 12) [99].

Covalent saccharide enzyme and oxocarbenium-ion-like intermediates are considered to be the used for catalytic mechanism of XETs and retaining  $\beta$ -glycosyl hydrolases. These intermediates have short lives in the reaction and they have been hydrolyzed by water molecule. In the first step of the reaction an acid residue is involved for activation of water molecule. However, it is believed that XETs postpone the hydrolysis reaction till the acceptor oligosaccharide complete the diffusion from the active fragment and finish transglycosylation [100].

The first 3D structure of XTH was modeled based on the *Populus tremula x tremuloides* XET16A (PttXET16A) (Figure 1.13). PttXET16A has  $\beta$ -jelly roll structure and it have substrate binding site that suitable for highly branched xyloglucans. It have conserved active site in GH16 even though it varies during the reaction. There are two antiparallel  $\beta$ -sheets with aromatic residues. Since PttXET16A is a model XTH, it has almost the same features with the other XTH members in GH16 family. PttXET16A also folded by C-terminal  $\alpha$ -helix followed by  $\beta$ -strand that appears in every XET-like molecules. The substrate binding site is conducted by many loops and  $\beta$ -turns as well as upper  $\beta$ -strands. There is a connection between the  $\beta$ -13 and  $\beta$ -14 strands that results a narrowing the width around 10 Å. Because of this cleft the acceptor binding site of the PttXET16A is more open from the 1,3-1,4  $\beta$ -glucanases but closer than k-carrageenases and the  $\beta$ -agarases [101].



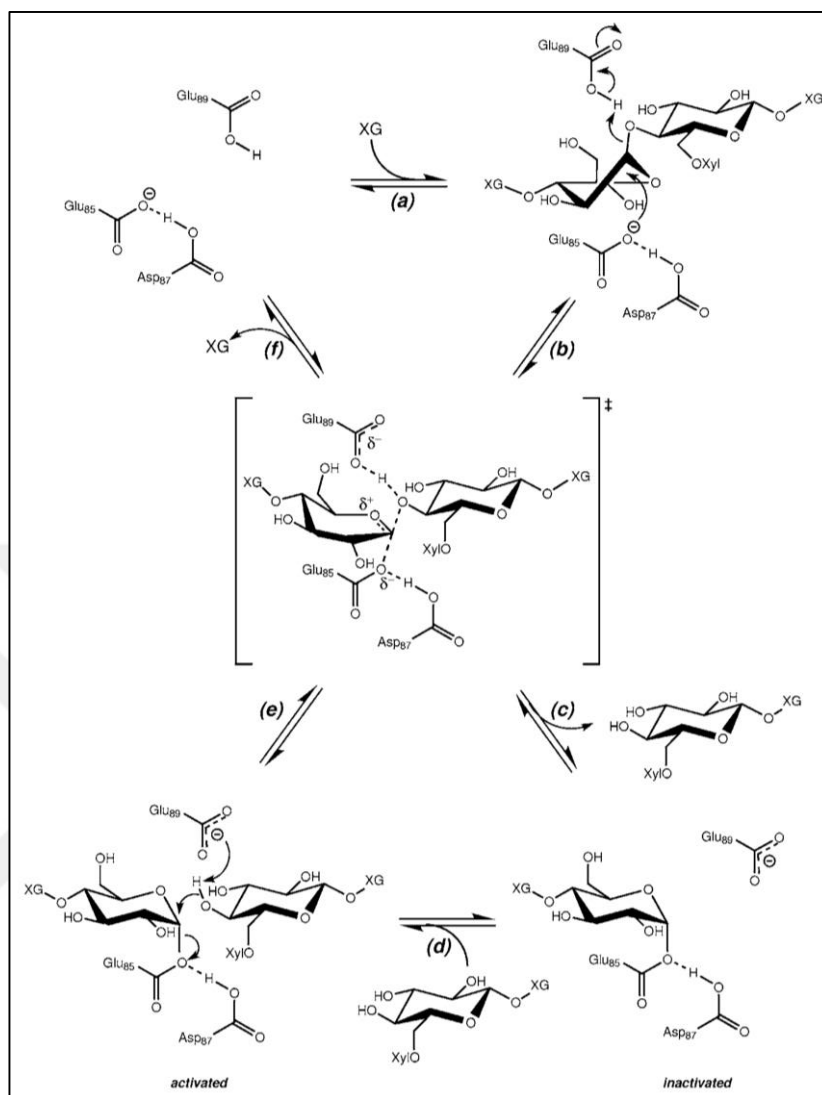


Figure 1.12. Chemical mechanism of the glycosyl transfer reaction by hydrolysis and transglycosylation [101].

The native XTH PtXET16A has amino acid sequence such as; “XETA AFAALRKPVDVAFGRNYVPTWAFDHIKYFNGGNEIQLHLDKYTGTFQSK GSYLFGHFMSQMKLVPGDSAGTVTAFYLSSQNSEH**DEIDFEFLGN**RRTGQPYILQTNVFTGGKGDREQRIYLWFDPTKEFHYSVLWNMYMIVFLVDDVPIRVFKNCKDLGVKFPFNQPMKIYSSLWNADDWATRGGLEKTDWSKAPFIASYRSFHIDGCEASVEAKFCATQGARWWDQKEFQDLDAFQYRRLSWVRQKYTIYNYCTDRSRYPSPMPPECKRDRDI” with the active site motif indicated as bold [102].

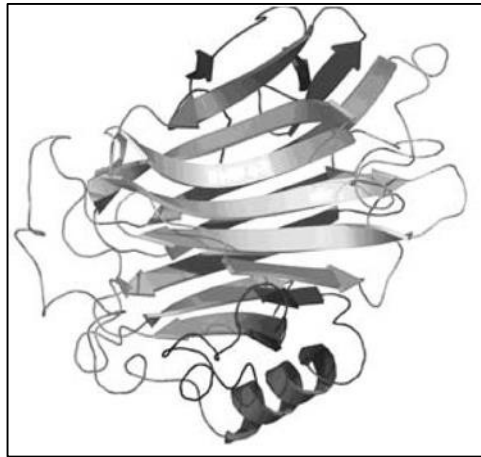


Figure 1.13. Structure of PttXET16A [101].

Cell wall elongation can be accomplished with the modifications of matrix polysaccharides. It can be increased or stopped based on the integration of the polymers. Cell extension can be done by binding newly synthesized xyloglucan and cellulose together with hydrogen bonds to the plasma membrane and microfibrils are joined with the xyloglucan chains. Another way of the cell wall modification for this purpose is endotransglycosylation of xyloglucan from the 4<sup>th</sup> glucose of 1,4- $\beta$ -linked backbone by an XTH enzyme (Figure 1.14) [103].

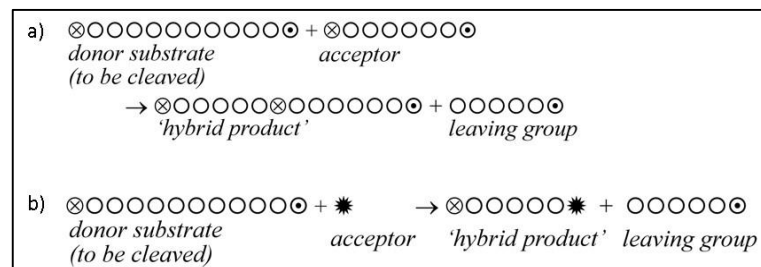


Figure 1.14. Representation of xyloglucan endotransglucosylase activity (empty circle; xyloglucan oligosaccharide, circle with dot; reducing sugar). a) Endotransglucosylation reaction between two xyloglucans. b) Endotransglucosylation reaction between xyloglucan and a xyloglucan oligosaccharide [33].

It is hard to decide whether an XTH enzyme may have hydrolysis activity as a member of the xyloglucan endohydrolase (XEH) family or transglycosylation activity as a member of the xyloglucan endotransglycosylases (XET). Nevertheless, transglycosylation can be

determined through the use of fluorescently labeled xyloglucan oligosaccharides in an activity assay [104]. In order to detect hydrolysis activity for XEH, water is used instead of oligosaccharides as an acceptor, and an appropriate assay used such as viscometry. Some of the XTH enzymes have only hydrolysis activity, while others may show hydrolase activity only when there is a lack of acceptor molecules [33,105].

Xyloglucan is commonly used donor among the XTHs but the exact donor preference of them is unclear since xyloglucan structure and molecular weight can change between plants and even between tissues of the same plant. Also it depends on the function of the XTH enzyme in a specific tissue. Generally xyloglucan oligosaccharides (XGOs) that have Glc<sub>4</sub> with rich xylosyl/glycosyl backbone are preferred by the XET enzymes [85,106]. The molecular weight of the donors can also be the deciding factor for XTHs and it can affect the reaction rate. Furthermore, the non-reducing end of the donor can be used as an acceptor instead of the labeled acceptor. In order to prevent these misleading situations, acceptor concentrations must not be low [33].

XTHs are involved in cell extension and they were detected in the elongated root parts of *Arabidopsis* and tobacco with the help of fluorescently labeled XGOs [107]. When cell division and expansion occurs, parts that perform cell division were showed higher *XTH* gene expressions or activity levels such as; root of formation aerenchyma, mesophyll air space, abscission zones and vascular tissues [91,108,109]. However, there are some exceptions indicates that XTH is not always have a role in the growth. One of the studies showed that *LeXTH2* gene from the tomato have been expressed in the non-elongating parts [110].

Almost 2000 genes are estimated that involves in synthesizing, modifying, or degrading cell wall molecules, which constitutes 10% of the overall genes of *Arabidopsis*. Characterization and the identifying the functions of these genes will provide the knowledge about the plant cell wall biosynthesis [111]. These various XTH enzymes have isoenzymes that may indicate us XTH enzymes can have lots of activities that is not discovered yet [96]. There are 33 *XTH* genes in *Arabidopsis thaliana* and these genes express different functions in different stage of the developmental stage and tissues [104]. For example *AtXTH5*, *AtXTH12*, *AtXTH13*, *AtXTH14*, *AtXTH17*, *AtXTH18*, *AtXTH19*, *AtXTH20*, *AtXTH26* and *AtXTH31* genes expressed in roots and *AtXTH3*, *AtXTH17*, *AtXTH22* and *AtXTH23* genes are expressed in higher levels when it was treated with auxin and brassinolide. However when *Arabidopsis*

was treated only with auxin, *AtXTH19* gene expression was upregulated whereas *AtXTH15* and *AtXTH21* genes were down-regulated. Additionally when *Arabidopsis* was treated only with brassinolide *AtXTH4* and *AtXTH5* genes were upregulated [112]. More than 29 *XTH* genes were found in rice (*Oryza sativa*), 41 genes were identified in poplar (*Populus trichocarpa*) and 25 of the *XTH* genes were found in tomato (*Solanum lycopersicum*) [113–115].

It has been known that monocot plants have as almost 1-5% of xyloglucan in their primary cell wall where dicot plants have nearly 20-25%. Even though monocots have less amounts of xyloglucan, the large *XTH* families of monocots raises the suspicion about the usage of a substrate beside the xyloglucan by *XTH* enzyme. Therefore, molecular modeling and characterization of the *XTH* must be performed in order to clarify the roles of genes in the various plants [29].

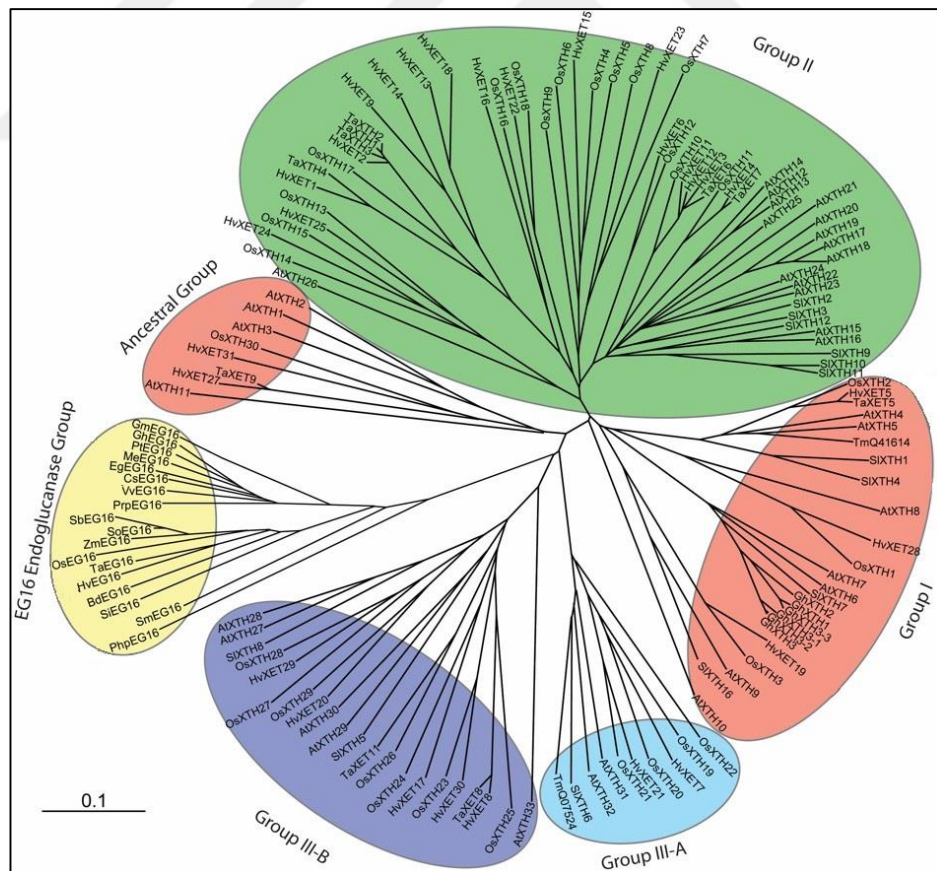


Figure 1.15. Phylogenetic tree of XTH enzymes according to their on amino acid sequences.

gi GhEG16 GhEG16	-----MADP-AL-----HHQ--IQPIKEI---AIDYTP EACTHCPV	30
gi HvEG16 HvEG16	-----MASERDQH---EHLRPDG---TEPLARI---AVDYTPDACRHAPE	36
gi OsEG16 OsEG16	MASESE--C---VAVAEPPHMH---VHLHPDG---TEPLAHI---AVDYCP EACHHASE	45
gi OsXTH30 OsXTH30	MVFQVQPPWLLLLLHLIAIAVLLLVAVDSVPPAPAPPVAVTFDDNYVATYGGDGYHLVNQ	60
gi BdXTH2 BdXTH2	MAASNVPWLLLLLILLPAALV---SPQATAAAPQPTPAFDENYVPSYGDGYHLVDM	56
gi GhEG16 GhEG16	SNSITLTFDHRGGARWRSTTRFLYGT-FTSLIQCPKGNTSGLNFNILYSSLEG--DKSQD	87
gi HvEG16 HvEG16	SGEIHVYDDRGGARWRSRFLPGGAVAAAVRAPAGDTTGLNLYLSSLEG--SGDND	94
gi OsEG16 OsEG16	DGEIHVYDDRGGARWRSRFLPGGAVAAATIRAPAGDTAGLNLYLSSLEG--SRDND	103
gi OsXTH30 OsXTH30	GTQISLTLDKSSGAGFRSKLMYGSGF-FHMRIVKVPAGYTAGVVTAYLAS EPDNDV--QD	117
gi BdXTH2 BdXTH2	GTEIRLTLDRRNGAGFVSKLRF GSGF-FHMRIVKPSGYTAGVVTAFY LASDSS--APDRD	113
gi GhEG16 GhEG16	EIDFEFLGKD---KTIVQTNYYTTGTGNREQIHDLGDFDCSDGFHEYTIKWNPDSEI EWID	144
gi HvEG16 HvEG16	EIDFEFLGND---KRAVQTNFFVAGSGGREAVHELPF DSSDGFHHYAVAWDAEAI EWRVD	151
gi OsEG16 OsEG16	EIDFEFLGHD---KCAVQTNFHVAGGGGREQIHVLPFDSSDGFHHYAIAMGADAI EWRID	160
gi OsXTH30 OsXTH30	EVDFEFLGDKDGNPITLQTNVFGHGDRERLRLWFDP AADFHDYSILWNPFFHLVIFVD	177
gi BdXTH2 BdXTH2	EVDFEFLGNVDGKPI TLQTNVFNHGHDREQLRLS LWFDP AADFHDYRILWNCFQIVL FVD	173
gi GhEG16 GhEG16	GKVVKA EKK E---GEAFPEK-PMFLYASVNDASYIAEGQWTGPYIGCDVPYVCLYKDI	199
gi HvEG16 HvEG16	GEVLRREERD---GEEPWPEK-PMFLYASFWDASGVDEGRWGTGTYHGRDAPYVCSYRDV	207
gi OsEG16 OsEG16	GELIRREERVA---GEPWPEK-PMFLYASVNDASHINDGKWTGTYHGRDAPYVCSYRDI	215
gi OsXTH30 OsXTH30	ETPVRVLKNLTSRGP EFFEPAK-PMRPRGSVNDASDNATDGGRTKVDWARAPFTA AAFQGF	236
gi BdXTH2 BdXTH2	ETPVRVLRNLTGSVPDYEFPEK-QMVVQGSVNDGSDNATDGGRTKVDW SRGPFAAEFRGF	232
gi GhEG16 GhEG16	QVPVSTAVECSCDS-----	213
gi HvEG16 HvEG16	RVPVALSTEEEEECQD---DAD-----AGDEADAAGAAEEEEEMDAGDG	250
gi OsEG16 OsEG16	RVPLALSL EDEEDPYKCACVGDASAATAAADAAEQVDAGDAPA-AAAAADAAEEVDAGDA	274
gi OsXTH30 OsXTH30	AVDACAAAA-----GGGVSSDDCGSPD---TMMINGGEYRRLTAAQQAAAYDVRG-N-	284
gi BdXTH2 BdXTH2	DVAGCANTS-----STPC---DSQSSP---GMMINGGGYRSLSAEQHAAYENVRN-KY	278
gi GhEG16 GhEG16	-----	213
gi HvEG16 HvEG16	ED-----	252
gi OsEG16 OsEG16	PAATAAADVAEQVDAGDVPASAAAADAVKEVDAGAGKD	312
gi OsXTH30 OsXTH30	LTYDYCTD-NSKKRP-VPPPECSFT-----	307
gi BdXTH2 BdXTH2	MNYDYCTD-KGRFKN-KLPAECSYA-----	301

Figure 1. 16 The amino acid sequence comparison of the XTH enzymes from ancestral group and EG16 group members. In the second and third paragraphs the "DEI/VDFEFLG" motif indicated by the boxes is the preserved catalytic domain.

XTH enzymes can be grouped in 4 different subfamily according their amino acid sequences named as; Group I, Group II, Group III and Ancestral Group [33,112] (Figure 1.15). The biochemical mechanisms or preferences of the XTH enzymes are not different between the groups but Group I and Group II generally have XET activity and Group III have XEH activity [33]. The genes that are the members of ancestral groups such as *OsXTH30* (*Oryza sativa*) and *BdXTH2* (*Brachypodium distachyon*) and from the EG16 group *OsXTH31* and *HvEG16* (*Hordeum vulgare*) can compared in order to observe their similarities and differences among each other (Figure.1.16). When various genes from both groups is observed the conserved active site motif can visualized in every amino acid sequences of the enzymes.

It has been observed that *Equisetum* has an endotransglucosylase enzyme activity (MLG:xyloglucan endotransglucosylase; MXE) that resembles a xyloglucan endotransglucosylase (XET) which uses xyloglucan as acceptor substrates and MLG as a donor substrate in its reactions. Poalean MLG and *Equisetum* MLG may not have the same purposes in their cells according to the studies. MLG ratios increases by ageing in *Equisetum* tissues while MLG has been found more in poalean during the early stages of young tissues [49].

### 1.10. POLYSACCHARIDE AND OLIGOSACCHARIDE SUBSTRATES

There are structural differences between the polysaccharides that are used as donor substrates. Barley  $\beta$ -glucan (BBG) is comprised of  $\beta$ -1,3- and  $\beta$ -1,4-linked D-glucosyl residues. Hydroxyethyl cellulose (HEC) have  $-\text{OCH}_2\text{CH}_2$  groups linked to glucose that normally cellulose does not contain. This provides HEC molecule to become soluble unlike cellulose which is insoluble, but it restrict the hydrogen bonding. Tamarind seed xyloglucan (TXG) is consist of of  $\beta$ -D-(1.4) linked glucosyl units with the attachment of  $\alpha$ -1,6-xylosyl to glycosyl backbone and  $\beta$ -1,2-galactosyl units attached to xylosyl residues (Figure 1.17).

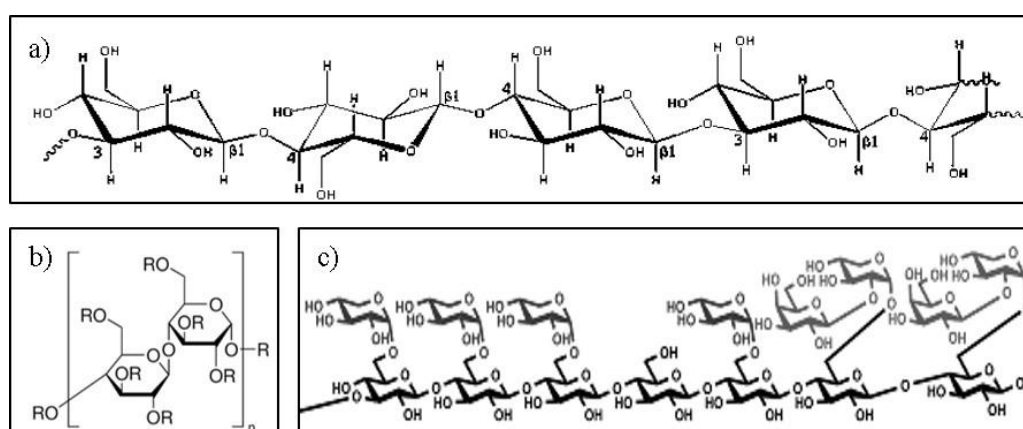


Figure 1.17. Representation of some of the main polysaccharides that are used as donors.

a) BBG, b) HEC, c) TXG

Oligosaccharides also shows differences based on their glycosidic bonds in their structure. The backbone of Xyloglucan oligosaccharides (XGO) composed of  $\beta$ -D-glucosyl residues linked by  $\beta$ -1-4 linkages.

1,3:1,4- $\beta$ -glucotetraose A (BA) has  $\beta$ -1,3-,  $\beta$ -1,4-,  $\beta$ -1,4 linkages between glycosyl residues, where 1,3:1,4- $\beta$ -glucotetraose B (BB) has  $\beta$ -1,4-,  $\beta$ -1,4-,  $\beta$ -1,3- and 1,3:1,4- $\beta$ -glucotetraose C (BC) consists of  $\beta$ -1,4-,  $\beta$ -1,3- and  $\beta$ -1,4- residues. All of the 1,3:1,4- $\beta$ -glucotetraoses have 4 of glycosyl residues.

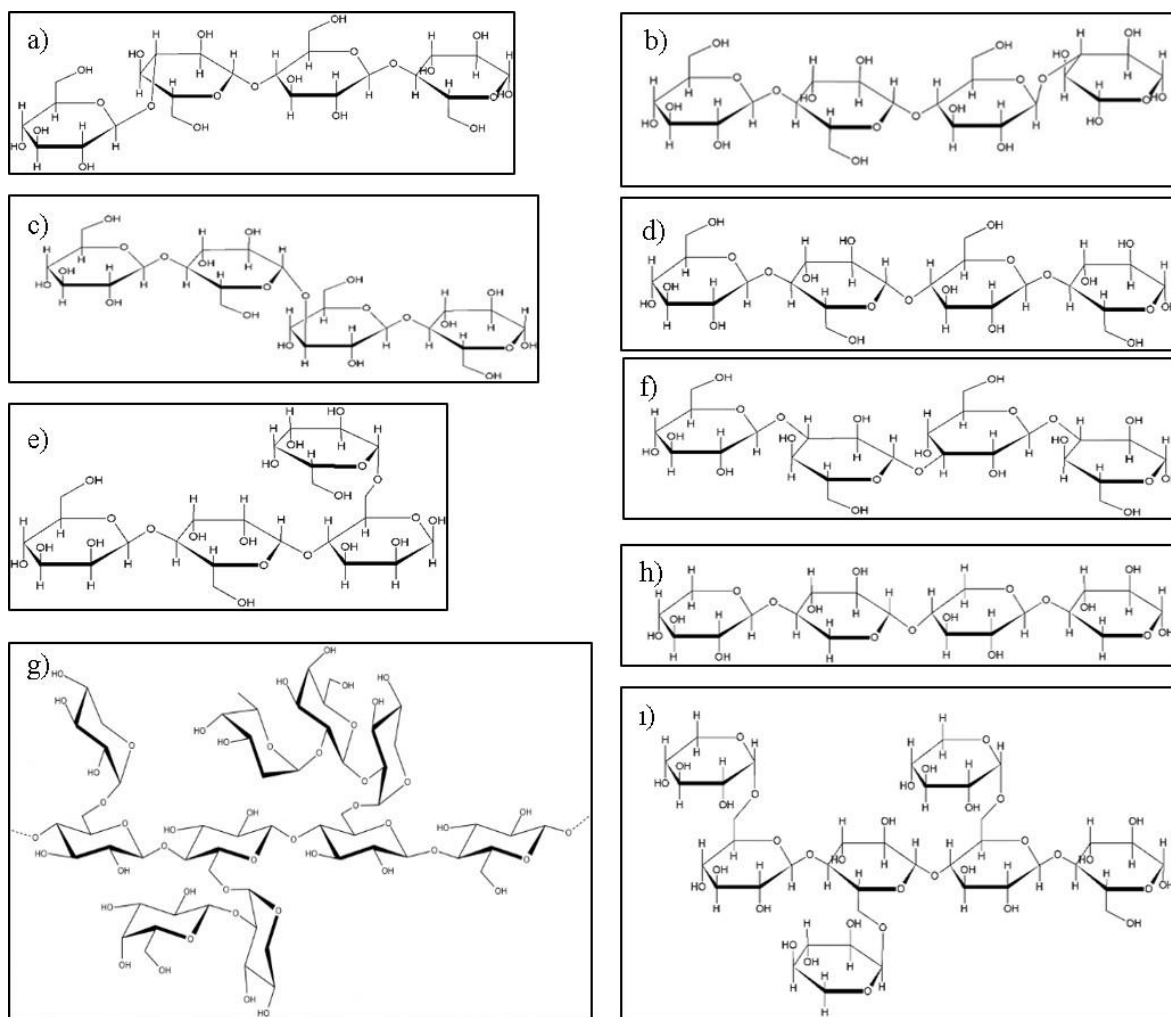


Figure 1.18. Oligosaccharides that are used as acceptor substrates. a) BA, b) BB, c) BC, d) CT, e) GM, f) LT, g) XGO, h) XT, i) X7.

1,4- $\beta$ -cellotetraose (CT) is made of  $\beta$ -1,4-linked glycosyl residues which is used for the representation of cellulose. Galactosyl mannan (GM) is made of 3 mannose residues with  $\beta$ -1,4-linked galactose residues by  $\alpha$ -1,6-linkage. Di-galactosyl mannan

(DGM) has 5 mannose structure that is linked by  $\beta$ -1,4-linkage and there are linkages between the 3<sup>rd</sup> and 4<sup>th</sup> mannose residues and galactose by  $\alpha$ -1,6-linkage.

Laminaritetraose (LT) is formed of 4 glycosyl residues that is linked by  $\beta$ -1,3-linkage. 1,4- $\beta$ -D-xylotetrose (XT) is a representative of xylan and consist of  $\beta$ -1,4-linked xylopyranosyl residues. Xyloglucan heptasaccharides (X7) made of 4 of the glucosyl residues linked by  $\beta$ -(1,4)-linkage.

### 1.11. HETEROLOGOUS EXPRESSION AND THE *PICHELIA PASTORIS* SYSTEM

Plant products in various areas such as; textile, food, pharmaceuticals, detergents, biofuels can be developed by modifying plants by understanding their biosynthesis process, gene family, structure and enzymatic mechanisms [12]. Developing these technologies within a living organism is difficult to sustain and time consuming, therefore *in vivo* and *in vitro* experiments must be performed. Heterologous techniques have been used to identify and manipulate the targeted protein since the recombinant organisms produce and release the functional protein from the cellular machinery [116].

*Pichia pastoris* is one of the yeast species that is commonly used as an expression system. *P. pastoris* is preferable to produce proteins compared to other expression systems since it is a eukaryote, it can manage post-translational modifications such as; glycosylation, phosphorylation, and sulphation. In order to characterize enzymatic proteins, the protein product must be obtained as close to the naturally produced protein as possible. Bacterial strains can also be used for protein expression, but they are not the first choice for glycosylated protein production, although they can be produced in shorter times [117]. *P. pastoris* is a better choice for producing *N*-glycosylated enzymes such as XTHs and previous studies have demonstrated that *P. pastoris* can produce XTH enzyme with the correct folding and formation [118]. Also, *P. pastoris* cells can grow in higher densities compared to mammalian cells and is easier to handle. The basic strategy is inserting the coding region of your gene into the expression vector, introducing the linearized vector into *P. pastoris*, collecting data about the expressed proteins and examining its substrate preferences [116].

Careful selection of the promoters is necessary to obtain larger amount of targeted proteins [117]. AOX1 (Alcohol oxide 1) is a yeast promoter that has many advantages. The protein



transcription of the targeted protein can be regulated while being controlled with the repression or depression system. AOX1 can express large amount of protein even if the protein is toxic to the host. The induction of the protein production can be managed easily by the methanol addition in to the media. AOX1 promoter can repress the protein transcription until the cells can achieve cell growth first and not overexpress the protein production when it is too early [116]. The amount of methanol is also important; it can damage the cell culture if an excess amount of methanol is used and cause a reduction in protein expression. Also, if the protein will be used as a food product, methanol usage may not be proper [119].

AOX1 is preferred since *P. pastoris* can use methanol as a carbon source since it is a methylotrophic organism. Additionally, in this heterologous expression system, proteins can be secreted outside of the cells and can be purified easily without disrupting the cells (Macauley-Patrick et al., 2005).

The main aim of this study is investigation of characterizing different XTH enzymes from various plant species of both the ancestral and EG16 group including; *OsXTH30*, *OsXTH31* from *Oryza sativa*, *BdXTH2* from *Brachypodium distachyon* and *HvEG16* from *Hordeum vulgare* system. The donor and acceptor polysaccharide preferences of these enzymes were examined with activity assays and kinetic studies. Information obtained from heterologous protein expression, purification and enzyme substrate characterization will let us understand the substrate specificities of XTH, evolutionary patterns and the role of the XTH enzyme in the cell wall biosynthesis and modification. Since XTH enzymes play important roles in strengthening and modification in the cell wall, fruit ripening, and resisting abiotic stress, knowledge from this study can lead to further investigations and also help to develop various plant-based areas including biofuel production, paper and textile industries, wood, biotic and abiotic stress resistances, fruit ripening and seed germination.

## 2. MATERIALS

### 2.1. EQUIPMENT AND MATERIALS

Equipment and materials were supplied from several companies according to the Table 2.1.

Table 2.1. List of equipment, materials and company names.

<b>Equipment and Materials</b>	<b>Company</b>
AKTA Primeplus Chromatography System	GE Healthcare Life Sciences, UK
New Brunswick 44/44R Incubator Shaker	Eppendorf Innova, USA
0.2 ml PCR Tubes	ISOLAB, Germany.
1.5 and 2 ml Centrifuge Tubes	ISOLAB, Germany.
1100 Series High-Performance Liquid Chromatography (HPLC)	Agilent Technologies, USA
200 $\mu$ l, and 1000 $\mu$ l Pipette Tips	Axygen Scientific, USA
5424 Microcentrifuge	Eppendorf Innova, USA
Arium Pro Ultrapure Water System	Sartorius, Germany
Avanti J-E High Speed Centrifuge	Beckman Coulter, USA
BioSep-SEC 4000 Column	Phenomenex, USA
ChemiDoc™ XRS+ System	Bio-rad, USA
Dialysis Tubing Cellulose Membrane	Sigma-Aldrich, USA
Drying and Heating Chamber	Binder, Germany
Elite 300 Plus Power Supply	Wealtec, USA
Forma™ 900 Series -86°C Upright Ultra-Low Temperature Freezer	Thermo Fisher Scientific, USA
Gene Pulser	Bio-rad, USA
Heater/Refrigerated Circulator	VWR, USA
HiPrep™ 26/10 Desalting Column	GE Healthcare Life Sciences, UK
His-Trap™ FF 5 ml Column	GE Healthcare Life Sciences, UK
Inoculation Loops	ISOLAB, Germany.

Micropipettes	Eppendorf Innova, USA
Microsart® e.jet Vacuum Laboratory Pump	Sartorius, Germany
Mighty Small II for 8x9Cm Gels	Hofer, USA
Minisart® SRP15 Syringe Filters	Sartorius, Germany
MS-H280-Pro Circular-top LED Digital Hotplate Stirrers	Scilogex, USA
NanoDrop 2000c Ultraviolet–visible (UV-Vis) Spectrophotometer	Thermo Fisher Scientific, USA
Nichel- Nitrioltriacetic Acid (Ni-NTA) Spin Columns	Qiagen, USA
Pechiney Plastic Packaging	Parafilm “M”, USA
Petri dish	ISOLAB, Germany.
Power Source 300V Electrophoresis Power Supply	VWR, USA
Rocking Platform Shaker	VWR, USA
SUB Aqua 12 Plus	Grant, UK
SUB Aqua 26 Plus	Grant, UK
Superdex 75 16/100 Size Exclusion Column	GE Healthcare Life Sciences, UK
T100™ Thermal Cycler	Bio-rad, USA
Trans-Blot Turbo™ Transfer System	Bio-rad, USA
Ultrospec 3000 UV/Visible Spectrophotometer	Pharmacia Biotech, UK
UV Transilluminator	Sigma-Aldrich, USA
Whatman Cellulose Filter Paper	Sigma-Aldrich, USA

## 2.2. CHEMICALS

Chemicals were supplied from several companies according to the Table 2.2.

Table 2.2. List of chemicals and company names.

<b>Chemicals</b>	<b>Company</b>
Amersham™ ECL™ Prime Western Blotting Detection Reagent	GE Healthcare Life Sciences, UK
Maximo Taq DNA Polymerase	GeneOn, Germany
Rb pAb to 6x His-tag	Abcam, UK
1 kb plus DNA ladder	Thermo Fisher Scientific, USA
10X Green Restriction Buffer	Thermo Fisher Scientific, USA
10X Reaction Buffer	GeneOn, Germany
10X Standard Taq Reaction Buffer	New England BioLabs (NEB), UK
2-Propanol, Ammonium di-Hydrogen Phosphate	PanReac AppliChem, Spain
50 bp DNA ladder	Thermo Fisher Scientific, USA
50X Tris-Acetate EDTA (TAE) Buffer	Bio-rad, USA
6X DNA Loading Dye	Thermo Fisher Scientific, USA
Acetic acid 100%	Sigma-Aldrich, USA
Acetone ≥ 99.5%	Sigma-Aldrich, USA
Acrylamide 30%	Sigma-Aldrich, USA
Agar	Sigma-Aldrich, USA
Agarose	Sigma-Aldrich, USA
Ammonium Acetate	Sigma-Aldrich, USA
Ammonium Phosphate Monobasic	Sigma-Aldrich, USA
Ammonium Sulphate	Sigma-Aldrich, USA
Bovine Serum Albumin (BSA)	Sigma-Aldrich, USA
Bradford Reagent	Sigma-Aldrich, USA
Calcium Chloride (CaCl <sub>2</sub> )	Avantor, USA
Chloramphenicol	Sigma-Aldrich, USA
ClaI	New England BioLabs (NEB), UK
Distilled Water (DNase/RNase free)	Thermo Fisher Scientific, USA
Dithiothreitol (DTT)	Thermo Fisher Scientific, USA
DraI	New England BioLabs (NEB), UK
D-sorbitol	Sigma-Aldrich, USA

EasySelect Pichia Expression Kit	Thermo Fisher Scientific, USA
EasySelect <i>Pichia pastoris</i> Expression Kit	Thermo Fisher Scientific, USA
Ethanol Absolute	Sigma-Aldrich, USA
Ethidium Bromide	Sigma-Aldrich, USA
Formaldehyde Solution	Sigma-Aldrich, USA
Formic Acid 98-100%	PanReac AppliChem, Spain
Gel Extraction Kit	Macherey-Nagel, Germany
Gene Pulser Cuvette	Bio-rad, USA
Glass Beads Acid Washed	Sigma-Aldrich, USA
Glycerol approx 87%	Sigma-Aldrich, USA
Glycine	PanReac AppliChem, Spain
Hydroxyethyl Cellulose	Sigma-Aldrich, USA
Imidazole	Sigma-Aldrich, USA
Immun star WesternC Chemiluminescent Kit	Bio-rad, USA
Isopropyl- $\beta$ -D-thiogalactopyranosid (IPTG)	Peqlab, Germany
iQ SYBR Green Supermix	Bio-rad, USA
Kanamycin Sulphate	Thermo Fisher Scientific, USA
Lyticase from <i>Arthrobacter luteus</i> lyophilized powder	Sigma-Aldrich, USA
Magnesium Chloride (MgCl <sub>2</sub> )	Kapa Biosystems, USA
Methanol, Bromophenol blue	PanReac AppliChem, Spain
NotI	Thermo Fisher Scientific, USA
Nuclease-Free Water	Thermo Fisher Scientific, USA
NucleoSpin Gel and PCR Clean-up Kit	Macherey-Nagel, Germany
NucleoSpin Plasmid Kit	Macherey-Nagel, Germany
PageRuler Prestained Protein Ladder	Thermo Fisher Scientific, USA
Peptone from casein	Merck Millipore, USA
Peptone from meat	Merck Millipore, USA
pGEM-T Easy Vector System	Promega, USA
Phenol:Chloroform 5:1	Sigma-Aldrich, USA
Phenylmethylsulfonyl Fluoride (PMSF)	PanReac AppliChem, Spain
Pichia EasyComp Transformation Kit	Thermo Fisher Scientific, USA

Pierce BCA Protein Assay Kit, D(+)-Sucrose 99.7%	Thermo Fisher Scientific, USA
Potassium Carbonate 99+%	Thermo Fisher Scientific, USA
Potassium Chloride $\geq 99.0\%$	Sigma-Aldrich, USA
Potassium Phosphate Dibasic	Sigma-Aldrich, USA
Potassium Phosphate Monobasic	Sigma-Aldrich, USA
pPICZ $\alpha$ -C Expression Vector	Thermo Fisher Scientific, USA
Silver Nitrate	Sigma-Aldrich, USA
SMD1168H <i>Pichia pastoris</i> Yeast Strain	Thermo Fisher Scientific, USA
Sodium Acetate	Sigma-Aldrich, USA
Sodium Carbonate anhydrous	PanReac AppliChem, Spain
Sodium Chloride	Sigma-Aldrich, USA
Sodium Dodecyl Sulphate	PanReac AppliChem, Spain
Sodium Hydroxide Solution 40 %, D(+)- Glucose	PanReac AppliChem, Spain
Sodium Phosphate Monobasic Dihydrate	Sigma-Aldrich, USA
Sodium Sulphate	Sigma-Aldrich, USA
T4 DNA Ligase	Thermo Fisher Scientific, USA
TALON Superflow Metal Affinity Resin	Takara Bio, USA
Taq DNA Polymerase	New England BioLabs (NEB), UK
Tetramethylethylenediamine (TEMED)	PanReac AppliChem, Spain
Transblot Turbo transfer pack Midi format 0.2 um nitrocellulose	Bio-rad, USA
Trichloroacetic acid (TCA)	Merck Millipore, USA
Tris Buffered Saline (TBS) powder	Santa Cruz Biotechnology, USA
Trizma base	Fisher Scientific, USA
Tween 20	Sigma-Aldrich, USA
XbaI	New England BioLabs (NEB), UK
Yeast Extract	Sigma-Aldrich, USA
Yeast Nitrogen Base	Sigma-Aldrich, USA
Zeocin antibiotic	Thermo Fisher Scientific, USA

Polysaccharides that were used as donor substrates were a kind gift from Megazyme International Ireland. Hydroxyethylcellulose (HEC) was supplied from Sigma-Aldrich, USA (Table 2.3.).

Oligosaccharides that were used as acceptor substrates were also a kind gift from Megazyme International Ireland (Table 2.4.)

Table 2.3. Polysaccharide donors listed with abbreviations and catalog numbers.

<b>Polysaccharide Donors</b>	<b>Abbreviations</b>	<b>Catalog no</b>
Barley $\beta$ -glucan	BBG	P-BGBM
Carob galactomannan	CM	P-GALML
Hydroxyethyl cellulose	HEC	54290
Guar galactomannan	GM	P-GGMMV
Konjac Glucomannan	KM	P-GLCML
Tamarind seed xyloglucan	TXG	P-XYGLN
Wheat arabinoxylan	WA	P-WAXYM

Table 2.4. Oligosaccharide acceptors listed with abbreviations and catalog numbers.

<b>Acceptor Substrates</b>	<b>Abbreviations</b>	<b>Catalog number</b>
1,3:1,4- $\beta$ -glucotetraose A	BA	O-BGTETA
1,3:1,4- $\beta$ -glucotetraose B	BB	O-BGTETB
1,3:1,4- $\beta$ -glucotetraose C	BC	O-BGTETC
1,4- $\beta$ -cellotetraose	CT	O-CTE
Di-galactosyl mannopentaose	DGM	O-GGM5
Galactosyl mannotriose	GM	O-GM3
Laminaritetraose	LT	O-LAM4
1,4- $\beta$ -mannotetrose	MT	O-MTE
1,4- $\beta$ -D-xylotetrose	XT	O-XTE
Xyloglucan heptasaccharides	X7	O-X3G4
Xyloglucan Oligosaccharides	XGO	O-XGHON

OsXTH30 (*Oryza sativa*), BdXTH2 (*Brachypodium distachyon*), HvXTH10 (*Hordeum vulgare*), OsXTH31 (*Oryza sativa*) genes were supplied from the GeneScript, USA.





### **3. METHODS**

#### **3.1. TARGET ENZYME SELECTION**

Target xyloglucan endotransglucosylase/hydrolase enzymes were selected the two group. OsXTH30 and BdXTH2 enzymes were chosen from the ancestral group and HvEG16-10, OSEG16-31 enzymes were chosen from the EG16 group. These codon optimized genes were selected for the heterologous expression.

#### **3.2. PRODUCTION AND PURIFICATION OF OSXTH30, HVEG16-10, OSEG16-31**

##### **3.2.1. Reproducing Colonies and Preparation of Glycerol Stock**

The competent cells DH5 $\alpha$  E.coli, which includes the plasmid with the gene of interest pPICZ $\alpha$ -C/OsXTH30, was reproduced in 10 ml of low salt Luria-Bertani (LB) broth (1% Tryptone 0.5% Yeast Extract 0.5% NaCl pH 7.5). Zeocin antibiotic was added to LB culture as 10  $\mu$ l to make the final concentration of the antibiotic 100  $\mu$ g/ $\mu$ l. LB culture was started at 37°C and 180 rpm overnight. Glycerol stock was prepared 180  $\mu$ l of %87 glycerol with the addition of 820  $\mu$ l of overnight culture. Glycerol stock was kept at -80°C to reuse during the experiments.

##### **3.2.2. Plasmid Isolation**

Plasmid isolation to pPICZ $\alpha$ -C-OsXTH30, pPICZ $\alpha$ -C-OsXTH31, pPICZ $\alpha$ -C-HvEG16-10 in overnight LB culture were performed with Macherey-Nagel NucleoSpin Plasmid kit. Overnight LB cultures with plasmids were centrifuged at 3320g for 10 minutes. Supernatants were discarded and the pellets were re-suspended completely with 500  $\mu$ l resuspension buffer named "Buffer A1". 500  $\mu$ l of "Buffer A2" was added to the tubes and inverted 6-8 times. Tubes were incubated at room temperature for 5 minutes until lysate clearly appears. 600  $\mu$ l of "Buffer A3" was added to each tube and inverted 6-8 times until blue samples turn

completely colorless. Tubes were centrifuged for 10 min at 11,000 g. NucleoSpin Plasmid/Plasmid (NoLid) Columns were placed in Collection Tubes and 750  $\mu$ l of supernatants were transferred to each column. Tubes were centrifuged for 1 min at 11,000g. Flow-through was discarded and NucleoSpin Plasmid Columns were placed in the collection tubes. This step was repeated until there were not any remaining lysate. 500  $\mu$ l of “Buffer AW” (preheated to 50°C) were added to tubes and centrifuged for 1 min at 11,000g. Flow-through was discarded and NucleoSpin Plasmid Columns were placed in the collection tubes. 600  $\mu$ l of “Buffer A4” (100 ml ethanol was added to the bottle before used) were added to tubes and centrifuged for 1 min at 11,000g. Flow-through was discarded and NucleoSpin Plasmid Columns were placed to empty the collection tubes. Tubes were centrifuged for 2 min at 11,000 rpm to dry silica membrane. NucleoSpin Plasmid/Plasmid (NoLid) Column was placed in a 1.5 ml microcentrifuge tubes and 50  $\mu$ l of nuclease free water were added to the tubes and incubated for 1 min at room temperature. Tubes were centrifuged 1 min at 11,000g. After the plasmids had been isolated, DNA content was measured with the Nanodrop 2000c UV-Vis Spectrometer.

### **3.2.3. Preparation of the *Pichia pastoris* Competent cells**

*Pichia pastoris* SMD1168H cells were cultured in a streaking Yeast Extract Peptone Dextrose (YPDS; 1% (w/v) yeast extract, 20% (w/v) peptone, 10% (v/v) dextrose) Agar plate at 30°C in an incubator for 4 days. One of the colonies was picked and 10 ml of YPDS agar (YPDS Agar; 1% (w/v) yeast extract, 20% (w/v) peptone, 10% (v/v) dextrose, 2% (w/v) agar) culture was started at 30°C through overnight in a shaking incubator of 160 rpm. 50 ml of overnight culture was diluted to OD<sub>600</sub> of 0.15-0.20 in a volume of 50 ml of YPD in a flask. *P. pastoris* culture was grown until the OD<sub>600</sub> reaches 5. The culture was centrifuged at 500g for 5 min at RT and the supernatant was discarded. The pellet was resuspended in 9 ml of ice cold BEDS solution (10 mM bicine-NaOH, pH 8.3, 3% (v/v) ethylene glycol, 5% (v/v) (dimethyl sulfoxide) DMSO, and 1 M sorbitol) and 1 ml of 1.0M Dithiothreitol (DTT) solution. The cell suspension was incubated for 5 min at 100 rpm in 30°C shaking incubator. The culture was centrifuged at 500g for 5 min at RT and resuspended in 1 ml of BEDS solution. Competent cells were aliquoted and divided as 200  $\mu$ l in each 1.5 ml microcentrifuge tubes and stored at -80 °C for following transformation process.

### 3.2.4. Plasmid Digestion

pPICZ $\alpha$ -C/OsXTH30, pPICZ $\alpha$ -C/OsXTH31, pPICZ $\alpha$ -C/HvEG16 plasmids were digested with DraI (10,000 units) enzyme to plasmid become linear. The amount of enzyme was optimized for the reaction. NEBuffer4, DraI, pPICZ $\alpha$ -C/OsXTH30 (10 $\mu$ g) and water were mixed to reach reaction volume up to 70  $\mu$ l.

The mixture was incubated at 37°C for 100 min. Linearization was checked by agarose gel electrophoresis. 0.5 g of agarose was mixed in 50 ml of 1X Tris-acetate-EDTA Buffer (24.2% (w/v) Trisma-Base, 2.71% (v/v) glacial acetic acid, 10% (v/v) 0.5 M of EDTA (pH 8.0)) and 0.8  $\mu$ l of Ethidium Bromide (10 mg/ml) was added after it dissolves to obtain 1% (w/v) agarose gel. Digested and undigested plasmids were loaded to the agarose gel and run at 120V for 20 minutes.

### 3.2.5. Phenol Extraction and Ethanol Precipitation of Plasmid DNA

To obtain pure plasmid Phenol extraction and ethanol precipitation was performed. One volume of phenol:chloroform:isoamyl alcohol (25:24:1) was added to DNA sample and vortexed. The sample was centrifuged at RT for 5 min at 2000 rpm. The upper aqueous phase was removed carefully and transferred to a new tube without carrying any phenol product. 0.1 volume of 3 M of NaOAc (pH 5.5) and 2.5 volume of absolute ethanol was added. Tubes were incubated at -20°C overnight. Samples were centrifuged at 4°C for 15 min at 14,000 rpm. After the supernatants had been carefully removed, 2 volumes of 80% ethanol were added and incubated at RT for 5 min. Samples were centrifuged at 4°C for 5 min and supernatants were totally removed until there was no ethanol remaining. Samples were dried at 50°C for 5 min and 10  $\mu$ l of ddH<sub>2</sub>O was added to the sample. 1  $\mu$ l of this sample was taken and mixed with 9  $\mu$ l of ddH<sub>2</sub>O water to prepare a diluted sample.

### 3.2.6. *Pichia pastoris* Transformation

Linearized plasmids pPICZ $\alpha$ -C/OsXTH30, pPICZ $\alpha$ -C/OsXTH31 and pPICZ $\alpha$ -C/HvEG16 were transformed into *P. pastoris* competent cells by taking 4  $\mu$ l of plasmid and mix it with 40  $\mu$ l of competent *P. pastoris* cells in an electroporation cuvette. 2.0 mm electroporation cuvettes were prepared for each plasmid sample for diluted and undiluted plasmids and incubated on ice for 2 min. One volume of 1 M sorbitol (18.215 % (w/v)) was mixed with one volume of YPD. Bio-Rad Gene Pulser was used for electroporation at 1.5 kV, 25  $\mu$ F and 200  $\Omega$ . After electroporation 1 ml of sorbitol and YPD mixture was added to each sample. Samples were transferred into 15 ml of falcons and incubated at 30°C for 2 hours in shaking incubator. After incubation falcons had been centrifuged and 850  $\mu$ l of the supernatant was discarded. The rest of the samples were resuspended with the remaining supernatant. *P. pastoris* colonies were cultured in Zeocin antibiotic containing (final concentration: 100  $\mu$ g/ $\mu$ l) YPDS agar plates and incubated at 30°C for 4 days. Antibiotic resistant transformant colonies were selected from the plates.

### 3.2.7. Selection of Colonies Which Producing The Target Enzyme

Randomly selected colonies were subcultured in Zeocin containing (final concentration: 100  $\mu$ g/ $\mu$ l) YPDS agar plates and incubated at 30°C for 4 days. Each of the colonies were cultured in 10 ml of Buffered Glycerol Complex Medium (BMGY; 1% (w/v) yeast extract, 10% (w/v) peptone, 0.01% (v/v) 1 M potassium phosphate buffer, 0.01% (v/v) yeast nitrogen base, 0.0002% (v/v) 500X biotin, 0.00115 % (v/v) 87% glycerol) and incubated 30°C at 200rpm until the OD<sub>600</sub> value reaches 4-6. *P. pastoris* cells were centrifuged at 4000 g and supernatant was discarded. *P. pastoris* cells were resuspended in 10 ml of Buffered Methanol Complex Medium (BMMY; 1% (w/v) yeast extract, 10% (w/v) peptone, 0.01% (v/v) 1 M potassium phosphate buffer, 0.01% (v/v) yeast nitrogen base, 0.0002% (v/v) 500X biotin, 0.01% methanol) and incubated at 22°C in 175 rpm shaking incubator. Throughout the incubation, 1% methanol was added to the cultures in every 24 hours for 5 days. After 5 days of incubation, cells were precipitated and supernatants were kept for later observations.

Trichloroacetic Acid (TCA) and Acetone precipitation were performed using the supernatants. 900  $\mu$ l of supernatant was taken and mixed with the 100  $\mu$ l of 100% TCA

(142.86% (w/w) TCA). After the proteins were observed milky white, samples were vortexed and incubated on ice for 1 hour. Samples were centrifuged at 4°C at 12,000g for 10 min. Supernatants were removed carefully and 800 µl of -20°C HPLC-pure acetone was added to the tubes. Samples were vortexed even though proteins didn't dissolve in acetone but aimed to discard an excess amount of TCA and incubated at -80°C overnight. Proteins were precipitated by centrifugation at 6500 g at 4°C for 10 min. After the supernatant was discarded samples were washed with 200 µl of -20°C HPLC-pure acetone and incubated in -20°C for 30 minutes. Tubes were centrifuged at 6500 g at 4°C for 10 min and the washing step was repeated. After the final centrifugation, 6500 g at 4°C for 10 min acetone was discarded completely and samples were waited on ice to dry all the acetone from pellets. Pellets were dissolved in 30 µl of ultrapure water.

30 µl of protein solution was mixed with 30 µl of Leammli buffer and incubated at 95°C for 7 min then waited on the ice. Protein samples were visualized with Sodium Dodecyl Sulfate Polyacrylamide Gel Electrophoresis (SDS-PAGE) method. 12% Resolving gel (32.6% (v/v) ddH<sub>2</sub>O, 40% (v/v) 30% acrylamide, 25.3% (v/v) 1.5 M Tris pH 8.8, 1.0% (v/v) 10% SDS, 1.0% (v/v) 10% Ammonium persulfate (APS), 0.04% (v/v) TEMED) and 5% Stocking gel (68% (v/v) ddH<sub>2</sub>O, 16.6% (v/v) 30% acrylamide, 12.6% (v/v) 1.0 M Tris pH 6.8, 1.0% (v/v) 10% SDS, 1.0% (v/v) 10% Ammonium persulfate (APS), 0.04% (v/v) TEMED) were prepared. Protein samples were loaded on the gel and samples were run at 300V for 1 hour. Proteins in the gel were stained with Coomassie Brilliant dye for 30 min. Distilled water was used for destaining. The molecular weight of the target protein was visualized. Another %12 polyacrylamide gel was prepared to use in Western blotting. Same protein samples were loaded and run at 300V for 1 hour. Transfer Pack 0.2 µm nitrocellulose membrane was used in order to transfer proteins from the gel and Bio-Rad Transblot Turbo system was used. 3% Skimmed dry milk powder (5% (w/v)) was mixed with Tris Buffered Saline-Tween 20 (TBS-T; 31.52% 1 M Tris-HCl, 9% (w/v) NaCl, 0.5% (v/w) tween-20) to block the unwanted proteins in the membrane overnight. 2 µl of Abcam Anti-6X His antibody was mixed with 10 ml TBS-T. The solution was added to the membranes and incubated for 1 hour. TBS-T was used for washing membranes for 5 min. This washing step was repeated. 10 ml of Phosphate-buffered saline solution pH 7.4 (PBS; 0.8% (w/v) NaCl, 0.02% (w/v) KCl, 0.178% (w/v) Na<sub>2</sub>HPO<sub>4</sub>, 0.027 (w/v) K<sub>2</sub>HPO<sub>4</sub>) was used the wash membrane for 10 min. Luminol Enhancer and Peroxidase solution from the Amersham<sup>TM</sup> ECL<sup>TM</sup> Prime

Western Blotting Detection Reagent kit was used to detect protein in the membrane and both images of the membranes were taken with ChemiDoc™ XRS+ System with Image Lab™ Software.

### **3.2.8. Enzyme Activity Assay**

Enzyme activity assay was used for the determination of the colonies which producing the most actively synthesizing XTH enzyme. Acceptors and donors that were planned to be used listed with their abbreviations in Table 2.1 and Table 2.2. Oligosaccharides that were used as acceptors were tagged with fluorescent sulforhodamine dye and all stocks were diluted to 50 mM before used. Donor polysaccharides were prepared as 0.8% (w/v) for stock solutions and they were diluted to 0.4% (w/v) with 0.2 M ammonium acetate before used in the experiments. Optimum pH values for the donors were determined by the optimum activity with pH for each enzyme.

2 µl of the supernatant of the colonies were taken for each colony mixed with 10 µl of 0.4% TXG donor and 1 µl of 50 mM of XGO acceptor. Reaction tubes were incubated at 30°C for 24 hours. 6 µl of formic acid was added to each reaction to stop the enzymatic reaction. 11 µl of ultrapure water was added and total reaction volume was become 30 µl. Reactions were analyzed with the Agilent 1100 Series High-Performance Liquid Chromatography (HPLC) with fluorescent detector (FLD). 15 µl of the reaction was injected to HPLC and it was separated by BioSep-SEC 4000 column, 75x7.80 mm. Flow rate was 0.5 ml/min and mobile phase was used as 0.1 M pH 6.0 ammonium acetate with containing 20% acetonitrile. Separation of fluorescently labeled polysaccharides and oligosaccharides were analyzed with the ChemStation software. The colonies that are producing the enzyme actively were selected with the analysis of HPLC.

### **3.2.9. Large Scale Production and Protein Purification**

Colonies that are producing the target enzyme actively were selected and large scale production was started with those colonies. Selected colony for each of the enzyme was subcultured and incubated in 10 ml of BMGY at 30 °C with 200 rpm shaking incubator for 16-18 hours. 780 µl from the BMGY overnight culture was taken and added to the 6

Erlenmeyer flasks of 500 ml capacity filled with 100 µl of BMGY and it was incubated at 30°C with 200 rpm shaking incubator for 16-18 hours. BMGY cultures were precipitated at 22°C in 3220g for 10 min and supernatants were discarded before cells were transferred into the BMMY. Pellets were resuspended in BMMY and the BMMY amounts were completed up to 100 ml (500 ml volume Erlenmeyer flask) or 200 ml (1 lt volume Erlenmeyer flask). BMMY production of OsXTH30 enzyme were 3 lt and 1,7 lt of BMMY. BMMY cultures were incubated at 22 °C in 175 rpm shaker incubator for 5 days. Throughout the incubation, 1% methanol was added to the cultures in every 24 hours for 5 days. The sample was taken from the culture to analyze enzymatic activity. After 5 days cells were precipitated at 22°C in 3220g for 10 min. All supernatants were filtered with 0.2 µM RC filters. Ammonium sulfate precipitation was performed at 4°C with %90 saturation level. Samples were centrifuged at 4 °C and 12,000 g for 15 minutes to precipitate the proteins. After the supernatant had been discarded, pellets were resuspended in 20 mM pH 7.4 sodium phosphate buffer. To get rid of the excess amount of ammonium sulfate before affinity chromatography, the protein solution was put in cellulose membranes to perform dialysis. 15 lt of 20 mM Sodium phosphate buffer pH 7.4 (0.06% (w/v) NaH<sub>2</sub>PO<sub>4</sub>·2H<sub>2</sub>O, 0.43% (w/v) Na<sub>2</sub>HPO<sub>4</sub>·2H<sub>2</sub>O) was prepared and cooled at 4 °C. Cellulose membranes filled with protein solutions were put in sodium phosphate buffer and buffer solution was changed in every 3 hours for 2 times.

HisTrap FF column with AKTAprime plus system was used to purify 6X-His tagged proteins. If the HisTrap FF column was not used for a while “stripping and recharging” method was used. In this method binding buffer pH 7.4 with low imidazole concentration (0.59% (v/v) 0.64 M of NaH<sub>2</sub>PO<sub>4</sub>·2H<sub>2</sub>O, 3.24% (v/v) 0.5 M of Na<sub>2</sub>HPO<sub>4</sub>·2H<sub>2</sub>O, 10% (v/v) 5M of NaCl, 0.25% (v/v) 2M of imidazole) was loaded to the HisTrap FFcolumn and it was charged with NiSO<sub>4</sub> solution. The sample was mixed with imidazole (final concentration 5M) and NaCl (final concentration 2M) and loaded onto the column. 6X-His tagged proteins were eluted with the elution buffer pH 7.4 with higher concentration of imidazole (0.59% (v/v) 0.64 M of NaH<sub>2</sub>PO<sub>4</sub>·2H<sub>2</sub>O, 3.24% (v/v) 0.5 M of Na<sub>2</sub>HPO<sub>4</sub>·2H<sub>2</sub>O, 10% (v/v) 5M of NaCl, 25% (v/v) 2M of imidazole).

Elution buffer was replaced with 0.1 M of ammonium acetate pH 6.0 solution with Buffer Exchange/Size Exclusion Chromatography method using HiPrep 20/10 DeSalting column. The enzyme solution was concentrated with Millipore Centrifugal Units before loaded to

HiPrep 20/10 DeSalting column. The protein solution was eluted in ammonium acetate and the fractions with target proteins were separated. For the final separation, Superdex 75 16/100 size exclusion column was used 0.1 M of ammonium acetate pH 6.0 was used as mobile phase. The protein solution was eluted to fractions and stored at 4 °C. Target fractions were pulled together.

### **3.2.10. Bradford Protein Assay**

Protein amount of the purified proteins were measured by Bradford Assay. Bovine Serum Albumin (BSA) standards were used to determine the calibration curve. Concentration of the BSA standards were 0.1 mg/ml, 0.8 mg/ml, 0.6 mg/ml, 0.4 mg/ml, 0.2 mg/ml and 0.1 mg/ml. Each of the 10 µl of BSA standards was mixed with 190 µl of Bradford reagent in 96 well plate. The plate was incubated at RT for 5 min in the dark. After the incubation, the absorbance of standards and protein samples were measured with a spectrophotometer at 595 nm. A standard curve was plotted as absorbance values at 595 nm versus protein concentration in µg/ml. The protein concentrations were determined using the standard curve.

### **3.2.11. Western Blot, Silver Nitrate Staining and Dot Blot Analysis**

Purified protein samples were separated on 12% polyacrylamide gel by their molecular weights and then proteins were detected with the help of antibodies with Western blot analysis as mentioned before. Another 12% polyacrylamide gel was used to identify proteins intensity by using Silver Nitrate staining. After the protein samples were run through, the gel waited in fixation solution (30% (v/v) EtOH, 10% (v/v) acetic acid) for overnight. After the fixation solution was discarded and the gel was washed with 0.8 mM sodium thiosulfate for 1 min. Gel was washed with distilled water for 1 min twice. 12mM of Silver Nitrate solution (0.00127) % (w/v)) was put onto the gel and incubated in the dark for 40 min. Gel was washed with distilled water. Developer solution (3% (w/v) potassium carbonate, 0.025% (v/v) formalin, 10 % (v/v) sodium thiosulfate) was put onto the gel and waited until the bands were visualized. After the band formation becomes sufficient developer solution was discarded and stop solution (4% (v/v) Tris base, 2 % (v/v) acetic acid) was added and the gel



was incubated for 30 min. Images were taken with ChemiDoc™ XRS+ System with Image Lab™ Software.

Dot blot analysis was performed to visualize the activity of the enzymes by their luminescence level. Enzyme reaction was set as explained before using TXG donor and XGO acceptor for 24 hours. Enzyme reaction and ammonium acetate (control) were put on onto Whatman Cellulose Filter Paper drop by drop. The paper was dried then it was washed with water overnight. After the paper was dried again luminescence levels were observed under UV Transilluminator.

### **3.2.12. pH Optimization and Activity Analysis**

To characterize enzymes the optimum pH that the enzyme shows the highest activity must be found. Different pH values were tried with TXG-XGO couples to find the highest activity. Reactions were set as described before and McIlvaine buffer used for dilution of the TXG stock for obtaining different pH values. Concentrated enzymes were diluted if it is needed. After the incubation at 30°C, the activities were measured by HPLC.

Enzyme activities were tested after the enzyme purifications. The OsXTH30, BdXTH2, OsEG16-31 and HvEG16-10 enzymes were tested with different donors and acceptors as mentioned in Table 2.1 and Table 2.2 were used with different time intervals. Enzyme activity with these donors and acceptors were measured with HPLC and calculated as picokatal/mg. Specific activities were calculated for enzymes and their percentages were compared to each other.

### **3.3. ENZYME KINETIC ANALYSIS OF BDXTH2**

The kinetic values of the BdXTH2 enzyme have been computed considering the reaction rate and the concentration of the substrate. Thus, calculations were done by the activity changes with different concentrations of donor and acceptors. The effect of the donor polysaccharides was not only depending on the concentration but also depending on the reaction volume and viscosity. The activity of different TXG concentrations from 0.05 to 0.8% giving reactions with 50 µM of X7 was calculated to find optimum donor concentration to avoid the negative

effect of viscosity of donor. Enzyme reaction trials were repeated at least 3 times and reactions were analyzed by HPLC. Optimum TXG concentration was selected and tested with X7 concentrations from 1  $\mu\text{M}$  to 1000  $\mu\text{M}$ . Reaction velocity was calculated according to activities of the enzyme during incubation and it was calculated as  $\mu\text{M}/\text{min}$  for the Michaelis-Menten curve. Lineweaver-Burke curve was plotted using the reaction velocity and final concentration value of the X7. Kinetic calculations were done according to the Lineweaver-Burke graph of the BdXTH2 enzyme with using TXG-X7 couple. Sample studies were applied to HEC-X7 couple and kinetic values were calculated.



## 4. RESULTS

### 4.1. PRODUCTION AND PURIFICATION OF OSXTH30

#### 4.1.1. Big Scale Production and Purification of OsXTH30 in 3 lt of BMMY Medium

##### 4.1.1.1. Transformation into *Pichia Pastoris* and Positive Colony Selection of OsXTH30

Linearized pPICZ $\alpha$ -C/OsXTH30 samples was transformed into *Pichia pastoris* and plated in YPDS agar. Plain YPDS agar plates and YPDS agar that treated with Zeocin antibiotic plates were used as empty control (Figure 4.1 a, b). There were not any grown colonies as expected. Nontransformant *P. pastoris* was plated to the Zeocin including YPDS agar plates and there were not any colonies as expected (Figure 4.1 c) because *P. pastoris* is not resistant to Zeocin antibiotic. Nontransformant colonies were observed in YPDS agar plate without Zeocin antibiotic that inoculated with *P. pastoris* (Figure 4.1 d). Transformant pPICZ $\alpha$ -C/OsXTH30 *P. pastoris* colonies were grown in the YPDS agar including Zeocin antibiotic since pPICZ $\alpha$ -C plasmid have Zeocin resistant genes (Figure 4.1 e). These transformant colonies were selected randomly and 12 of the colonies were subcultured in YPDS agar with Zeocin antibiotic. After they incubated for 4 days at 30°C each of the colonies were inoculated at 10 ml of BMGY medium. Then cells were transferred to 10 ml of BMMY medium with 1% methanol addition for 5 days. TCA acetone precipitation was performed to 12 of the selected colonies in order the precipitate OsXTH30 proteins. During the TCA acetone precipitation colony number 3 and 4 were contaminated and analysis were continued with the rest of the colonies.

Enzyme activities were measured to test which one of the colony have the most activity. Precipitated proteins of the colonies were loaded to 12% polyacrylamide gel then the Coomassie staining and Western blotting for SDS-PAGE were performed in order to observe production of the OsXTH30 protein (Figure 4.1.).

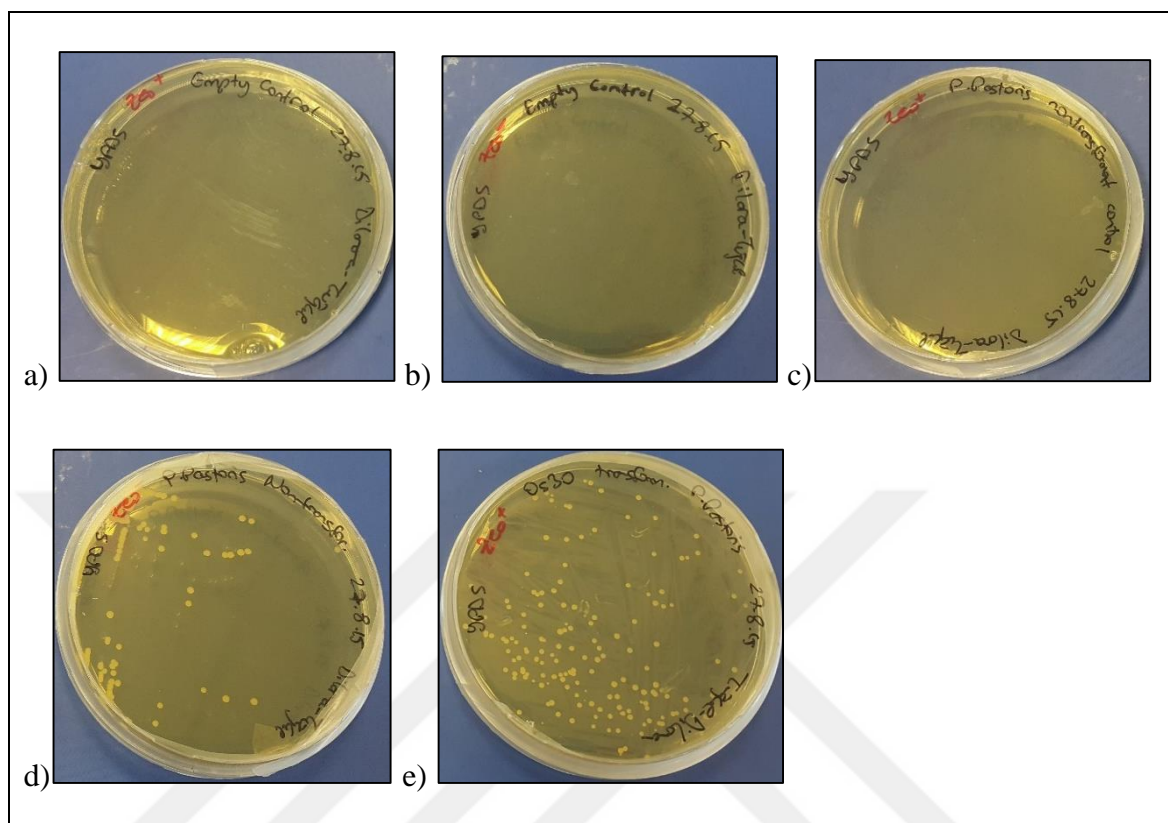


Figure 4.1. YPDS agar with transformant and nontransformant *P. pastoris* colonies for colony selection of pPICZ $\alpha$ -C/OsXTH30 a) YPDS agar with Zeocin antibody. b) YPDS agar without Zeocin antibody. c) YPDS agar with Zeocin antibody inoculated with nontransformant *P. pastoris* cells. d) YPDS agar without Zeocin antibody inoculated with nontransformant *P. pastoris* cells. e) YPDS agar with Zeocin antibody inoculated with transformant *P. pastoris* cells.

The molecular weight of the pPICZ $\alpha$ -C/OsXTH30 that heterologously expressed by the *P. pastoris* theoretically calculated as 33 kDa. Protein bands of the target enzyme were observed between 40-55 kDa in the gel image of the Coomassie staining and Western blotting (Figure 4.2) except the colony number 11 in the Western blotting image (Figure 4.2.b). Several protein bands were also observed in the both images that presumed to be contaminant proteins.

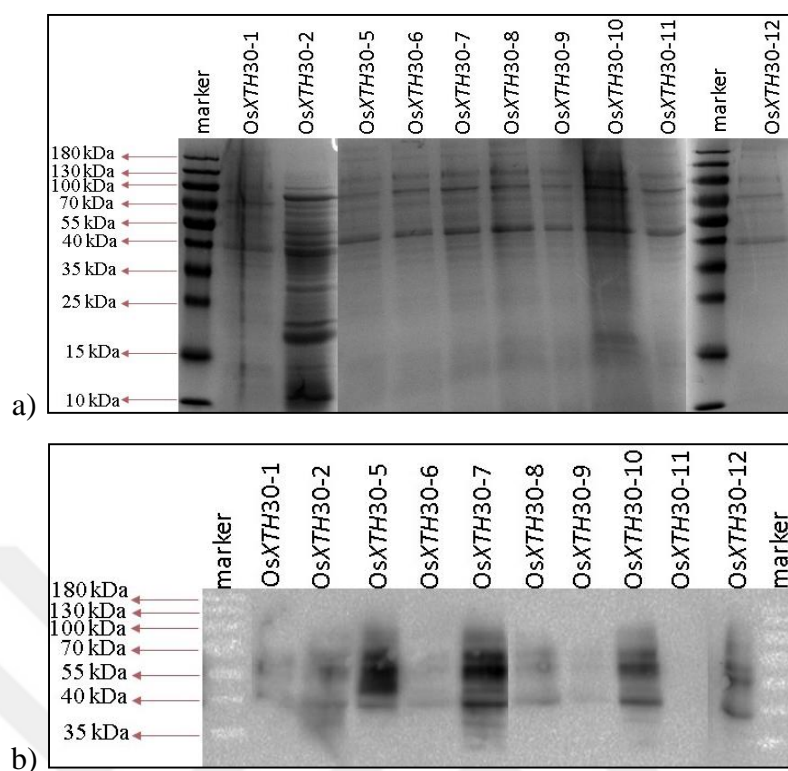


Figure 4.2. Detection of OsXTH30 protein produced by heterologous expression of transformant *P. pastoris* colonies by using SDS-PAGE. a) Coomassie brilliant blue stained SDS-PAGE gel of transformed OsXTH30 enzyme producing *P. pastoris* colonies from 1 to 12. b) Western blotting analysis to SDS-PAGE gel using Anti-6X His tag antibody of transformed OsXTH30 enzyme producing *P. pastoris* colonies from 1 to 12. Protein marker band sizes and colony numbers are indicated on the image.

Although the protein band of colony number 9 were faint than the others, according to the enzyme activity analysis, colony 9 was selected as the most active enzyme producing colony.

#### 4.1.1.2. Expression of OsXTH30 in *Pichia pastoris*

Transformant *P. pastoris* colony 9 was selected for expression of OsXTH30 and big scale production was started in 3 lt of BMMY medium with the addition of %1 v:v methanol in every 24 hours for 5 days. Samples were taken for enzyme activity analysis during the production and purification steps. Enzyme reactions were performed with TXG-XGO donor-acceptor couple with no dilution for 24 hours. During the methanol induction, activity of the

enzyme was increasing by time but after the purification step with affinity chromatography enzyme activity was started to decrease. (Table 4.1).

Table 4.1. The enzyme activities of undiluted OsXTH30 enzyme along the production and purification periods with TXG-XGO donor acceptor couple for 24 hours.

Stage of the taken sample	Volume of the sample	Fluorescence (Lu)
Methanol Induction Day 3	100 ml	226,2
Methanol Induction Day 4	100 ml	4452
Methanol Induction Day 5	100 ml	8023,3
Affinity Chromatography Purification by HisTrap FFColumn	60 ml	4435,5

#### *4.1.1.3. Purification of OsXTH30 Enzyme with Chromatography*

After dialysis of the protein sample, 6X-His tagged OsXTH30 protein was purified with affinity chromatography method and GE Healthcare HisTrap FF column that recharged with Nickel ions. Firstly, the proteins that were not 6X-His tagged were eluted from the column. Then 6X-His tagged proteins were eluted from the column in elution buffer and observed as the second peak in the chromatogram (Figure 4.3). OsXTH30 protein fractions from 1 to 13 were collected and purification of the enzyme was continued with these fractions. Fraction range was determined according their absorbance values.

16/100 gel filtration column was used to eliminate the contaminants with affinity chromatography from the protein solution and OsXTH30 protein samples were separated into the fractions. Absorbance value of the first peak was lower than the second peak and fractions from 43 to 94 were stored for analysis (Figure 4.4).

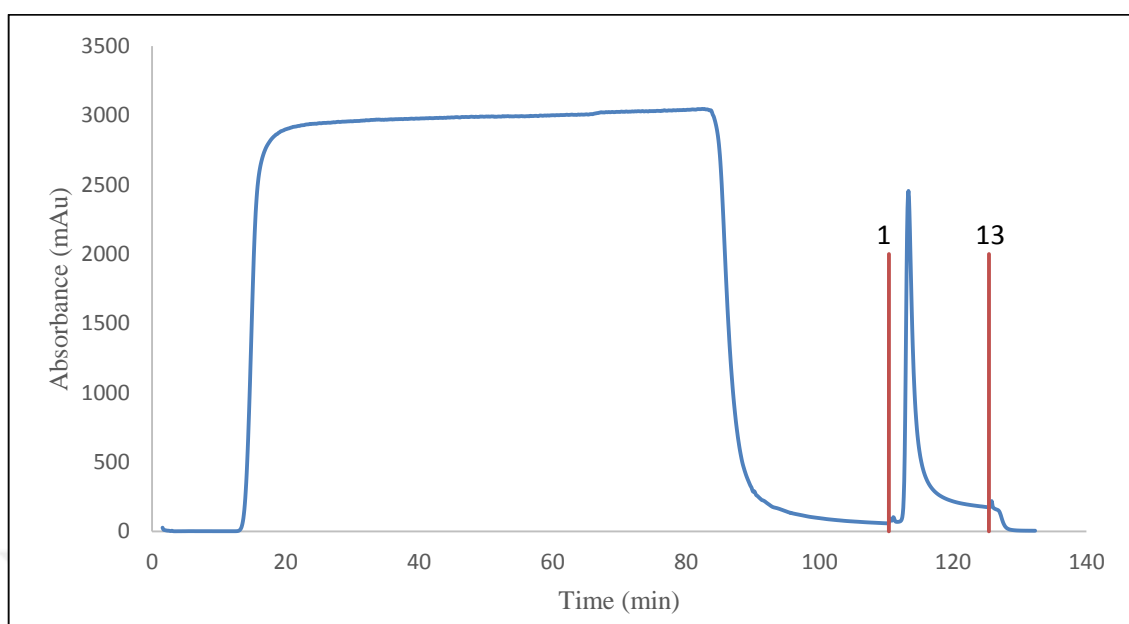


Figure 4.3. Purification OsXTH30 protein by the affinity chromatography of using the GE Healthcare HisTrap FF column.

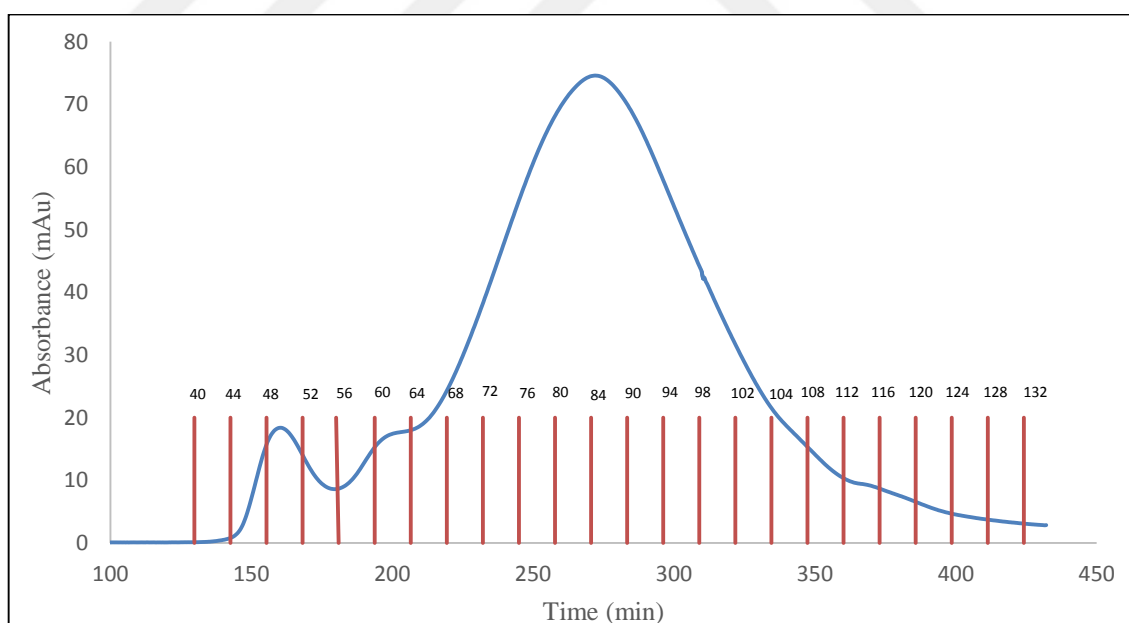


Figure 4.4. The GE Healthcare Superdex 75 16/100 size exclusion column chromatogram of OsXTH30 enzyme.

GE Healthcare HiPrep 26/10 Desalting column was used for buffer exchange. OsXTH30 proteins were collected in 0.1 M of ammonium acetate solution. GE Healthcare Superdex

75/16 size exclusion column was used to separate OsXTH30 protein solution and the first peak was containing the fractions of the targeted proteins. Fractions 44 to 94 were collected for protein detection and enzyme activity analysis.

#### ***4.1.1.4. Detection of OsXTH30 Enzyme Using SDS-PAGE, Western Blotting, Silver Nitrate Staining and Dot Blot Analysis***

Purities of the OsXTH30 protein fractions from 43 to 94 were observed with SDS-PAGE and Western blot analysis. Each of the fractions were loaded on the SDS-PAGE gel and proteins were visualized with Western blotting by using Anti-6X His tag antibody. Protein fractions were also loaded to the second SDS-PAGE gel and proteins were visualized with silver nitrate staining (Figure 4.5).

According to the result of Western blot analysis (Figure 4.5.a-b) of OsXTH30 enzyme, protein bands were between 40-55 kDa, even though molecular weight of OsXTH30 enzyme was about 33 kDa. Thicker bands were observed between fractions of 46 to 70. Protein bands were started to get fainter from fractions of 85. Protein bands were not observed at fraction number 43 and between fractions of 88 to 94. Silver nitrate staining gel image results of the purified the OsXTH30 were not clear (Figure 5.1.c-d). Protein bands were also observed around 40-55 kDa but various bands were also visualized that assumed to be contaminant proteins. Fractions from 43 to 100 were visualized with dot blot analysis. Fractions from 46 to 97 were brighter than the others.



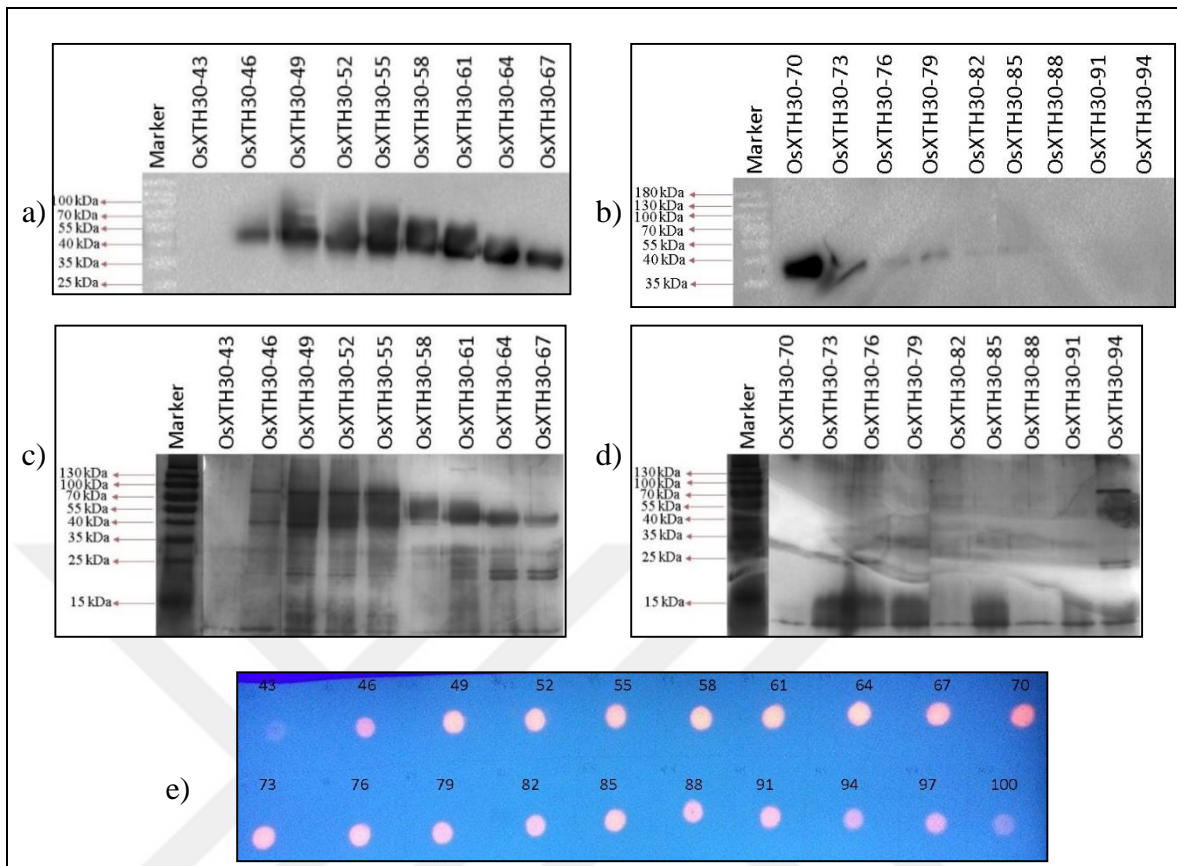


Figure 4.5. Analysis of the OsXTH30 protein fractions from 46 to 94 after purification with GE Healthcare Superdex 75 16/100 gel filtration column a) OsXTH30 protein fractions analysis from 43 to 67 by Western blotting using Anti-6X His tag antibody. b) OsXTH30 protein fractions analysis from 70 to 94 by Western blotting using Anti-6X His tag antibody. c) OsXTH30 protein fractions analysis from 43 to 67 by silver nitrate staining. d) OsXTH30 protein fractions analysis from 70 to 94 by silver nitrate staining. e) Dot blot analysis of the fractions from 43 to 100. Protein marker band sizes and fraction numbers are indicated on the image.

As a result of these analysis, fractions were pulled together into 2 groups according to their purities. Fractions from 46 to 57 were named as pool 1 (impure pool) and fractions from 58 to 70 were named as pool 2 (pure pool). Protein pools were analyzed with silver nitrate staining. Each pool was concentrated with Millipore Amicon Ultra-15 Centrifugal Filter Units up to 1 ml.

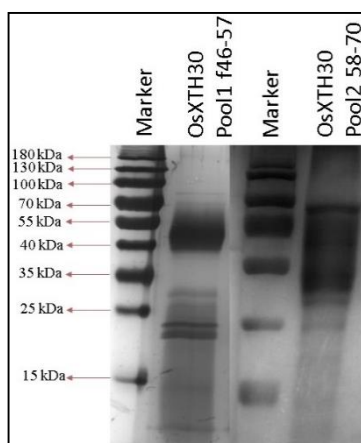


Figure 4.6. Western blot analysis of the OsXTH30 protein of pool 1 (f46-57) and pool 2 (f58-70). Protein marker band sizes and fraction numbers are indicated on the image.

#### ***4.1.1.5. Bradford Assay and the Enzyme Activity Analysis***

Protein concentrations of OsXTH30 enzyme were measured with Bradford Assay. Standard curve was graphed using the BSA standards with 1, 0.8, 0.6, 0.4, 0.2 and 0.1 mg/ml concentrations (Figure 4.7).

Protein absorbance of the pool 1 (f46-57) and pool 2 (f58-70) were measured at 595 nm by spectrophotometer. Concentrations of the protein pools were calculated according to the BSA standard curve. The concentration of the pool 1 (f46-57) were higher than the pool 2 (f58-70) (Table 4.2).

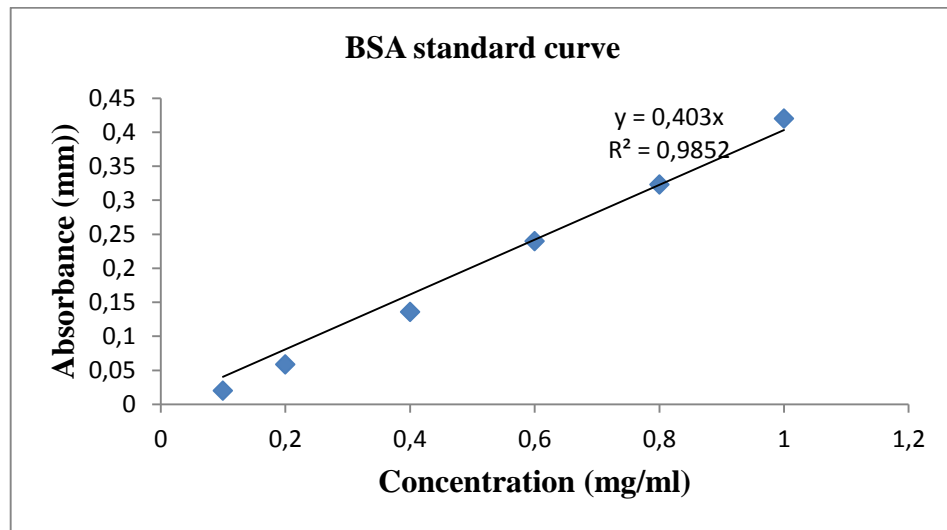


Figure 4.7. Standard curve of Bradford assay using BSA measured at 595 nm.

Table 4.2. Protein fraction concentrations of purified pools belongs to the OsXTH30 enzyme.

<b>Fraction range of the pools</b>	<b>Protein Concentration (mg/ml)</b>
Pool 1 (f46-57)	2,3176 mg/ml
Pool 2 (f58-70)	0,0002 mg/ml

The enzyme activities of the pool 1 (f46-57) and pool 2 (f58-70) were measured with TXG-XGO donor-acceptor couple without dilution. Even though the concentration and the fluorescence values of pool 1 (f46-57) were higher than the pool 2 (f58-70), specific activity of the pool 2 (f58-70) in picokatal/mg was higher than the pool 1.

Table 4.3. The enzyme activities of purified pools belongs to the OsXTH30 enzyme.

<b>Protein Fractions</b>	<b>Donor-Acceptor Couple</b>	<b>Dilution Factor</b>	<b>Incubation time</b>	<b>Fluorescence (Lu)</b>	<b>Picokatal/mg protein</b>
Pool 1 (f46-57)	TXG-XGO	No dilution	1 hour	392.2	0,000314
Pool 2 (f58-70)	TXG-XGO	No dilution	1 hour	116.8	1,005498

Although the activity of the enzyme was detected in both enzyme pools, it was observed that the activity of the enzyme was decreasing by time and it was decided that amount of the activity was not enough to continue the enzyme kinetic studies. The heterologous protein production of the OsXTH30 enzyme was repeated with the colony 9.

#### **4.1.2. Big Scale Production and Purification of OsXTH30 in 1.7 lt of BMMY Medium**

##### ***4.1.2.1. Expression of OsXTH30 in Pichia pastoris***

Big scale heterologous production of OsXTH30 with the colony 9 was repeated. Colony 9 was inoculated to BMGY and then the transformant cells were transferred to BMMY medium to start big scale production of 1.7 lt in BMMY. Methanol induction was performed by adding %1 v:v methanol to the BMMY culture in every 24 hours for 3 days and transformant *P. pastoris* cells were precipitated at the end of the incubation period. Supernant of the protein solution was filtrated with 0.22  $\mu$ M 0.2 filters. Proteins were precipitated with the ammonium sulfate solution and precipitated proteins were resuspended in sodium phosphate buffer. Dialysis was performed in order to getting rid the excess amount of the ammonium sulfate. OsXTH30 proteins were purified using the chromatography techniques.

During the production and purification of the OsXTH30 enzyme samples were analyzed for the enzyme activity. Enzyme reactions were performed with TXG-XGO donor-acceptor couple for 1 hours from the different volumes of enzyme samples (Table 4.4).

Table 4.4. The enzyme activities of undiluted OsXTH30 enzyme along the production and purification periods with TXG-XGO donor acceptor couple for 1 hour.

Stage of the taken sample	Volume of the sample	Fluorescence (Lu)
BMGY big scale	100 ml	11.3
Methanol Induction Day 1	100 ml	139
Methanol Induction Day 2	100 ml	462.6
After ammonium sulfate precipitation	120 ml	4899.1
Dialysis	117 ml	4435.5
Buffer exchange with HiPrep 20/10 Desalting Column	65 ml	1810.3

#### *4.1.2.2. Purification of OsXTH30 Enzyme with Chromatography*

Protein sample of the 6X His tagged OsXTH30 enzyme was purified after dialysis with GE Healthcare HisTrap FF column using affinity chromatography technique. Contaminant proteins without 6X His tag were eluted from the column until the end of the 60<sup>th</sup> min. The second peak was belong to the 6X His tagged OsXTH30 enzyme and proteins were collected in fractions (Figure 4.8).

Buffer exchange was performed with GE Healthcare HiPrep 26/10 Desalting column. Protein contaminants were eliminated using the GE Healthcare Superdex 75 16/100 gel filtration size exclusion column and OsXTH30 enzyme was collected in fractions (Figure 4.8).

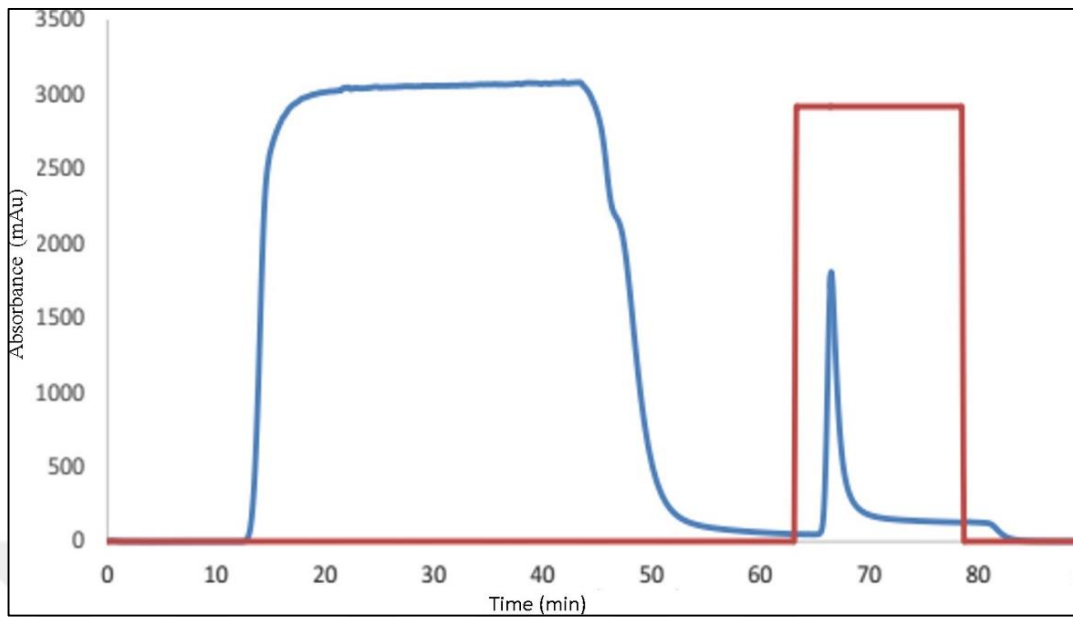


Figure 4.8. Chromatogram of heterologously expressed OsXTH30 enzyme using GE Healthcare HisTrap FF column.

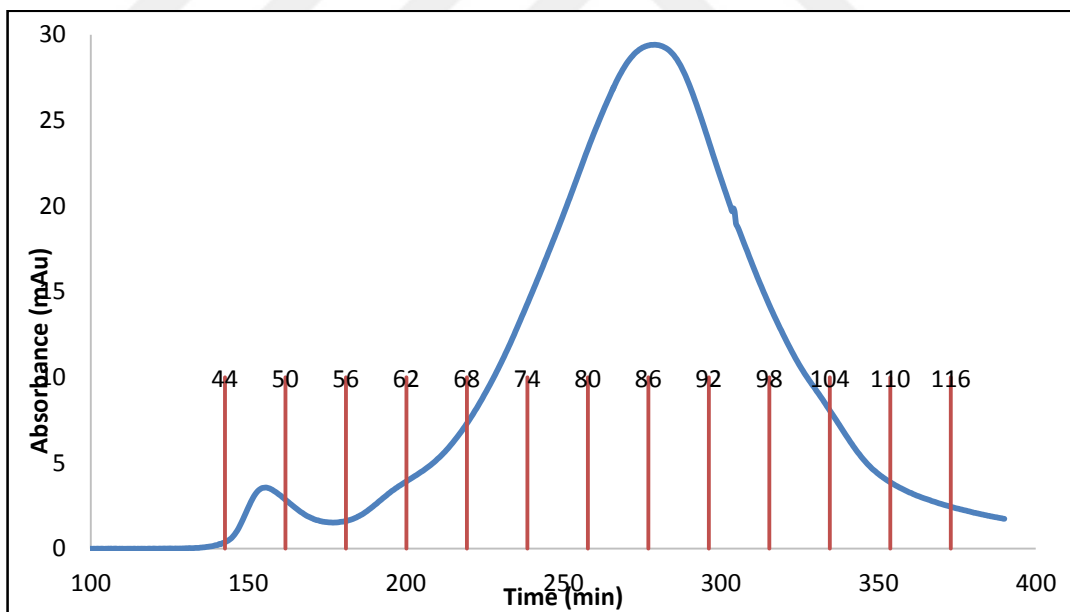


Figure 4.9. Chromatogram of heterologously expressed OsXTH30 enzyme using The GE Healthcare Superdex 75 16/100 size exclusion column.

#### ***4.1.2.3. Detection of OsXTH30 Enzyme Using SDS-PAGE, Western Blotting, Silver Nitrate Staining***

Enzyme fractions of the purified OsXTH30 enzyme were collected and concentrated to 1.5 ml with the Millipore Centrifugal Units. Protein analysis of the fractions were performed by using SDS-PAGE, Western Blotting and silver nitrate staining techniques. Each fractions were analyzed in order to observe the size of the protein and targeting the fraction range.

Expected bands of fractions were not observed from SDS-PAGE analysis with polyacrylamide gel electrophoresis and silver nitrate staining (Figure 4.10) even though activity were observed in enzyme activity analysis results. Western Blotting images showed that some protein fraction bands were observed at about 35 kDa and 70 kDa, which were not related to molecular weight of the target enzyme. However, there was no consistency between the fractions due to some problems during the experiment.

The results of the enzyme assay and the chromatogram of the GE Healthcare Superdex 75 16/100 gel filtration chromatography of the OsXTH30 protein were examined together and the fractions were pooled to give 3 protein pools. Then pools were concentrated with Millipore Amicon Ultra-15 Centrifugal Filter Units. The fraction groups forming pool 1, pool 2 and pool 3 were respectively as follows; fractions 45-56, fractions 57-65 and fractions 66-101.

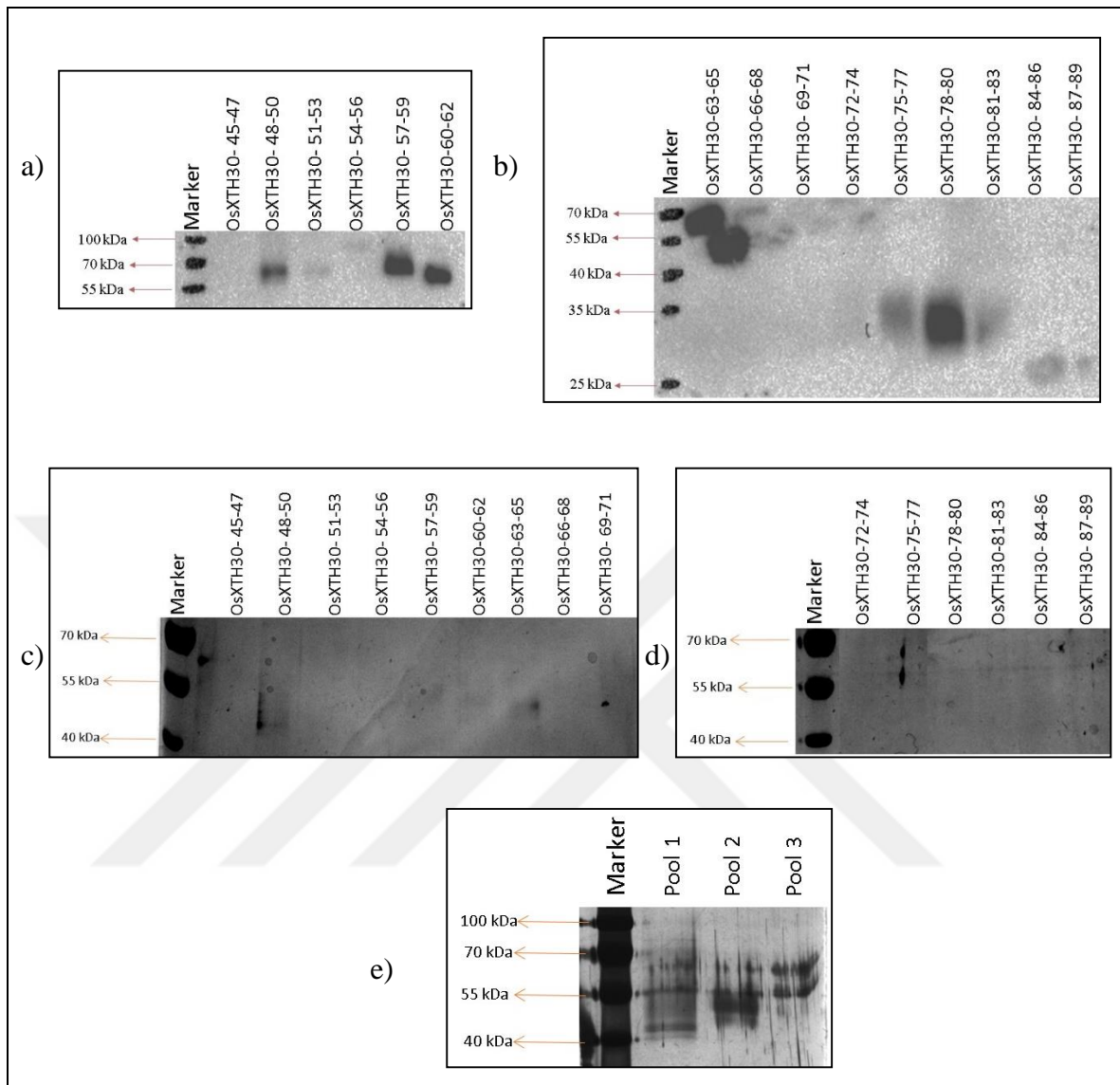


Figure 4.10. Analysis of the protein content of OsXTH30 protein in fractions resulting from GE Healthcare Superdex 75 16/100 gel filtration chromatography. a) Western blot analysis of the OsXTH30 fractions between 45 and 62 using anti-6X His antibody. b) Western blot analysis of the OsXTH30 fractions between 43 and 89 using anti-6X His antibody. c) SDS-PAGE silver nitrate staining of OsXTH30 protein fractions between 45 and 71. d) SDS-PAGE silver nitrate staining of OsXTH30 protein fractions between 72 and 89. e) Silver nitrate staining of OsXTH30 protein fraction that were separated into 3 pools as; Fractions 45-56 (pool 1), fractions 57-65 (pool 2) and fractions 66-101 (pool3). Protein marker band sizes and fraction numbers are indicated on the image.



#### 4.1.2.4. Bradford Assay and the Enzyme Activity Analysis

Standard curve was graphed using the BSA standards with 0.6, 0.4, 0.1 and 0.05 mg/ml concentrations (Fig 4.11). Protein concentration of the 3 pools were calculated according to the standard curve equation.

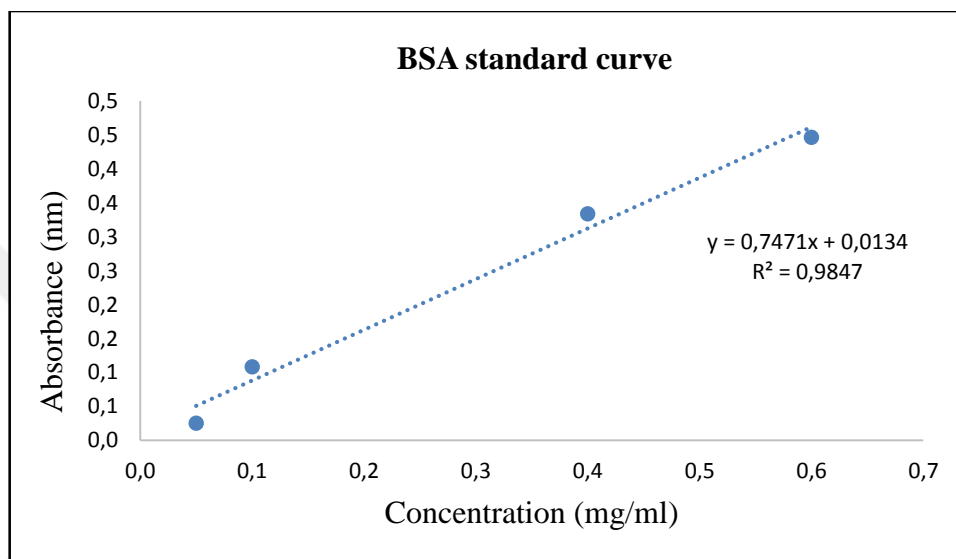


Figure 4.11. Standard curve of Bradford assay using BSA measured at 595 nm.

Table 4.5. Protein concentrations of purified OsXTH30 enzyme pools.

Sample Name	Protein concentration (mg/ml)
Pool 1 (45-56)	0
Pool 2 (57-65)	0,023
Pool 3 (66-101)	0,094

The activities of the fraction were tested with TXG-XGO donor- acceptor couple and the enzymatic activity of the product was measured using a HPLC system fluorescence detector and quantified as fluorescence quantities (Figure 4.12).

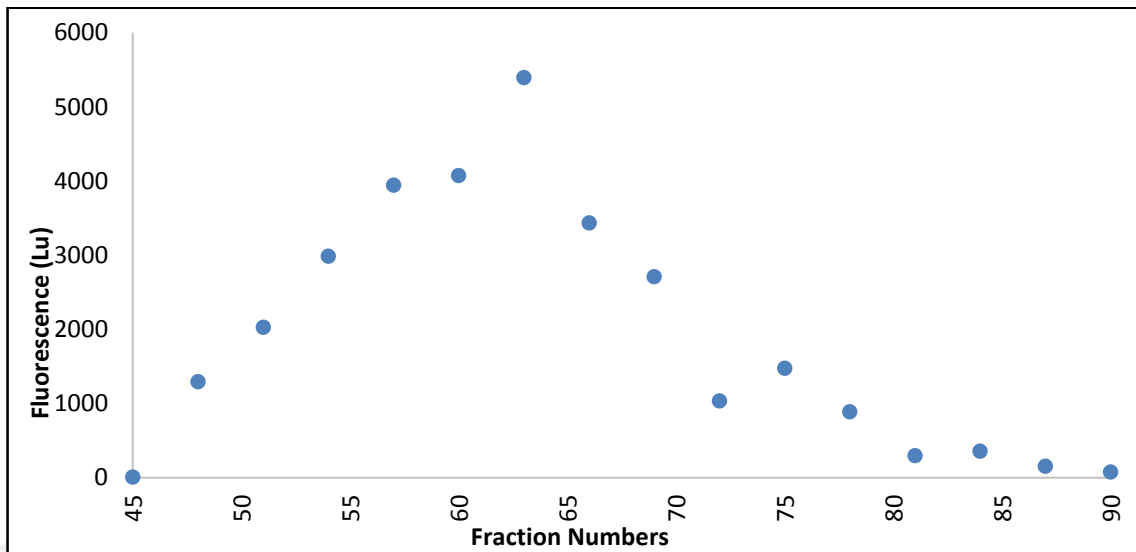
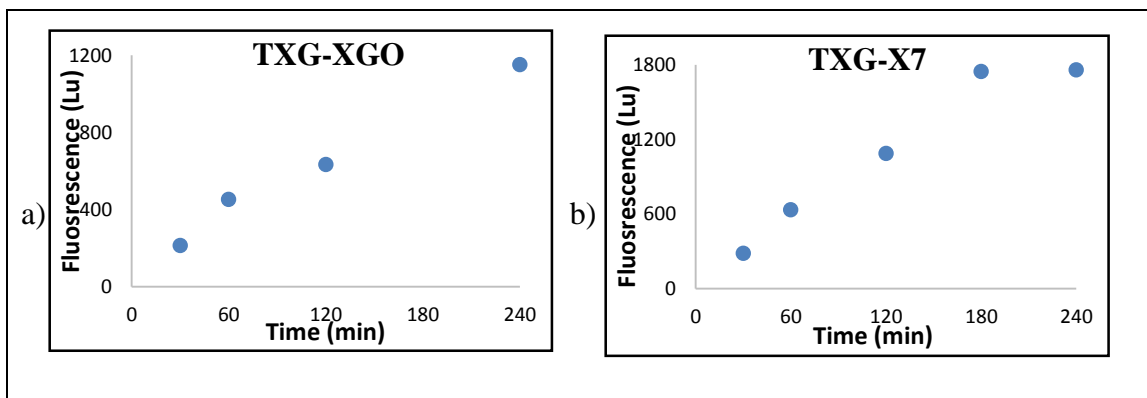


Figure 4. 12. Enzyme activity results of the OsXTH30 enzyme after the GE Healthcare Superdex 75 16/100 gel filtration column. Enzyme reactions were set by using TXG-XGO donor-acceptor couples detected by the HPLC.

The concentration of OsXTH30 enzyme pools was measured by the BSA assay (Table 4.5.). As a result of the Bradford analysis, it was determined that sufficient amounts of protein was not obtained to continue analyzes. However, activity tests were performed with pairs of TXG-XGO, TXG-X7, HEC-XGO and HEC-X7 donor-acceptor pairs for the specific activity using with pool 2 enzyme fractions (Figure 4.13.).



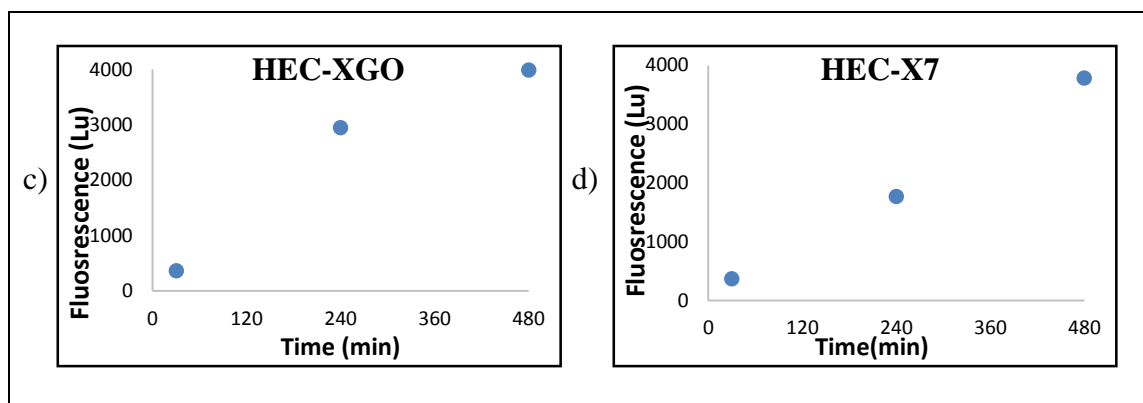


Figure 4.13. The enzyme activity-time plot of different polysaccharide-oligosaccharide substrate pairs of OsXTH30 enzyme. a) The enzyme activity-time plot drawn with the amount of the area calculated at 30, 60, 120, 240 minutes of the TXG-XGO substrate pair. b) The enzyme activity-time plot drawn with the amount of the area calculated at 30, 60, 120, 240 minutes of the TXG-X7 substrate pair. c) The enzyme activity-time plot drawn with the amount of the area calculated at 30, 240, 480 minutes of the HEC-XGO substrate pair. d) The enzyme activity-time plot drawn with the amount of the area calculated at 30, 60, 120, 240 minutes of the TXG-X7 substrate pair.

As a result of the activity tests, it was observed that the OsXTH30 enzyme lost its activity over time and it was decided that amount of the activity was not enough to continue the enzyme kinetic studies.

## 4.2. CHARACTERIZATION OF BDXTH2

### 4.2.1. pH Optimization

BdXTH2 enzyme was heterologously expressed previously and gathered into 3 different pools. In order to determine the optimum activity of the BdXTH2 enzyme, optimum pH of the enzyme must be determined. McIlvaine buffer was used with wide range of pH values. Enzyme activities were detected with pool 1 and TXG-XGO reactions at 30°C for 60 min with HPLC system.

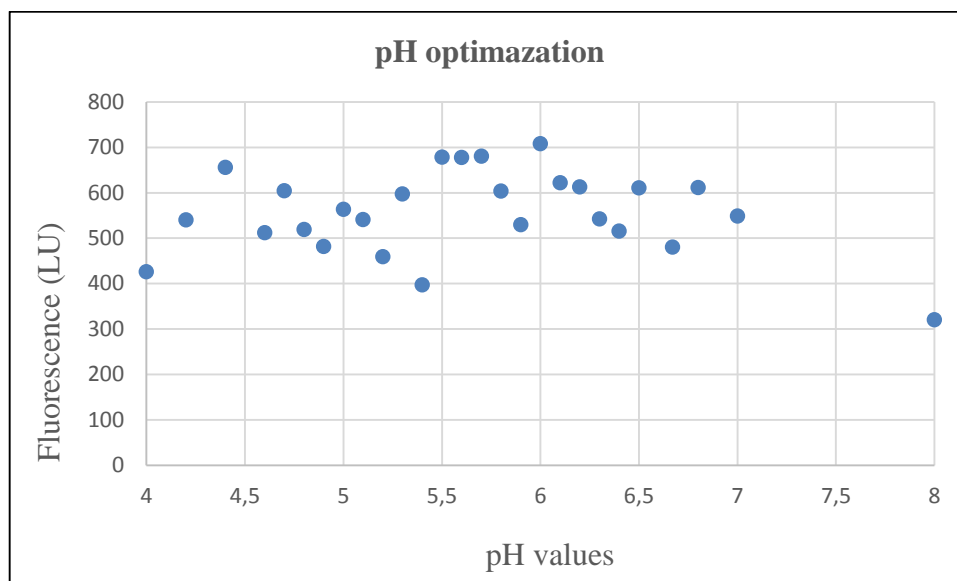


Figure 4.14. pH optimization of the BdXTH2 by using the TXG-XGO couples that have different pH values prepared with McIlvaine buffers.

The optimum pH value was selected for BdXTH2 enzyme as 6 and the enzyme activities were performed in this pH (Figure 4.14).

#### 4.2.2. Enzyme Activity Analysis

Specific enzyme activity of the BdXTH2 enzyme was determined using with pool 2. Different substrate couples were tested and activities were indicated as picokatal/mg. Specific activities of TXG, HEC and BBG donors with XGO acceptor couples were calculated. TXG-X7 couple was showed higher activity than the TXG-XGO. HEC-XGO and BBG-BB couple was exhibited the highest activity.

Table 4.6 Specific enzyme activity of BdXTH2 with different substrate couples. Specific activities were calculated according to the TXG-XGO percentage.

<b>Donor-acceptor couple</b>	<b>Specific Activity (Picokatal/mg protein)</b>	<b>Relative activity of %TXG-XGO</b>	<b>Relative activity of %HEC-XGO</b>	<b>Relative activity of %BBG-XGO</b>
TXG-BA	1,746	4,621		
TXG-BB	6,582	17,423		
TXG-BC	3,647	9,655		
TXG-CT	4,149	10,982		
TXG-GM	0,752	1,991		
TXG-LT	0,566	1,499		
TXG-XT	4,347	11,508		
TXG-X7	37,777	100,000		
TXG-XGO	35,175	93,113		
HEC-BA	6,766	17,911	37,018	
HEC-BB	11,050	29,250	60,452	
HEC-BC	5,209	13,789	28,499	
HEC-CT	9,010	23,849	49,291	
HEC-XT	3,826	10,127	20,931	
HEC-X7	15,829	41,901	86,600	
HEC-XGO	18,278	48,385	100,000	
BBG-BA	2,484	6,575		30,344
BBG-BB	8,186	21,668		100,000
BBG-BC	5,017	13,280		61,291
BBG-CT	5,079	13,446		62,054
BBG-LT	1,662	4,398		20,299
BBG-XT	3,350	8,867		40,921
BBG-XGO	5,671	15,012		69,282
WA-X7	0,001	0,003		
WA-XGO	0,001	0,004		

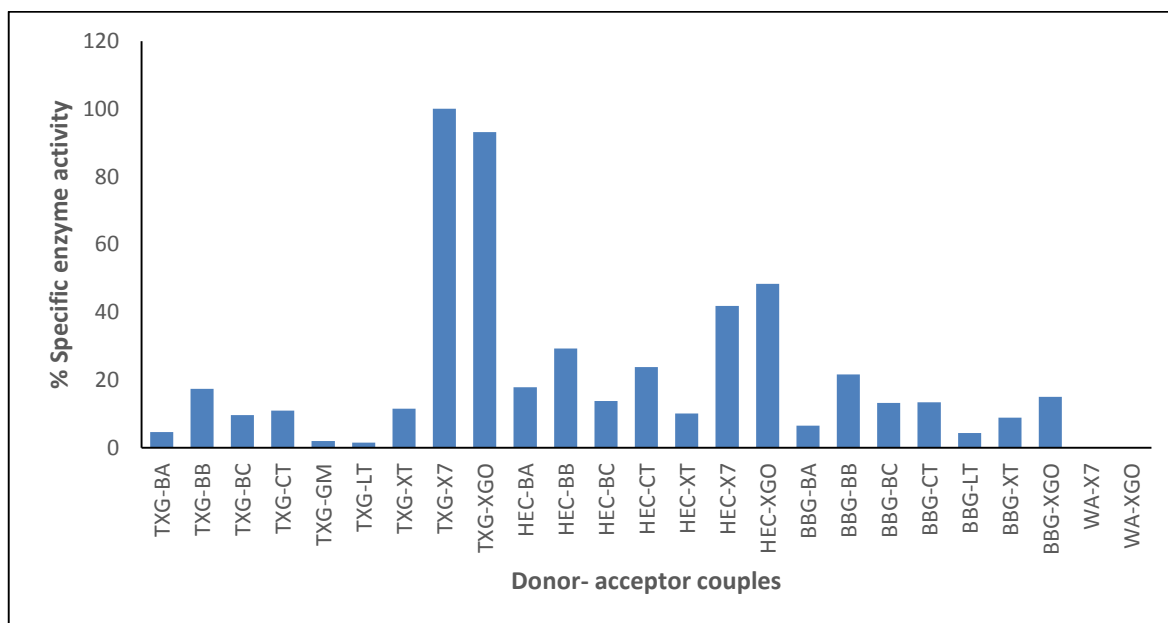


Figure 4.15. Relative Specific enzyme activities of BdXTH2 according to the Table 4.6. TXG-XGO couple was used for comparison.

### 4.2.3. Kinetic Studies

Kinetic studies were carried out with the TXG-X7 and HEC-X7 donor acceptor couples with since they have high specific activities. In order to continue kinetic studies, maximum activity giving reaction conditions must be determined. For this purpose optimum TXG concentration were determined. The activity of different TXG concentrations from 0.8% w:v to 0.1% w:v were tested in order to prevent negative affect of the viscosity with 50 $\mu$ M of X7. BdXTH2 enzyme were tested with pool 3 with 1/70 dilution in 1 hour reaction.

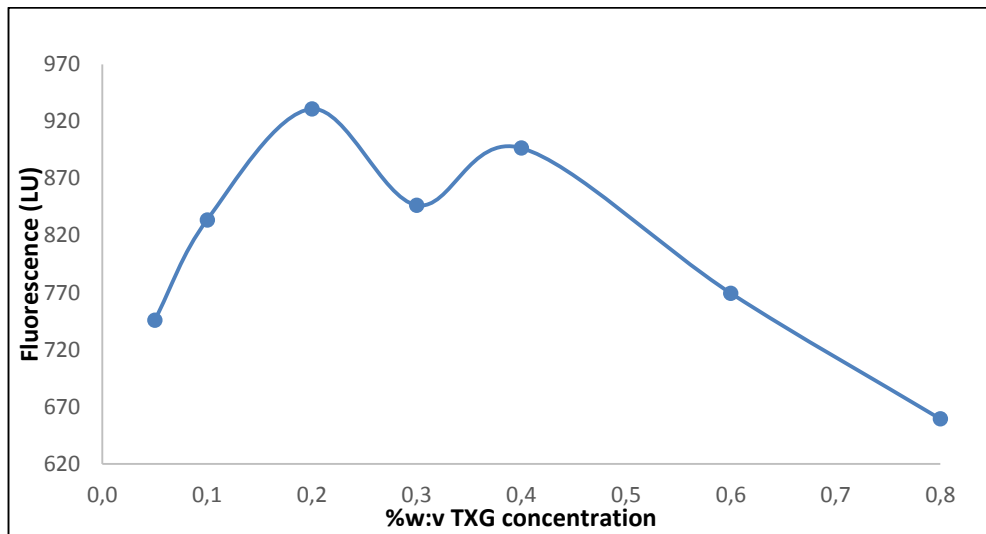


Figure 4.16. Detection of the optimum TXG concentration using with 50 $\mu$ M of X7 for BdXTH2 activity.

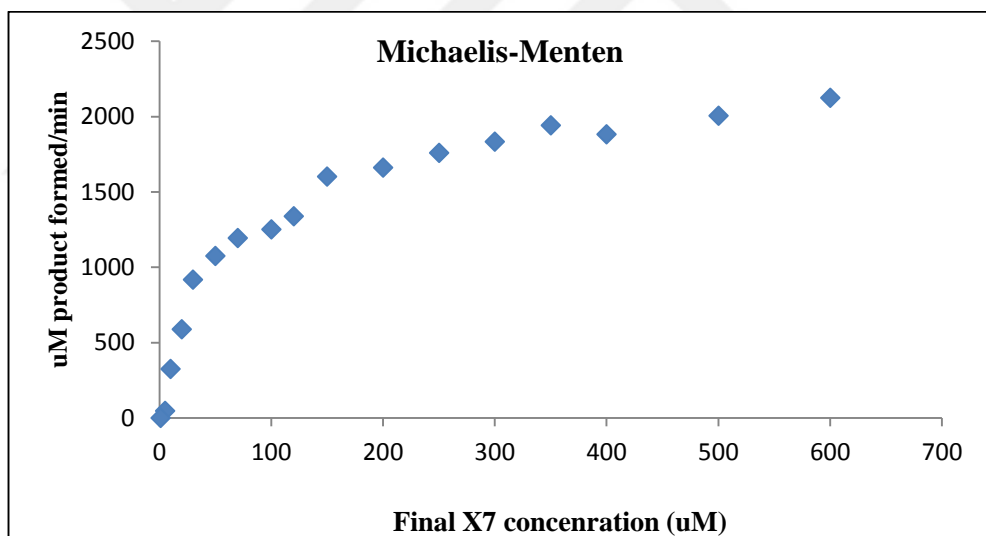


Figure 4.17. Detection of the optimum X7 concentration with %0.2 w:v of TXG for BdXTH2 activity.

The optimum TXG substrate concentration was selected as 0.2 % (Figure 4.16) and with this concentration the optimum substrate concentration was calculated.

The activity of different concentrations of X7 substrate from 1  $\mu$ M to 600  $\mu$ M were tested with 0.2% w:v of TXG. According to the Michaelis-Menten graph, the curve was reached to plateau phase at 250  $\mu$ M of X7 concentration (Figure 4.17).

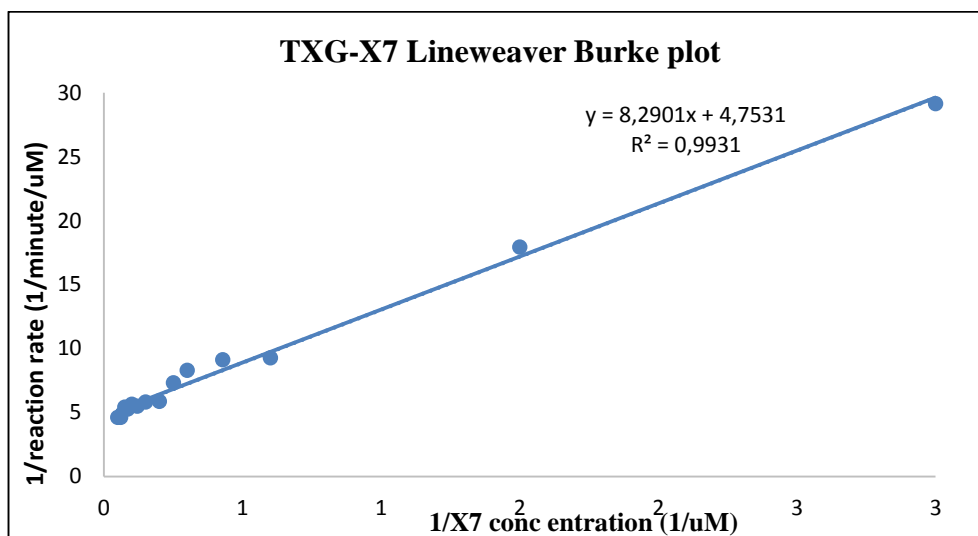


Figure 4.18. Lineweaver-Burke graph of BdXTH2 enzyme with 0.2% of TXG with various X7 concentration.

Kinetic calculations of BdXTH2 enzyme were calculated based on the TXG-X7 Lineweaver-Burk graph (Figure 4.18). As a result of kinetic studies with the TXG-X7 couple, it was calculated that BdXTH2 enzyme had  $V_{max}$  value 0,2104  $\mu\text{M}/\text{min}$ ,  $K_m$  value 1,74  $\mu\text{M}$  and  $K_{cat}$  value 104188,1905  $\text{min}^{-1}$ .

### 4.3. PRODUCTION AND PURIFICATION OF OSEG16-31 AND HVEG16-10

#### 4.3.1. Positive Colony Selection of OsEG16-31 and HvEG16-10

Linearized pPICZ $\alpha$ -C/OsEG16-31 and pPICZ $\alpha$ -C/HvEG16-10 were transformed into *Pichia pastoris* then plated in YPDS agar plates with Zeocin antibiotic. 18 colonies were picked from the each enzyme plates and they were subcultured again in YPDS agar plates with Zeocin. After the transformant *P. pastoris* colonies were grown for 4 days at 30°C each of the colonies were incubated in 10 ml of BMGY medium. Then cells were transferred to 10 ml of BMMY medium with 1% methanol addition for 5 days. TCA acetone precipitation was performed to 18 of the selected colonies in order the precipitate OsEG16-31 and HvEG16-10 proteins.



The activity of the colonies of OsEG16-31 and HvEG16-10 proteins and protein expressions of the first 9 colonies were visualized by the enzyme activity assay and SDS-PAGE analysis and Western blotting (Figure 4.17).

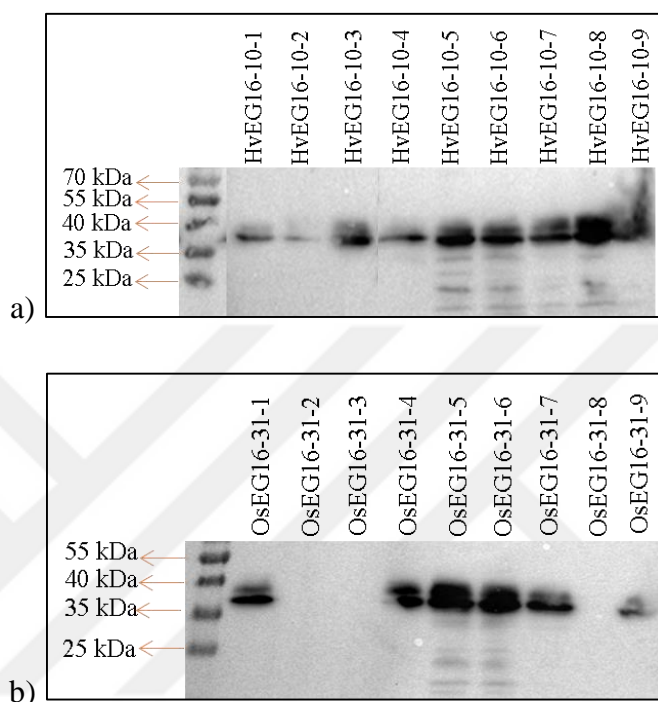


Figure 4.19. Detection of heterologously expressed HvEG16 and OsEG1631 enzymes of selected colonies using polyacrylamide gel electrophoresis. a) Western blot analysis of HvEG16 colonies between 1 and 9 using 6X-His tag antibody. b) Western blot analysis of OsEG1631 colonies between 1 and 9 using 6X-His tag antibody.

Colonies of HvEG16-10 from 1 to 4 have protein bands as between 33.2 kDa as expected and colonies from 5 to 9 were also visualized between 35-40 kDa but with other impurities. OsEG16-31 colony numbers of 1, 4, 5, 6, 7 and 9 have shown protein bands with other impurities mainly between 35-40 kDa (Figure 4.19).

Although both OsEG16-31 and HvEG16-10 colonies were observed to have protein expressions in some of the colonies when the enzyme activities were tested, there were not any activity observed with HPLC. Therefore, big scale production and enzyme activity analysis could not achieved.

## 5. DISCUSSION

The main aim of this study is to examine the various groups of XTH enzymes, their substrate specificities and mechanism of action of active site configurations. XTH enzymes are being explored extensively all over the world due to the growing evidence and distribution on the importance of various plant cell wall processes. It has been reported that XTH has many roles such as seed germination, fruit ripening, and protection from abiotic stresses, cell enlargement and strengthening in the cell wall [113,120–123]. However, sufficient studies have not been made on substrate specificity and substrate binding about the heterotransglycosylation activity of these enzymes. Substrate specificity of these enzymes will be useful for plant studies if information about the mode of action is obtained.

XTH enzymes are part of the CAZy Glycoside Hydrolase 16 family according to their protein sequences [124]. There are other enzymes that catalyze transglycosylation reactions in the family but XTHs are the only plant based sequences [125]. For this reason, it can provide valuable information on XTH genes evolution from hydrolases and the mechanism of substrate linkage and preference. This study investigated the impact of XTH that obtained from OsXTH30, OsEG16-31 (*Oryza sativa*), BdXTH2 (*Brachypodium distachyon*) and HvEG16-10 (*Hordeum vulgare*) to the substrate recognition, binding and cleavage mechanism. These enzymes were tried to fully be characterized after they have been heterologously expressed by *P. pastoris*.

One of the problematic factors about the process of heterologous expression system was optimizing the yeast expression. The temperature, methanol addition, incubation time of the heterologous expression system was optimized in order to obtain active enzyme producing colonies.

The production of OsXTH30 was performed firstly with the cloning of OsXTH30 gene to pPICZ $\alpha$ -C vector. After achieving inserting OsXTH30 gene successfully into pPICZ $\alpha$ -C, plasmids were transformed to *P. pastoris*. In order to expressing target enzymes AOX1 promoter was upregulated by %1 of methanol induction. The big scale expression of OsXTH30 with BMMY was performed and the protein production was purified with chromatography steps. After the purification of OsXTH30 protein, sufficient amount of activity could not observed to continue for enzyme kinetic studies. The chromatography

steps may cause the problem. The pH value of the buffer solutions for eliminating protein from the columns could have change by the temperature. The other reason being unsuccessful purification step could be from the elution step. His-tagged proteins may stuck to the column and could not be eluted from the column. Also methanol addition may not enough to promote AOX1 and the express the proteins. Additionally, protein folding could change the result of the activities. There could be protease contamination problem that inhibits the expression of the enzymes and resulted the degradation of the proteins. For this reason kinetic studies of OsXTH30 enzyme could not achieved since there was not enough activity to continue. However there were enough activity to observe reactions of TXG-XGO, TXG-X7, HEC-XGO and HEC-X7 donor acceptor substrate couples (Figure 4.13).

In order to observe proteins SDS-PAGE, western blot and silver nitrate staining were performed. However the theoretically calculated molecular weights of the targeted enzymes were generally not achieved. It was assumed that glycosylation of the proteins may cause the extension of the molecular weight.

OsEG16-31 and HvEG16-10 enzymes were also produced by heterologous expression by *P. pastoris*. After small scale production of these enzymes there were colonies that assumed to express target protein. Although there were not any transferase activity by the HPLC measurements. It was presumed that these EG16 family genes may have hydrolase activity that could have checked by the ELSD detector.

The BdXTH2 enzyme which produced and purified by another member of our study group was successfully characterized. Specific activities and relative activities of the donor-acceptor substrate couples were calculated. TXG-X7 donor-acceptor couple was shown the highest activity among the others. BdXTH2 has also showed 93.1 % relative activity with TXG-XGO couple compared to TXG-X7. The second donor that showed the highest activity was HEC. HEC-XGO couple have the highest activity among the HEC couples. Also HEC-X7 couples were detected as 41.9% relative activity. Lastly, BdXTH2 was observed to have % 21.7 of BBG-BB and % 15 of BBF-XGO activity.

Optimum concentrations of TXG and X7 substrates were selected for the kinetic studies of BdXTH2. The highest activity was observed with 0.2% of TXG. When the donor concentration exceed 0.4%, viscosity was also increased and caused reduction in enzyme activity.

Michaelis-Menten graph was used in order to select final concentration of X7 as 280  $\mu\text{M}$  for gaining optimum enzyme activity. Then Lineweaver-Burke graph was used for kinetic calculations. The maximum rate;  $V_{\text{max}}$  of BdXTH2 with TXG-X7 was calculated as 0.2104  $\mu\text{M}/\text{min}$ ,  $K_{\text{m}}$  value was 1,74  $\mu\text{M}$  and  $K_{\text{cat}}$  value was 104188,1905  $\text{min}^{-1}$ .

As a result, BdXTH2 enzyme characterization and kinetic studies were accomplished successfully. Due to the problem of production and purification, OsXTH30, OsEG16-31 and HvEG16-10 enzymes could not be characterized. For further studies OsXTH30, OsEG16-31 and HvEG16-10 could be expressed by using different expression system.



## 6. CONCLUSION

The plant cell wall in which XTH enzymes are active is the most important part of the plant that protects itself from environmental factors and interacts with the environment. It is important to understand the structures, functions and interactions of carbohydrates and proteins in the plant cell wall in order to increase yield and to protect the plant from external stresses and to manipulate the plant properties. OsEG16-31 and HvEG16-10 enzymes should show hydrolase activity but that activity could not be observed with the HPLC fluorescence detector. Active BdXTH2 enzyme was successfully expressed and purified and it showed the highest activity with the TXG-X7 substrate couple. The other donor acceptor couples where the BdXTH2 enzyme was highly active were HEC-XGO and BBG-BB.

The kinetic studies of XTH enzymes and substrate preference may play an important role in plant preference for breeders. It will also provide invaluable information on how the existing higher plant XTH genes can be modified to alter substrate binding properties. The information gained in this study may lead to the cell walls of plants containing beta-glucan, especially barley, wheat, rice and maize, to be modified for cell growth, nutrition, stress tolerance and biofuels. This may lead to cis-genic approaches that are more attractive to consumers.

## REFERENCES

- [1] N. Farrokhi, R.A. Burton, L. Brownfield, M. Hrmova, S.M. Wilson, A. Bacic, G.B. Fincher, Plant cell wall biosynthesis: Genetic, biochemical and functional genomics approaches to the identification of key genes, *Plant Biotechnol. J.*, 4: 145–167, 2006.
- [2] N.C. Carpita, M. Defernez, K. Findlay, B. Wells, D. a Shoue, G. Catchpole, R.H. Wilson, M.C. McCann, Cell wall architecture of the elongating maize coleoptile, *Plant Physiol.*, 127: 551–565, 2001.
- [3] A.H. Liepman, R. Wightman, N. Geshi, S.R. Turner, H.V. Scheller, Arabidopsis - A powerful model system for plant cell wall research, *Plant J.*, 61: 1107–1121, 2010.
- [4] Z.A. Popper, Evolution and diversity of green plant cell walls, *Curr. Opin. Plant Biol.*, 11: 286–292, 2008.
- [5] R.A. Burton, G.B. Fincher, Plant cell wall engineering: Applications in biofuel production and improved human health, *Curr. Opin. Biotechnol.*, 26: 79–84, 2014.
- [6] C. Somerville, S. Bauer, G. Brininstool, M. Facette, T. Hamann, J. Milne, E. Osborne, A. Paredez, S. Persson, T. Raab, S. Vorwerk, H. Youngs, Toward a Systems Approach to Understanding Plant Cell Walls, *Science (80-. )*, 306: 2206–2211, 2004.
- [7] S. Vorwerk, S. Somerville, C. Somerville, The role of plant cell wall polysaccharide composition in disease resistance, *Trends Plant Sci.*, 9: 203–209, 2004.
- [8] H. Motose, M. Sugiyama, H. Fukuda, A proteoglycan mediates inductive interaction during plant vascular development, *Nature*, 429: 873–878, 2004.
- [9] Q. Hall, M.C. Cannon, The cell wall hydroxyproline-rich glycoprotein RSH is essential for normal embryo development in Arabidopsis, *Plant Cell*, 14: 1161–1172, 2002.
- [10] W.D. Reiter, Biosynthesis and properties of the plant cell wall, *Curr. Opin. Plant Biol.*, 5: 536–542, 2002.
- [11] Z.A. Popper, S.C. Fry, Widespread occurrence of a covalent linkage between xyloglucan and acidic polysaccharides in suspension-cultured angiosperm cells, *Ann. Bot.*, 96: 91–99, 2005.
- [12] D.J. Cosgrove, Growth of the plant cell wall, *Nat. Rev. Mol. Cell Biol.*, 6: 850–861, 2005.
- [13] J. Vogel, K. Keegstra, M. Pauly, Unique aspects of the grass cell wall This review comes from a themed issue on Physiology and metabolism Edited, *Curr. Opin. Plant*

- Biol.*, 11: 301–307, 2008.
- [14] I.M. Saxena, R.M. Brown, Cellulose biosynthesis: Current views and evolving concepts, *Ann. Bot.*, 96: 9–21, 2005.
- [15] M.S. Doblin, I. Kurek, D. Jacob-Wilk, D.P. Delmer, Cellulose biosynthesis in plants: From genes to rosettes, *Plant Cell Physiol.*, 43: 1407–1420, 2002.
- [16] O. Lerouxel, D.M. Cavalier, A.H. Liepman, K. Keegstra, Biosynthesis of plant cell wall polysaccharides - a complex process, *Curr. Opin. Plant Biol.*, 9: 621–630, 2006.
- [17] T. Arioli, L. Peng, A.S. Betzner, J. Burn, W. Wittke, W. Herth, C. Camilleri, J. Plazinski, R. Birch, A. Cork, J. Glover, J. Redmond, R.E. Williamson, Molecular Analysis of Cellulose Biosynthesis in Arabidopsis, *Science (80-. )*, 279: 717–720, 1998.
- [18] K. Keegstra, J. Walton,  $\beta$ -Glucans—Brewer’s Bane, Dietician ’ s Delight, *Science (80-. )*, 311: 1872–1873, 2006.
- [19] S. Djerbi, M. Lindskog, L. Arvestad, F. Sterky, T.T. Teeri, The genome sequence of black cottonwood (*Populus trichocarpa*) reveals 18 conserved cellulose synthase (CesA) genes, *Planta*, 221: 739–746, 2005.
- [20] R.A. Burton, N.J. Shirley, B.J. King, A.J. Harvey, G.B. Fincher, The CesA gene family of barley Quantitative analysis of transcripts reveals two groups of co-expressed genes, *Plant Physiol.*, 134: 224–236, 2004.
- [21] J.E. Burn, Functional Analysis of the Cellulose Synthase Genes CesA1, CesA2, and CesA3 in Arabidopsis, *PLANT Physiol.*, 129: 797–807, 2002.
- [22] N.G. Taylor, R.M. Howells, A.K. Huttly, K. Vickers, S.R. Turner, Interactions among three distinct CesA proteins essential for cellulose synthesis, *Proc. Natl. Acad. Sci.*, 100: 1450–5, 2003.
- [23] D.J. Cosgrove, Growth of the plant cell wall, *Nat. Rev. Mol. Cell Biol.*, 6: 850–861, 2005.
- [24] C. Lloyd, J. Chan, Microtubules and the shape of plants to come, *Nat. Rev. Mol. Cell Biol.*, 5: 13–22, 2004.
- [25] T. a Richmond, C.R. Somerville, The cellulose synthase superfamily, *Plant Physiol.*, 124: 495–498, 2000.
- [26] R. a Burton, S. a Jobling, A.J. Harvey, N.J. Shirley, D.E. Mather, A. Bacic, G.B. Fincher, The genetics and transcriptional profiles of the cellulose synthase-like HvCslF gene family in barley, *Plant Physiol.*, 146: 1821–1833, 2008.

- [27] M.S. Doblin, F.A. Pettolino, S.M. Wilson, R. Campbell, R.A. Burton, G.B. Fincher, E. Newbigin, A. Bacic, D.P. Delmer, A Barley Cellulose Synthase-Like CSLH Gene Mediates (1,3; 1,4)- $\beta$ -D-Glucan Synthesis in Transgenic Arabidopsis, *Proc. Natl. Acad. Sci. U. S. A.*, 106: 5996–6001, 2009.
- [28] K.S. Dhugga, R. Barreiro, B. Whitten, K. Stecca, J. Hazebroek, G.S. Randhawa, M. Dolan, A.J. Kinney, D. Tomes, S. Nichols, P. Anderson, Guar Seed B -Mannan Synthase Is a Member of the Cellulose Synthase Super Gene Family, *Science (80-. )*, 303: 363–367, 2004.
- [29] G.B. Fincher, Revolutionary Times in Our Understanding of Cell Wall Biosynthesis and Remodeling in the Grasses, *Plant Physiol.*, 149: 27–37, 2009.
- [30] S.P. Hazen, J.S. Scott-Craig, J.D. Walton, Cellulose synthase-like (CSL) genes of rice, *Plant Physiol.*, 128: 336–340, 2002.
- [31] Y.S.Y. Hsieh, P.J. Harris, Xyloglucans of monocotyledons have diverse structures, *Mol. Plant*, 2: 943–965, 2009.
- [32] T.J. Bootten, P.J. Harris, L.D. Melton, R.H. Newman, Solid-state  $^{13}\text{C}$ -NMR spectroscopy shows that the xyloglucans in the primary cell walls of mung bean (*Vigna radiata* L) occur in different domains: A new model for xyloglucan-cellulose interactions in the cell wall, *J. Exp. Bot.*, 55: 571–583, 2004.
- [33] J.K.C. Rose, J. Braam, S.C. Fry, K. Nishitani, The XTH family of enzymes involved in xyloglucan endotransglucosylation and endohydrolysis: Current perspectives and a new unifying nomenclature, *Plant Cell Physiol.*, 43: 1421–1435, 2002.
- [34] Y. Kato, Matsuda Kazuo, Structural Investigation of  $\beta$ -D-glucan and Xyloglucan from Bamboo-Shoot Cell-Walls, *Carbohydr. Res.*, 109: 233–248, 1982.
- [35] Y. Kato, K. Matsuda, G. Xyl Xyl Xyl, G. — Xyl, -c Glc —, Bullet. Glc Glc —, B. Glc, B. Glc —, Xyloglucan in the Cell Walls of Suspension-Cultured Rice Cells "I", *Plant Cell Physiol*, 26: 4–3, 1985.
- [36] T. Hayashi, Xyloglucans in the Primary Cell Wall, *Annu. Rev. Plant Physiol. Plant Mol. Biol.*, 40: 139–168, 1989.
- [37] M.J. Peña, A.G. Darvill, S. Eberhard, W.S. York, M.A. O'Neill, Moss and liverwort xyloglucans contain galacturonic acid and are structurally distinct from the xyloglucans synthesized by hornworts and vascular plants, *Glycobiology*, 18: 891–904, 2008.
- [38] S.C. Fry, W.S. York, P. Albersheim, A. Darvill, T. Hayashi, J. ???P Joseleau, Y. Kato,



- E.P. Lorences, G.A. Maclachlan, M. McNeil, A.J. Mort, J.S. Grant Reid, H.U. Seitz, R.R. Selvendran, A.G.J. Voragen, A.R. White, An unambiguous nomenclature for xyloglucan derived oligosaccharides, *Physiol. Plant.*, 89: 1–3, 1993.
- [39] S.T. Tuomivaara, K. Yaoi, M.A. O'Neill, W.S. York, Generation and structural validation of a library of diverse xyloglucan-derived oligosaccharides, including an update on xyloglucan nomenclature, *Carbohydr. Res.*, 402: 56–66, 2015.
- [40] A. Schultink, L. Liu, L. Zhu, M. Pauly, Structural diversity and function of xyloglucan sidechain substituents, *Plants*, 3: 526–542, 2014.
- [41] D.M. Gibeaut, M. Pauly, A. Bacic, G.B. Fincher, Changes in cell wall polysaccharides in developing barley (*Hordeum vulgare*) coleoptiles, *Planta*, 221: 729–738, 2005.
- [42] M. Hoffman, Z. Jia, M.J. Peña, M. Cash, A. Harper, A.R. Blackburn, A. Darvill, W.S. York, Structural analysis of xyloglucans in the primary cell walls of plants in the subclass Asteridae, *Carbohydr. Res.*, 340: 1826–1840, 2005.
- [43] N. Obel, V. Erben, T. Schwarz, S. Kühnel, A. Fodor, M. Pauly, Microanalysis of plant cell wall polysaccharides, *Mol. Plant*, 2: 922–932, 2009.
- [44] S. Gille, A. de Souza, G. Xiong, M. Benz, K. Cheng, A. Schultink, I.-B. Reca, M. Pauly, O-acetylation of Arabidopsis hemicellulose xyloglucan requires AXY4 or AXY4L, proteins with a TBL and DUF231 domain, *Plant Cell*, 23: 4041–53, 2011.
- [45] L. von Schantz, F. Gullfot, S. Scheer, L. Filonova, L. Cicortas Gunnarsson, J. Flint, G. Daniel, E. Nordberg-Karlsson, H. Brumer, M. Ohlin, Affinity maturation generates greatly improved xyloglucan-specific carbohydrate binding modules, *BMC Biotechnol.*, 9: 92, 2009.
- [46] M. Pauly, L.N. Andersen, S. Kauppinen, L. V Kofod, W.S. York, P. Albersheim, a Darvill, A xyloglucan-specific endo-beta-1,4-glucanase from *Aspergillus aculeatus*: expression cloning in yeast, purification and characterization of the recombinant enzyme, *Glycobiology*, 9: 93–100, 1999.
- [47] M. Hrmova, V. Farkas, A.J. Harvey, J. Lahnstein, B. Wischmann, N. Kaewthai, I. Ezcurra, T.T. Teeri, G.B. Fincher, Substrate specificity and catalytic mechanism of a xyloglucan xyloglucosyl transferase HvXET6 from barley (*Hordeum vulgare* L), *FEBS J.*, 276: 437–456, 2009.
- [48] M.C. McCann, B. Wells, K. Roberts, Direct visualization of cross-links in the primary plant cell wall, *J. Cell Sci.*, 96: 323–334, 1990.
- [49] O. a. Zabolina, Xyloglucan and Its Biosynthesis, *Front. Plant Sci.*, 3: 2008–2012,

- 2012.
- [50] M.S. Buckeridge, C. Rayon, B. Urbanowicz, M.A.S. Tiné, N.C. Carpita, Mixed Linkage (1→3),(1→4)-β- d -Glucans of Grasses, *Cereal Chem.*, 81: 115–127, 2004.
- [51] S.C. Fry, K.E. Mohler, B.H.W.A. Nesselrode, L. Franková, Mixed-linkage β-glucan: Xyloglucan endotransglucosylase, a novel wall-remodelling enzyme from Equisetum (horsetails) and charophytic algae, *Plant J.*, 55: 240–252, 2008.
- [52] T.J. Simmons, D. Uhrín, T. Gregson, L. Murray, I.H. Sadler, S.C. Fry, An unexpectedly lichenase-stable hexasaccharide from cereal, horsetail and lichen mixed-linkage β-glucans (MLGs): Implications for MLG subunit distribution, *Phytochemistry*, 95: 322–332, 2013.
- [53] A. Iurlaro, G. Dalessandro, G. Piro, J.G. Miller, S.C. Fry, M.S. Lenucci, Evaluation of glycosidic bond cleavage and formation of oxo groups in oxidized barley mixed-linkage β-glucans using tritium labelling, *Food Res. Int.*, 66: 115–122, 2014.
- [54] A. Lazaridou, C.G. Biliaderis, Molecular aspects of cereal β-glucan functionality: Physical properties, technological applications and physiological effects, *J. Cereal Sci.*, 46: 101–118, 2007.
- [55] P.J. Wood, Cereal β-glucans in diet and health, *J. Cereal Sci.*, 46: 230–238, 2007.
- [56] N.C. Carpita, M.C. McCann, The functions of cell wall polysaccharides in composition and architecture revealed through mutations, *Plant Soil*, 247: 71–80, 2002.
- [57] D.U. Lima, W. Loh, M.S. Buckeridge, Xyloglucan-cellulose interaction depends on the sidechains and molecular weight of xyloglucan, *Plant Physiol. Biochem.*, 42: 389–394, 2004.
- [58] N.C. Carpita, M.C. McCann, The Maize Mixed-Linkage (1→3),(1→4)- β-D-Glucan Polysaccharide Is Synthesized at the Golgi Membrane, *Plant Physiol.*, 153: 1362–1371, 2010.
- [59] I. Sørensen, F.A. Pettolino, S.M. Wilson, M.S. Doblin, B. Johansen, A. Bacic, W.G.T. Willats, Mixed-linkage (1,3),(1,4)-β-D-glucan is not unique to the Poales and is an abundant component of Equisetum arvense cell walls, *Plant J.*, 54: 510–521, 2008.
- [60] J.M. Labavitch, P.M. Ray, Structure of hemicellulosic polysaccharides of Avena sativa coleoptile cell walls, *Phytochemistry*, 17: 933–937, 1978.
- [61] S. Wada, P.M. Ray, Matrix polysaccharides of oat coleoptile cell walls, *Phytochemistry*, 17: 923–931, 1978.

- [62] C. Lee, Q. Teng, R. Zhong, Y. Yuan, Z.-H. Ye, Functional roles of rice glycosyltransferase family GT43 in xylan biosynthesis, *Plant Signal. Behav.*, 9: e27809, 2014.
- [63] H.V. Scheller, P. Ulvskov, Hemicelluloses, *Annu. Rev. Plant Biol.*, 61: 263–289, 2010.
- [65] A. Oikawa, H.J. Joshi, E.A. Rennie, B. Ebert, C. Manisseri, J.L. Heazlewood, H.V. Scheller, An integrative approach to the identification of arabidopsis and rice genes involved in xylan and secondary wall development, *PLoS One*, 5: 2010.
- [66] M. Bosch, C.D. Mayer, A. Cookson, I.S. Donnison, Identification of genes involved in cell wall biogenesis in grasses by differential gene expression profiling of elongating and non-elongating maize internodes, *J. Exp. Bot.*, 62: 3545–3561, 2011.
- [67] D. Chiniquy, V. Sharma, a. Schultink, E.E. Baidoo, C. Rautengarten, K. Cheng, a. Carroll, P. Ulvskov, J. Harholt, J.D. Keasling, M. Pauly, H. V. Scheller, P.C. Ronald, XAX1 from glycosyltransferase family 61 mediates xylosyltransfer to rice xylan, *Proc. Natl. Acad. Sci.*, 109: 17117–17122, 2012.
- [68] T. Jeoh, C.I. Ishizawa, M.F. Davis, M.E. Himmel, W.S. Adney, D.K. Johnson, Cellulase digestibility of pretreated biomass is limited by cellulose accessibility, *Biotechnol. Bioeng.*, 98: 112–122, 2007.
- [69] B. Yang, C.E. Wyman, Effect of Xylan and Lignin Removal by Batch and Flowthrough Pretreatment on the Enzymatic Digestibility of Corn Stover Cellulose, *Biotechnol. Bioeng.*, 86: 88–95, 2004.
- [70] S. Manna, B.H. McAnalley, Determination of the position of the O-acetyl group in a  $\beta$ -(1  $\rightarrow$  4)-mannan (acemannan) from *Aloe barbardensis* Miller, *Carbohydr. Res.*, 241: 317–319, 1993.
- [71] I.C.M. Dea, A. Morrison, Chemistry and Interactions of Seed Galactomannans, *Adv. Carbohydr. Chem. Biochem.*, 31: 241–312, 1975.
- [72] H. Zhang, K. Nishinari, M.A.K. Williams, T.J. Foster, I.T. Norton, A molecular description of the Gelation Mechanism of Konjac Mannan, *Int. J. Biol. Macromol.*, 30: 7–16, 2002.
- [73] T.R. Society, R. Society, B. Sciences, Non-Cellulosic Structural Polysaccharides in Algal Cell Walls III Mannan in Siphonous Green Algae Author ( s ): Eva Frei and R D Preston Source : Proceedings of the Royal Society of London Series B , Biological Sciences , Vol 169 , No Publi, 169: 127–145, 2013.

- [74] H. Meier, J.S.G. Reid, Reserve Polysaccharides Other Than Starch in Higher Plants, *Plant Carbohydrates I*, i: 418–471, 1982.
- [75] M.G. Handford, T.C. Baldwin, F. Goubet, T.A. Prime, J. Miles, X. Yu, P. Dupree, Localisation and characterisation of cell wall mannan polysaccharides in *Arabidopsis thaliana*, *Planta*, 218: 27–36, 2003.
- [76] A.H. Liepman, C.J. Nairn, W.G.T. Willats, I. Sorensen, A.W. Roberts, K. Keegstra, Functional Genomic Analysis Supports Conservation of Function Among Cellulose Synthase-Like A Gene Family Members and Suggests Diverse Roles of Mannans in Plants, *Plant Physiol.*, 143: 1881–1893, 2007.
- [77] I. Moller, I. Sørensen, A.J. Bernal, C. Blaukopf, K. Lee, J. Øbro, F. Pettolino, A. Roberts, J.D. Mikkelsen, J.P. Knox, A. Bacic, W.G.T. Willats, High-throughput mapping of cell-wall polymers within and between plants using novel microarrays, *Plant J.*, 50: 1118–1128, 2007.
- [78] F. Goubet, C.J. Barton, J.C. Mortimer, X. Yu, Z. Zhang, G.P. Miles, J. Richens, A.H. Liepman, K. Seffen, P. Dupree, Cell wall glucomannan in *Arabidopsis* is synthesised by CSLA glycosyltransferases, and influences the progression of embryogenesis, *Plant J.*, 60: 527–538, 2009.
- [79] B.L. Ridley, M.A. O’Neill, D. Mohnen, Pectins: Structure, biosynthesis, and oligogalacturonide-related signaling, *Phytochemistry*, 57: 929–967, 2001.
- [80] M.A. O’Neill, T. Ishii, P. Albersheim, A.G. Darvill, Rhamnogalacturonan II: structure and function of a borate cross-linked cell wall pectic polysaccharide, *Annu. Rev. Plant Biol.*, 55: 109–39, 2004.
- [81] T. Matsunaga, T. Ishii, S. Matsumoto, M. Higuchi, A. Darvill, P. Albersheim, M.A. O’Neill, Occurrence of the primary cell wall polysaccharide rhamnogalacturonan II in pteridophytes, lycophytes, and bryophytes Implications for the evolution of vascular plants, *Plant Physiol.*, 134: 339–351, 2004.
- [82] M.E. Himmel, S.-Y. Ding, D.K. Johnson, W.S. Adney, M.R. Nimlos, J.W. Brady, T.D. Foust, Biomass recalcitrance: engineering plants and enzymes for biofuels production, *Science*, 315: 804–7, 2007.
- [83] D. Mohnen, Pectin structure and biosynthesis, *Curr. Opin. Plant Biol.*, 11: 266–277, 2008.
- [84] M. Jackson, C. L., Dreaden, T. M., Theobald, L. K., Tran, N. M., Beal, T. L., Eid, Pectin induces apoptosis in human prostate cancer cells: Correlation of apoptotic

- function with pectin structure, *Glycobiology*, 17: 805–819., 2007.
- [85] K. Nishitani, R. Tominaga, Endo-xyloglucan transferase, a novel class of glycosyltransferase that catalyzes transfer of a segment of xyloglucan molecule to another xyloglucan molecule, *J. Biol. Chem.*, 267: 21058–21064, 1992.
- [86] N.M. Steele, Z. Sulová, P. Campbell, J. Braam, V. Farkas, S.C. Fry, Ten isoenzymes of xyloglucan endotransglycosylase from plant cell walls select and cleave the donor substrate stochastically, *Biochem. J.*, 355: 671–9, 2001.
- [87] M.M. Purugganan, J. Braam, S.C. Fry, The Arabidopsis TCH4 xyloglucan endotransglycosylase Substrate specificity, pH optimum, and cold tolerance, *Plant Physiol.*, 115: 181–190, 1997.
- [88] M. Hrmova, V. Farkas, J. Lahnstein, G.B. Fincher, A barley xyloglucan xyloglucosyl transferase covalently links xyloglucan, cellulosic substrates, and (1,3;1,4)- $\beta$ -D-glucans, *J. Biol. Chem.*, 282: 12951–12962, 2007.
- [89] T.J. Simmons, K.E. Mohler, C. Holland, F. Goubet, L. Franková, D.R. Houston, A.D. Hudson, F. Meulewaeter, S.C. Fry, Hetero-trans- $\beta$ -glucanase, an enzyme unique to Equisetum plants, functionalizes cellulose, *Plant J.*, 83: 753–769, 2015.
- [90] S.C. Fry, R.C. Smith, K.F. Renwick, D.J. Martin, S.K. Hodge, K.J. Matthews, Xyloglucan endotransglycosylase, a new wall-loosening enzyme activity from plants, *Biochem. J.*, 282 ( Pt 3: 821–8, 1992.
- [91] D.M. Antosiewicz, M.M. Purugganan, D.H. Polisensky, J. Braam, Cellular localization of Arabidopsis xyloglucan endotransglycosylase-related proteins during development and after wind stimulation, *Plant Physiol.*, 115: 1319–1328, 1997.
- [92] J.E. Thompson, S.C. Fry, Restructuring of wall-bound xyloglucan by transglycosylation in living plant cells, *Plant J.*, 26: 23–34, 2001.
- [93] J.E. Thompson, S.C. Fry, Trimming and solubilization of xyloglucan after deposition in the walls of cultured rose cells, *J. Exp. Bot.*, 48: 297–305, 1997.
- [94] R.J. Redgwell, S.C. Fry, Xyloglucan Endotransglycosylase Activity Increases during Kiwifruit (*Actinidia deliciosa*) Ripening (Implications for Fruit Softening), *Plant Physiol.*, 103: 1399–1406, 1993.
- [95] Y.B. Liu, S.M. Lu, J.F. Zhang, S. Liu, Y.T. Lu, A xyloglucan endotransglucosylase/hydrolase involves in growth of primary root and alters the deposition of cellulose in Arabidopsis, *Planta*, 226: 1547–1560, 2007.
- [96] S. Romo, T. Jiménez, E. Labrador, B. Dopico, The gene for a xyloglucan

- endotransglucosylase/hydrolase from *Cicer arietinum* is strongly expressed in elongating tissues, *Plant Physiol. Biochem.*, 43: 169–176, 2005.
- [97] B.I. Cantarel, P.M. Coutinho, C. Rancurel, T. Bernard, V. Lombard, B. Henrissat, The Carbohydrate-Active EnZymes database (CAZy): An expert resource for glycogenomics, *Nucleic Acids Res.*, 37: 233–238, 2009.
- [98] V. Lombard, H. Golaconda Ramulu, E. Drula, P.M. Coutinho, B. Henrissat, The carbohydrate-active enzymes database (CAZy) in 2013, *Nucleic Acids Res.*, 42: 2014.
- [99] M.J. Baumann, J.M. Eklöf, G. Michel, A.M. Kallas, T.T. Teeri, M. Czjzek, H. Brumer, Structural evidence for the evolution of xyloglucanase activity from xyloglucan endo-transglycosylases: biological implications for cell wall metabolism, *Plant Cell*, 19: 1947–1963, 2007.
- [100] P. Johansson, Structural Studies of a Xyloglucan Endotransglycosylase from *Populus tremula* x *tremuloides* and Three Conserved Hypothetical Proteins from *Mycobacterium tuberculosis*, 2006.
- [101] P. Johansson, S. Denman, H. Brumer, Å.M. Kallas, H. Henriksson, T. Bergfors, T.T. Teeri, T.A. Jones, Crystallization and preliminary X-ray analysis of a xyloglucan endotransglycosylase from *Populus tremula* x *tremuloides*, *Acta Crystallogr. - Sect. D Biol. Crystallogr.*, 59: 535–537, 2003.
- [102] A. Gutmanas, Y. Alhroub, G.M. Battle, J.M. Berrisford, E. Bochet, M.J. Conroy, J.M. Dana, M.A. Fernandez Montecelo, G. Van Ginkel, S.P. Gore, P. Haslam, R. Hatherley, P.M.S. Hendrickx, M. Hirshberg, I. Lagerstedt, S. Mir, A. Mukhopadhyay, T.J. Oldfield, A. Patwardhan, L. Rinaldi, et al., PDBe: Protein data bank in Europe, *Nucleic Acids Res.*, 42: 2014.
- [103] T. Takeda, Y. Furuta, T. Awano, K. Mizuno, Y. Mitsuishi, T. Hayashi, Suppression and acceleration of cell elongation by integration of xyloglucans in pea stem segments, *Proc. Natl. Acad. Sci. U. S. A.*, 99: 9055–60, 2002.
- [104] J.L. Yang, X.F. Zhu, Y.X. Peng, C. Zheng, G.X. Li, Y. Liu, Y.Z. Shi, S.J. Zheng, Cell wall hemicellulose contributes significantly to aluminum adsorption and root growth in *Arabidopsis*, *Plant Physiol.*, 155: 1885–1892, 2011.
- [105] a Tabuchi, H. Mori, S. Kamisaka, T. Hoson, A new type of endo-xyloglucan transferase devoted to xyloglucan hydrolysis in the cell wall of azuki bean epicotyls, *Plant Cell Physiol.*, 42: 154–161, 2001.
- [106] R. Schröder, R.G. Atkinson, G. Langenkämper, R.J. Redgwell, Biochemical and

- molecular characterisation of xyloglucan endotransglycosylase from ripe kiwifruit, *Planta*, 204: 242–251, 1998.
- [107] K. Vissenberg, I.M. Martinez-Vilchez, J.P. Verbelen, J.G. Miller, S.C. Fry, In vivo colocalization of xyloglucan endotransglycosylase activity and its donor substrate in the elongation zone of *Arabidopsis* roots, *Plant Cell*, 12: 1229–1237, 2000.
- [108] I.N. Saab, M.M. Sachs, A flooding-induced xyloglucan endo-transglycosylase homolog in maize is responsive to ethylene and associated with aerenchyma, *Plant Physiol.*, 112: 385–391, 1996.
- [109] W. Xu, M.M. Purugganan, D.H. Polisensky, D.M. Antosiewicz, S.C. Fry, J. Braam, *Arabidopsis* TCH4, regulated by hormones and the environment, encodes a xyloglucan endotransglycosylase, *Plant Cell*, 7: 1555–1567, 1995.
- [110] C. Catalá, J.K. Rose, W.S. York, P. Albersheim, A.G. Darvill, A.B. Bennett, Characterization of a tomato xyloglucan endotransglycosylase gene that is down-regulated by auxin in etiolated hypocotyls, *Plant Physiol.*, 127: 1180–92, 2001.
- [111] K. Keegstra, Plant Cell Walls, *Am. Soc. Plant Biol.*, 154: 483–486, 2010.
- [112] R. Yokoyama, K. Nishitani, A comprehensive expression analysis of all members of a gene family encoding cell-wall enzymes allowed us to predict cis-regulatory regions involved in cell-wall construction in specific organs of *Arabidopsis*, *Plant Cell Physiol.*, 42: 1025–1033, 2001.
- [113] M. Saladié, J.K.C. Rose, D.J. Cosgrove, C. Catalá, Characterization of a new xyloglucan endotransglucosylase/hydrolase (XTH) from ripening tomato fruit and implications for the diverse modes of enzymic action, *Plant J.*, 47: 282–295, 2006.
- [114] R. Yokoyama, J.K.C. Rose, K. Nishitani, A Surprising Diversity and Abundance of Xyloglucan Endotransglucosylase / Hydrolases in Rice Classification and Expression Analysis 1, *Society*, 134: 1088–1099, 2004.
- [115] J. Geisler-Lee, M. Geisler, P.M. Coutinho, B. Segerman, N. Nishikubo, J. Takahashi, H. Aspeborg, S. Djerbi, E. Master, S. Andersson-Gunnerås, B. Sundberg, S. Karpinski, T.T. Teeri, L.A. Kleczkowski, B. Henrissat, E.J. Mellerowicz, Poplar carbohydrate-active enzymes Gene identification and expression analyses, *Plant Physiol.*, 140: 946–62, 2006.
- [116] S. Macauley-Patrick, M.L. Fazenda, B. McNeil, L.M. Harvey, Heterologous protein production using the *Pichia pastoris* expression system, *Yeast*, 22: 249–270, 2005.
- [117] R. Daly, M.T.W. Hearn, Expression of heterologous proteins in *Pichia pastoris*: A

- useful experimental tool in protein engineering and production, *J. Mol. Recognit.*, 18: 119–138, 2005.
- [118] H. Hohenblum, B. Gasser, M. Maurer, N. Borth, D. Mattanovich, Effects of Gene Dosage, Promoters, and Substrates on Unfolded Protein Stress of Recombinant *Pichia pastoris*, *Biotechnol. Bioeng.*, 85: 367–375, 2004.
- [119] C. Menéndez, L. Hernández, A. Banguela, J. País, Functional production and secretion of the *Gluconacetobacter diazotrophicus* fructose-releasing exo-levanase (LsdB) in *Pichia pastoris*, *Enzyme Microb. Technol.*, 34: 446–452, 2004.
- [120] J. Becnel, M. Natarajan, A. Kipp, J. Braam, Developmental expression patterns of Arabidopsis XTH genes reported by transgenes and Genevestigator, *Plant Mol. Biol.*, 61: 451–467, 2006.
- [121] S.K. Cho, J.E. Kim, J.A. Park, T.J. Eom, W.T. Kim, Constitutive expression of abiotic stress-inducible hot pepper CaXTH3, which encodes a xyloglucan endotransglucosylase/hydrolase homolog, improves drought and salt tolerance in transgenic Arabidopsis plants, *FEBS Lett.*, 580: 3136–3144, 2006.
- [122] D.J. Cosgrove, Expansive growth of plant cell walls, *Plant Physiol. Biochem.*, 38: 109–24, 2000.
- [123] N. Kido, R. Yokoyama, T. Yamamoto, J. Furukawa, H. Iwai, S. Satoh, K. Nishitani, The matrix polysaccharide (1;3,1;4)- $\beta$ -D-glucan is involved in silicon-dependent strengthening of rice cell wall, *Plant Cell Physiol.*, 56: 268–276, 2015.
- [124] A.M. Kallas, K. Piens, S.E. Denman, H. Henriksson, J. Fäldt, P. Johansson, H. Brumer, T.T. Teeri, Enzymatic properties of native and deglycosylated hybrid aspen (*Populus tremulaxtremuloides*) xyloglucan endotransglycosylase 16A expressed in *Pichia pastoris*, *Biochem. J.*, 390: 105–13, 2005.
- [125] M. Strohmeier, M. Hrmova, M. Fischer, A.J. Harvey, G.B. Fincher, J. Pleiss, Molecular modeling of family GH16 glycoside hydrolases: potential roles for xyloglucan transglucosylases/hydrolases in cell wall modification in the poaceae, *Protein Sci.*, 13: 3200–3213, 2004.